NASA Technical Paper 2938

October 1989

Optimized Resolved Rate Control of Seven-Degree-of-Freedom Laboratory Telerobotic Manipulator (LTM) With Application to Three-Dimensional Graphics Simulation

L. Keith Barker and
William S. McKinney, Jr.

NASA

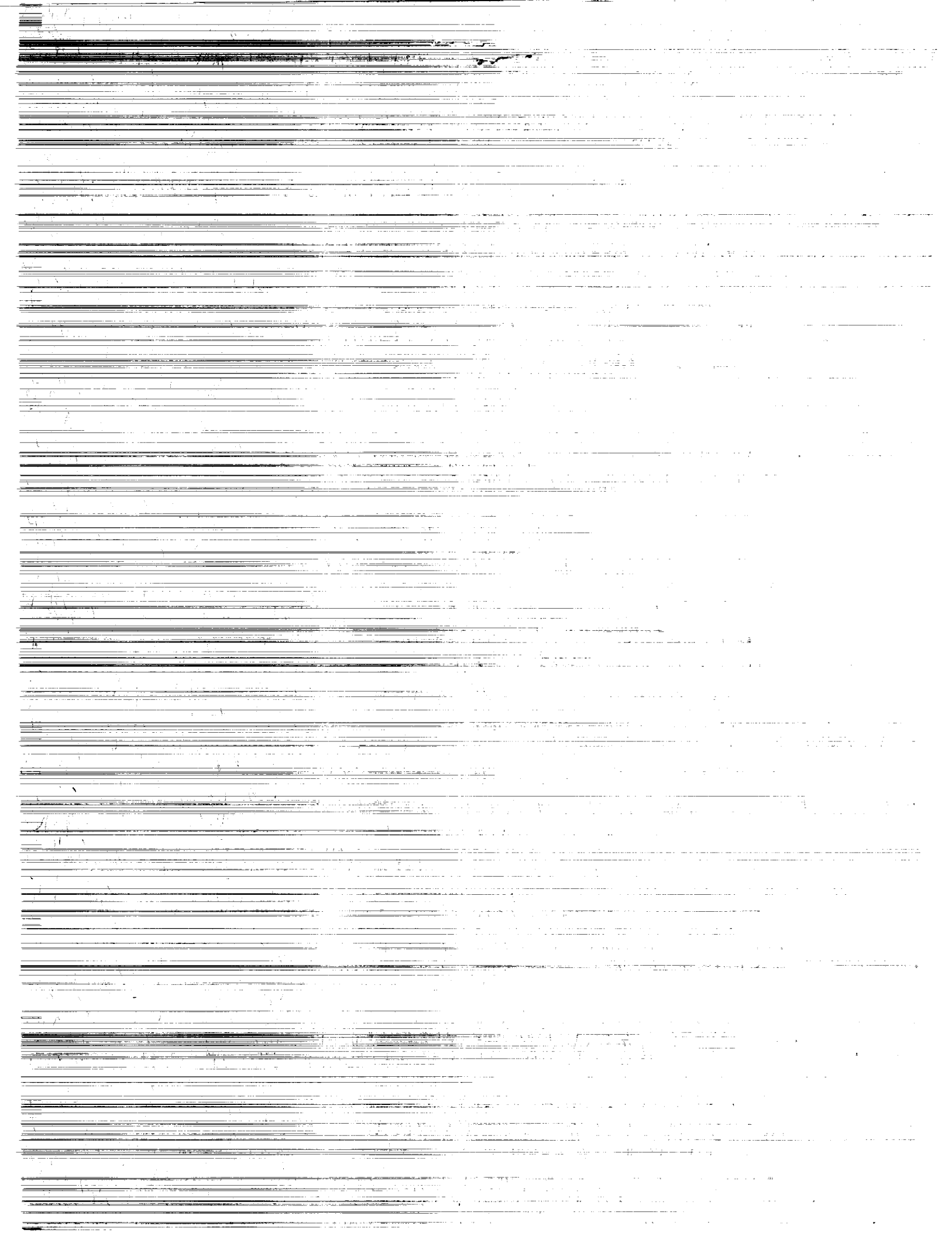

NASA Technical Paper 2938

1989

Optimized Resolved Rate Control of Seven-Degree-of-Freedom Laboratory Telerobotic Manipulator (LTM) With Application to Three-Dimensional Graphics Simulation

L. Keith Barker and
William S. McKinney, Jr.
Langley Research Center
Hampton, Virginia

National Aeronautics and Space Administration
Office of Management
Scientific and Technical Information Division

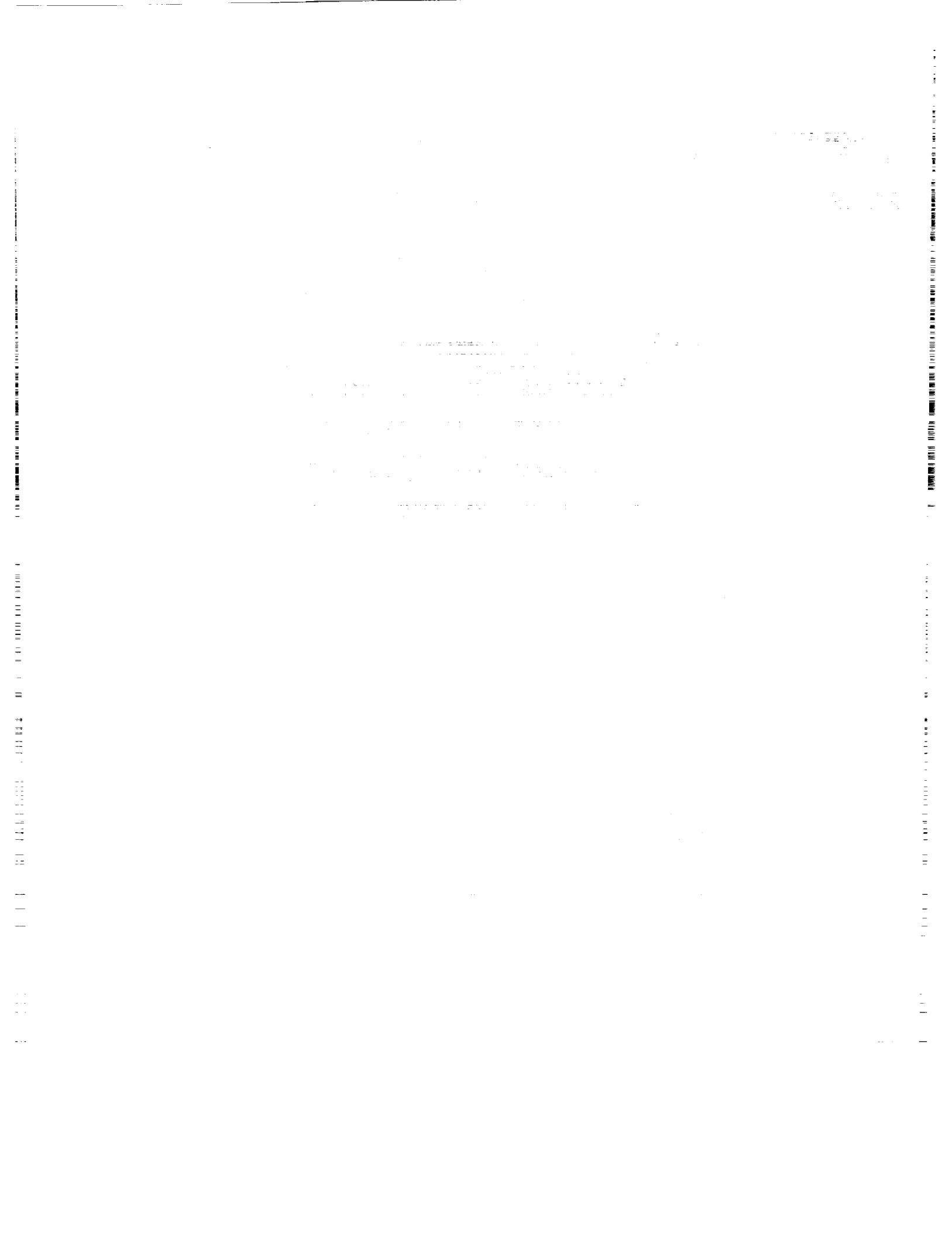

SUMMARY

An optimized resolved rate control scheme for real-time control of seven-degree-of-freedom manipulators with spherical wrists was recently developed at the Oak Ridge National Laboratory. The scheme generates a least-squares solution for joint angle rates, which move the robot hand at a commanded velocity while (optionally) trying to configure the arm to satisfy a specified performance criterion of joint angles.

The present paper discusses the use of this scheme for controlling a prototype of a seven-degree-of-freedom robot arm—the Laboratory Telerobotic Manipulator (LTM)—built by the Oak Ridge National Laboratory for NASA. Axis systems and homogeneous transformation matrices based on the Denavit-Hartenberg parameters are established for the LTM along with appropriate resolved rate control equations. When the optimization scheme cannot be used due to kinematic singularities that result in less than six degrees of freedom, special resolved rate equations are also presented.

A three-dimensional graphics model of the LTM was driven by velocity commands from a six-axis hand controller to assess the equations developed in this paper. For the motions simulated, the robot hand moves as commanded and the special resolved rate equations for kinematic singularities appear reasonable.

INTRODUCTION

The Laboratory Telerobotic Manipulator (LTM) is a seven-degree-of-freedom robot arm built by the Oak Ridge National Laboratory for NASA. A prototype structure with two of the arms (fig. 1(a)) has been delivered to the Langley Research Center for evaluation in ground-based research to assess the role of redundant degree-of-freedom arms in space operations. Each arm has three pitch-yaw joints (fig. 1(b)): one at the shoulder, another at the elbow, and a third at the wrist. The seventh degree of freedom is provided by a wrist roll joint. The problem of interest in this paper is velocity control of the LTM.

Velocity control is a popular way to control robot arms. The velocity of the robot hand is known (or commanded by an operator) and this velocity is resolved into joint angle rates (resolved rate control, ref. 1) to move the hand as commanded. Six independent joints are all that are needed for general movement of the hand in its workspace; but the LTM has a seventh joint, which means there are more choices for joint angle rates to move the hand as commanded. A reasonable solution from among the many choices is one for which the sum of the squares of the joint angle rates is the smallest—a least-squares solution. The solution may also be a trade-off between small rates and those rates which work toward satisfying a specified performance criterion of the joint angles.

An optimized resolved rate control scheme for seven-degree-of-freedom manipulators with spherical wrists (called Dubey's method in this paper (ref. 2)) is applied to the LTM. Dubey's method generates a least-squares solution for the joint angle rates which move the robot hand at the commanded velocity while (optionally) trying to configure the arm to satisfy a specified performance criterion of joint angles. In essence, Dubey's method is a fast way to compute the least-squares solution for arms like the LTM. Real-time control was the impetus for the development of the scheme.

A problem with using Dubey's method is that it requires selecting a column of the Jacobian matrix so that the remaining six columns (or, equivalently, six joint angle rates) are independent. A method to determine quickly which column to select is presented in this paper and is different from the approach in reference 3, a recent application of the scheme to the LTM. However, such a selection is not always possible—in which case the scheme does not apply—and alternate control equations are devised.

SYMBOLS

$\mathbf{A}_j^i$	homogeneous transformation matrix from axis system i to axis system j
a_i	Denavit-Hartenberg parameter, perpendicular distance between Z_{i-1} and Z_i
C_i	$\cos\theta_i$
d_i	Denavit-Hartenberg parameter, distance between coordinate systems $i-1$ and i along Z_{i-1}

$\mathrm{H}(\theta)$	scalar-valued performance criterion
$\nabla\mathrm{H}$	gradient of $\mathrm{H}(\theta)$
$\nabla\mathrm{H}_{\mathrm{arm}}$	gradient defined in equation (9)
$\nabla\mathrm{H}_{\mathrm{wrist}}$	gradient defined in equation (10)
$\mathbf{I}$	identity matrix
$\mathbf{J}$	Jacobian matrix (6 by 7)
$\mathbf{J}^{+}$	generalized inverse of $\mathbf{J}$
$\mathbf{J}_1$,$\mathbf{J}_2$,$\mathbf{J}_3$	submatrices of $\mathbf{J}$ (see eq. (8) or eq. (D2))
$\check{\mathbf{J}}_1$	submatrix (3 by 3) of $\mathbf{J}_1$
k	constant which determines rate of convergence to $\mathrm{H}(\theta)$
l_{ES}	length from elbow to shoulder (constant)
l_{HW}	length from hand to wrist (constant)
l_{WE}	length from wrist to elbow (constant)
l_{WS}	line-of-sight distance from wrist to shoulder
m	index which indicates component of $\dot{\phi}_{p,\mathrm{arm}}$ and $\dot{\phi}_{h,\mathrm{arm}}$ set to 0 and 1, respectively, when using Dubey's method
$\boldsymbol{p}_i^{i-1}$	position vector from joint axis system $i-1$ to joint axis system i; expressed in joint axis system $i-1$
$\mathbf{R}_j^i$	rotational part of homogeneous transformation matrix from axis system i to axis system j
$\mathrm{Rot}(S,\psi)$	rotation matrix (3 by 3) representing a rotation about S axis by angular amount ψ
S_i	$\sin\theta_i$
t	time, sec
$\mathbf{V}$	commanded translational velocity of robot hand
V_{T3},V_{P3},V_{R3}	thrusting, pitching, and rotating velocities of hand relative to line-of-sight from shoulder to wrist, used in forming equations to fully extend robot arm when elbow pitch angle θ_3 is involved
V_{T4},V_{P4},V_{R4}	thrusting, pitching, and rotating velocities of hand relative to line-of-sight from shoulder to wrist, used in forming equations to fully extend robot arm when elbow yaw angle θ_4 is involved
X_i,Y_i,Z_i	axes associated with joint $i+1$, Z_i is axis of rotation; also, unit vector along axis
X_μ,Y_μ,Z_μ	corresponding axes after rotation of axis system (X_2,Y_2,Z_2) by angle μ about Y_2; when both elbow joints are $\pm 90°$, velocity cannot be produced along X_μ
X_ν,Y_ν,Z_ν	corresponding axes after rotation of axis system (X_μ,Y_μ,Z_μ) by angle ν about Z_μ; with loss of shoulder and elbow pitch, velocity cannot be produced along Y_ν
x, y, z	coordinates

$\dot{\mathbf{x}}$	commanded velocity (translational and rotational) of robot hand
α_i	Denavit-Hartenberg parameter, angle between Z_{i-1} and Z_i, measured positively about positive X_i
β_i	constant joint angle offset bias
δ_2,δ_3,δ_4,δ_6	small positive angles used to specify singularity regions
θ_i	angle associated with joint i ($\theta_i = 0°$ for $i = 1$ to 7 in fig. 2)
θ_i'	Denavit-Hartenberg parameter, joint angle between X_{i-1} and X_i, measured positively about positive Z_{i-1}
θ_3^*,θ_4^*	last values of θ_3 and θ_4, respectively, before singularity region of special solution 1 was entered (fig. 6), initialized to initial values of θ_3 and θ_4
$\dot{\boldsymbol{\theta}}$	vector of seven joint angle rates
$\|\dot{\boldsymbol{\theta}}\|$	Euclidean norm of $\dot{\boldsymbol{\theta}}$
$\dot{\boldsymbol{\theta}}_{\text{arm}}$	vector of four arm joint angle rates $\dot{\theta}_1$, $\dot{\theta}_2$, $\dot{\theta}_3$, and $\dot{\theta}_4$
$\dot{\boldsymbol{\theta}}_{\text{opt}}$	optimized vector of seven joint angle rates
$\dot{\boldsymbol{\theta}}_{\text{opt,arm}}$	optimized vector of four arm joint angle rates
$\dot{\boldsymbol{\theta}}_{\text{wrist}}$	vector of wrist joint angle rates $\dot{\theta}_5$, $\dot{\theta}_6$, and $\dot{\theta}_7$
μ	angle between elbow-to-shoulder link and line-of-sight from shoulder to wrist (fig. 3)
ν	angle between Y_μ and $Z_\mu \times X_3$, used in showing velocity component that cannot be produced with loss of shoulder and elbow pitch (defined by eqs. (81) and (82))
ρ_1	angle from plane of X_0 and Z_0 to line of sight from shoulder to wrist when elbow is not yawed (fig. 5(a))
ρ_2	angle from X_1 axis to line of sight from shoulder to wrist when elbow is not pitched (fig. 5(b))
σ_1	angle between elbow-to-shoulder link and line of sight from shoulder to wrist when elbow is not yawed (fig. 5(a))
σ_2	angle between elbow-to-shoulder link and line of sight from shoulder to wrist when elbow is not pitched (fig. 5(b))
$\dot{\boldsymbol{\phi}}$	vector of joint angle rates (eq. (4))
$\dot{\boldsymbol{\phi}}_h$	homogeneous solution of equation (4)
$\dot{\boldsymbol{\phi}}_{h,\text{arm}}$	vector of four rates $\dot{\boldsymbol{\phi}}_h[1]$, $\dot{\boldsymbol{\phi}}_h[2]$, $\dot{\boldsymbol{\phi}}_h[3]$, and $\dot{\boldsymbol{\phi}}_h[4]$
$\dot{\breve{\boldsymbol{\phi}}}_{h,\text{arm}}$	subvector of $\dot{\boldsymbol{\phi}}_{h,\text{arm}}$
$\dot{\boldsymbol{\phi}}_{h,\text{wrist}}$	vector of three rates $\dot{\boldsymbol{\phi}}_h[5]$, $\dot{\boldsymbol{\phi}}_h[6]$, and $\dot{\boldsymbol{\phi}}_h[7]$
$\dot{\phi}_i$	component i of $\dot{\boldsymbol{\phi}}$
$\dot{\boldsymbol{\phi}}_p$	particular solution of equation (4)
$\dot{\boldsymbol{\phi}}_{p,\text{arm}}$	vector of four rates $\dot{\boldsymbol{\phi}}_p[1]$, $\dot{\boldsymbol{\phi}}_p[2]$, $\dot{\boldsymbol{\phi}}_p[3]$, and $\dot{\boldsymbol{\phi}}_p[4]$
$\dot{\breve{\boldsymbol{\phi}}}_{p,\text{arm}}$	subvector of $\dot{\boldsymbol{\phi}}_{p,\text{arm}}$

$\dot{\phi}_{p,\text{wrist}}$	vector of three rates $\dot{\phi}_p[5]$, $\dot{\phi}_p[6]$, and $\dot{\phi}_p[7]$
ω	commanded rotational velocity of robot hand
3-D	three-dimensional
Arm reference points:	
E	elbow
H	hand
S	shoulder
W	wrist

A dot over a quantity indicates the derivative with respect to time. A caret ($\hat{}$) over a vector indicates that the vector is expressed in base coordinates (X_0,Y_0,Z_0). The component index of a vector is listed as a subscript or in brackets ([ ]). If a vector has a label subscript, the component index is always listed in brackets. For example, the second component of the joint angle rate vector $\dot{\boldsymbol{\theta}}$ is $\dot{\boldsymbol{\theta}}_2$ or $\dot{\boldsymbol{\theta}}[2]$. The second component of the arm joint angle rate vector $\dot{\boldsymbol{\theta}}_{\text{arm}}$ is $\dot{\boldsymbol{\theta}}_{\text{arm}}[2]$.

DESCRIPTION OF APPENDIXES

To reduce material in the main body of the paper and to present other pertinent information, six appendixes have been included at the end of this paper. Appendix A lists the homogeneous transformation matrices $\mathbf{A}_{i-1}^{i}$, from joint axis system i to joint axis system $i-1$ and presents a fast way to compute the composite transformation matrix from the hand axis system to the base axis system (hand-to-base transformation $\mathbf{A}_0^7$). Appendix B extends the usefulness of the equations in the analysis by showing that operator inputs need not be restricted to the hand axis system (at wrist). Appendix C derives an example performance criterion which may be used to encourage movement away from some of the singularities of the LTM. Appendix D presents a method for computing quickly several submatrices of the Jacobian matrix in desired reference frames. The solution for the wrist joint angle rates is given in a generic form, which applies directly to four other similar equations in the analysis. Also, a means of dealing with the wrist singularity is presented. In appendix E an expression for a submatrix of the Jacobian is derived in the axis system of the second joint (shoulder yaw θ_2) for analyzing the singularities of the LTM. Appendix F describes a computer program used to implement the equations in this paper.

ANALYSIS

The LTM with axis systems is depicted in figure 2, where all joint angles are defined to be zero. In this initial position, θ_1, θ_3, and θ_5 produce a pitching motion of the hand; θ_2, θ_4, and θ_6 produce a yawing motion of the hand; and θ_7 rolls the hand. As the LTM moves, the X_2 axis is always aligned with the elbow-to-shoulder link; the X_4 axis is always aligned with the wrist-to-elbow link; and the Z_6 axis (and Z_7 axis) is always aligned with the hand-to-wrist link. By convention, θ_i rotates about Z_{i-1}. Denavit-Hartenberg parameters for the LTM are listed in table I. Homogeneous transformation matrices based on these parameters are given in appendix A.

The axis system chosen for operator inputs is the robot hand axis system (X_7,Y_7,Z_7), although this need not be true. (See appendix B.) A simplifying assumption is that $l_{HW} = 0$ to locate the origin of the hand axis system at the intersection of the rotational axes of the robot wrist. Thus, wrist rotation (θ_5, θ_6, and θ_7) does not translate the origin of the hand axis system.

A robot needs only six independent degrees of freedom to translate and orient its hand, so there is a redundant degree of freedom among the seven joints of the LTM. This redundant degree of freedom means different configurations of the arm can be used to produce identical motions of the hand (which can be important, for example, when reaching around obstacles), but the redundancy complicates real-time control.

Joint angle rates of a robot arm cause the hand to move at a velocity

$$\dot{\mathbf{x}} = \mathbf{J}\dot{\boldsymbol{\theta}} \tag{1}$$

where $\mathbf{J}$ is the Jacobian matrix and $\dot{\boldsymbol{\theta}}$ is a vector of joint angle rates. The idea of resolved rate control is to specify $\dot{\mathbf{x}}$ and calculate $\dot{\boldsymbol{\theta}}$.

Performance Criterion

A solution of equation (1), optimized by a specified scalar-valued performance criterion $\mathrm{H}(\theta)$ is (ref. 4)

$$\begin{aligned}\dot{\boldsymbol{\theta}}_{\mathrm{opt}} &= \mathbf{J}^{+}\dot{x} + k\left[\mathbf{I} - \mathbf{J}^{+}\mathbf{J}\right]\nabla\mathrm{H} \\ &= \mathbf{J}^{+}\left[\dot{x} - k\mathbf{J}\nabla\mathrm{H}\right] + k\nabla\mathrm{H}\end{aligned} \tag{2}$$

where $\dot{\boldsymbol{\theta}}_{\mathrm{opt}}$ is the vector of optimized joint angle rates, $\mathbf{J}^{+}$ is the generalized inverse of the Jacobian matrix, $\mathbf{I}$ is the appropriate identity matrix, and $\nabla\mathrm{H}$ is the gradient of the performance criterion. In this paper, $\mathbf{J}^{+}$ is computed by singular value decomposition of $\mathbf{J}$. The constant scalar k in equation (2) is a weighting factor which determines the trade-off between a least-squares solution for the joint angle rates ($\mathbf{J}^{+}\dot{\mathbf{x}}$), and a solution which optimizes the performance criterion $\mathrm{H}(\theta)$. As $|k| \rightarrow 0$, preference is given to minimizing joint angle rates. If the goal is to maximize $\mathrm{H}(\theta)$, k should be positive; if the goal is to minimize $\mathrm{H}(\theta)$, k should be negative. An example performance criterion which may be used to avoid some of the singularities of the LTM is discussed in appendix C.

Dubey's Method of Computing Optimized Joint Angle Rates

The method in reference 2 for calculating optimized joint angle rates for seven-degree-of-freedom robot arms (called Dubey's method in this paper) assumes that equation (2) can be expressed in the form

$$\dot{\boldsymbol{\theta}}_{\mathrm{opt}} = \dot{\boldsymbol{\phi}}_p - \frac{\dot{\boldsymbol{\phi}}_p \cdot \dot{\boldsymbol{\phi}}_h}{\dot{\boldsymbol{\phi}}_h \cdot \dot{\boldsymbol{\phi}}_h}\dot{\boldsymbol{\phi}}_h + k\nabla\mathrm{H} \tag{3}$$

where $\dot{\boldsymbol{\phi}}_p$ and $\dot{\boldsymbol{\phi}}_h$ are particular and homogeneous solutions, respectively, of the equation

$$\dot{\mathbf{x}} - k\mathbf{J}\nabla\mathrm{H} = \mathbf{J}\dot{\boldsymbol{\phi}} \tag{4}$$

(The reader should note the following nomenclature: Joint angle rates which are solutions of equation (1) are always denoted $\dot{\boldsymbol{\theta}}$. The Jacobian matrix and the performance criterion are both functions of the joint angle vector $\boldsymbol{\theta}$, formed by integrating $\dot{\boldsymbol{\theta}}$. Particular and homogeneous solutions of equation (4) are denoted $\dot{\boldsymbol{\phi}}_p$ and $\dot{\boldsymbol{\phi}}_h$, respectively, and are used to calculate an optimized $\dot{\boldsymbol{\theta}}$.)

Specifically, the particular solution $\dot{\boldsymbol{\phi}}_p$ satisfies

$$\dot{\mathbf{x}} - k\mathbf{J}\nabla\mathrm{H} = \mathbf{J}\dot{\boldsymbol{\phi}}_p \tag{5}$$

with one component of $\dot{\boldsymbol{\phi}}_p$ assigned the value 0 by choice, and the homogeneous solution satisfies the equation

$$0 = \mathbf{J}\dot{\boldsymbol{\phi}}_h \tag{6}$$

with one component of $\dot{\boldsymbol{\phi}}_h$ assigned the value 1 by choice. The component assigned the value 0 in $\dot{\boldsymbol{\phi}}_p$ corresponds to the component assigned the value 1 in $\dot{\boldsymbol{\phi}}_h$. Once the particular and homogeneous solutions are found, the homogeneous solution is multiplied by a scalar (the dot product of the two solutions divided by the dot product of the homogeneous solution with itself) and is subtracted from the particular solution. The gradient of the performance criterion times the rate-of-convergence constant is added to the result to form the optimized solution (eq. (3)). Dubey's method implicitly

assumes full rank for the 6 by 6 Jacobian submatrix which must be inverted in equations (5) and (6) to find the six unknown joint angle rates, respectively, of the particular and homogeneous solutions. An alternative method must be used if the Jacobian matrix has rank five or less (i.e., if the robot loses the ability to move along or rotate about some direction in Cartesian space). The advantage of Dubey's method is that the optimized solution can be found without formally computing the generalized inverse. For a more detailed discussion of Dubey's method, see references 2 and 5. The remainder of this analysis presents an efficient method for using Dubey's method to control the LTM and suggests some alternative solutions when the method cannot be used. However, these alternative solutions are by no means the only possible approaches for coping with singular configurations of the arm in which Dubey's method does not apply.

Particularized Algorithm for Dubey's Method

The vector $\dot{\mathbf{x}}$ in equation (4) is partitioned as

$$\dot{\mathbf{x}} = \begin{Bmatrix} \mathbf{V} \\ \hline \boldsymbol{\omega} \end{Bmatrix} \tag{7}$$

where $\mathbf{V}$ and $\boldsymbol{\omega}$ are commanded translational and rotational velocity vectors, respectively, of the hand axis system. Since the hand axis system is assumed to be located at the wrist in this paper, the wrist produces only rotational motions of the hand axis system, and equation (4) can be written as

$$\begin{Bmatrix} \mathbf{V} \\ \hline \boldsymbol{\omega} \end{Bmatrix} - k \left[\begin{array}{c|c} \mathbf{J}_1 & 0 \\ \hline \mathbf{J}_2 & \mathbf{J}_3 \end{array}\right] \begin{Bmatrix} \nabla \mathrm{H}_{\mathrm{arm}} \\ \hline \nabla \mathrm{H}_{\mathrm{wrist}} \end{Bmatrix} = \left[\begin{array}{c|c} \mathbf{J}_1 & 0 \\ \hline \mathbf{J}_2 & \mathbf{J}_3 \end{array}\right] \begin{Bmatrix} \dot{\boldsymbol{\phi}}_{\mathrm{arm}} \\ \hline \dot{\boldsymbol{\phi}}_{\mathrm{wrist}} \end{Bmatrix} \tag{8}$$

where

$$\nabla \mathrm{H}_{\mathrm{arm}} = \begin{Bmatrix} \partial \mathrm{H}/\partial\theta_1 \\ \partial \mathrm{H}/\partial\theta_2 \\ \partial \mathrm{H}/\partial\theta_3 \\ \partial \mathrm{H}/\partial\theta_4 \end{Bmatrix} \tag{9}$$

$$\nabla \mathrm{H}_{\mathrm{wrist}} = \begin{Bmatrix} \partial \mathrm{H}/\partial\theta_5 \\ \partial \mathrm{H}/\partial\theta_6 \\ \partial \mathrm{H}/\partial\theta_7 \end{Bmatrix} \tag{10}$$

$$\dot{\boldsymbol{\phi}}_{\mathrm{arm}} = \begin{Bmatrix} \dot{\phi}_1 \\ \dot{\phi}_2 \\ \dot{\phi}_3 \\ \dot{\phi}_4 \end{Bmatrix} \tag{11}$$

$$\dot{\boldsymbol{\phi}}_{\mathrm{wrist}} = \begin{Bmatrix} \dot{\phi}_5 \\ \dot{\phi}_6 \\ \dot{\phi}_7 \end{Bmatrix} \tag{12}$$

With respect to translational motion of the hand (the $\mathbf{V}$-part of eq. (8)), any redundancy must reside in the first four joints, since the three wrist joints cannot translate the hand (at wrist).

Dubey's method relies on being able to solve for six independent joint angle rate components, each of which is either a component of $\dot{\boldsymbol{\phi}}_{\mathrm{arm}}$ or $\dot{\boldsymbol{\phi}}_{\mathrm{wrist}}$. If $\mathbf{J}_3$ is not singular, the solution for $\dot{\boldsymbol{\phi}}_{\mathrm{wrist}}$ provides three of these components. The other three independent components must come from the four components of $\dot{\boldsymbol{\phi}}_{\mathrm{arm}}$, provided $\mathbf{J}_1$ has full rank.

Therefore, if $\mathbf{J}_3$ is not singular and if $\mathbf{J}_1$ has full rank, one of the components of $\dot{\boldsymbol{\phi}}_{\mathrm{arm}}$ is chosen to be 0 and 1, respectively, in forming the particular and homogeneous solutions of equation (8). The details of calculating these particular and homogeneous solutions follow.

Computation of the Particular Solution

Equation (8) allows formation of the particular solution from the translational and rotational velocity equations:

$$\mathbf{V} - k\mathbf{J}_1 \nabla \mathrm{H}_{\mathrm{arm}} = \mathbf{J}_1 \dot{\phi}_{p,\mathrm{arm}} \tag{13}$$

$$\omega - \mathbf{J}_2 \left[\dot{\phi}_{p,\mathrm{arm}} + k \nabla \mathrm{H}_{\mathrm{arm}} \right] - k\mathbf{J}_3 \nabla \mathrm{H}_{\mathrm{wrist}} = \mathbf{J}_3 \dot{\phi}_{p,\mathrm{wrist}} \tag{14}$$

Equation (13) is solved for $\dot{\phi}_{p,\mathrm{arm}}$ with one component assigned the value 0 by choice. Once $\dot{\phi}_{p,\mathrm{arm}}$ is calculated, equation (14) is solved for $\dot{\phi}_{p,\mathrm{wrist}}$.

For discussion purposes, set the mth component of $\dot{\phi}_{p,\mathrm{arm}}$ to 0 in equation (13) and delete the mth column of $\mathbf{J}_1$. Let the remaining submatrix of $\mathbf{J}_1$ be denoted by $\check{\mathbf{J}}_1$ and let the vector of the remaining three components of $\dot{\phi}_{p,\mathrm{arm}}$ be denoted by $\check{\dot{\phi}}_{p,\mathrm{arm}}$. Assuming that $\check{\mathbf{J}}_1$ is invertible, the reduced equation yields

$$\check{\dot{\phi}}_{p,\mathrm{arm}} = \check{\mathbf{J}}_1^{-1} \left[\mathbf{V} - k\mathbf{J}_1 \nabla \mathrm{H}_{\mathrm{arm}} \right] \tag{15}$$

By properly associating indices, one can assemble $\dot{\phi}_{p,\mathrm{arm}}$ from the components of $\check{\dot{\phi}}_{p,\mathrm{arm}}$ with the missing component given by $\dot{\phi}_{p,\mathrm{arm}}[m] = 0$.

Once $\dot{\phi}_{p,\mathrm{arm}}$ is known, equation (14) can be solved by

$$\dot{\phi}_{p,\mathrm{wrist}} = \mathbf{J}_3^{-1} \left[\omega - \mathbf{J}_2 \left(\dot{\phi}_{p,\mathrm{arm}} + k \nabla \mathrm{H}_{\mathrm{arm}} \right) - k\mathbf{J}_3 \nabla \mathrm{H}_{\mathrm{wrist}} \right] \tag{16}$$

Equation (16) formally represents the solution of equation (14), but simple expressions are derived in appendix D to expedite the calculation of $\dot{\phi}_{p,\mathrm{wrist}}$ and deal with the singularity of $\mathbf{J}_3$. Finally, the complete particular solution is

$$\dot{\phi}_p = \begin{Bmatrix} \dot{\phi}_{p,\mathrm{arm}} \\ \hline \dot{\phi}_{p,\mathrm{wrist}} \end{Bmatrix} \tag{17}$$

Computation of the Homogeneous Solution

Equation (8) allows formation of the homogeneous solution from the two equations:

$$0 = \mathbf{J}_1 \dot{\phi}_{h,\mathrm{arm}} \tag{18}$$

$$-\mathbf{J}_2 \dot{\phi}_{h,\mathrm{arm}} = \mathbf{J}_3 \dot{\phi}_{h,\mathrm{wrist}} \tag{19}$$

Equation (18) can be expressed in the form:

$$0 = \check{\mathbf{J}}_1 \check{\dot{\phi}}_{h,\mathrm{arm}} + \begin{Bmatrix} \mathbf{J}_1[1,m] \\ \mathbf{J}_1[2,m] \\ \mathbf{J}_1[3,m] \end{Bmatrix} \dot{\phi}_{h,\mathrm{arm}}[m] \tag{20}$$

where removing the mth column of $\mathbf{J}_1$ leaves the submatrix $\check{\mathbf{J}}_1$ and removing the mth component from $\dot{\phi}_{h,\mathrm{arm}}$ leaves $\check{\dot{\phi}}_{h,\mathrm{arm}}$.

Recall that the value 1 is assigned to the mth component of the homogeneous solution in Dubey's method. Consequently, with the assignment $\dot{\phi}_{h,\mathrm{arm}}[m] = 1$, the solution of equation (20) is

$$\check{\dot{\phi}}_{h,\mathrm{arm}} = -\check{\mathbf{J}}_1^{-1} \begin{Bmatrix} \mathbf{J}_1[1,m] \\ \mathbf{J}_1[2,m] \\ \mathbf{J}_1[3,m] \end{Bmatrix} \tag{21}$$

By properly associating indices, one can assemble $\dot{\phi}_{h,\text{arm}}$ from the components of $\dot{\check{\phi}}_{h,\text{arm}}$, with the missing component given by $\dot{\phi}_{h,\text{arm}}[m] = 1$. Note that $\check{\mathbf{J}}_1^{-1}$ appears in both equations (15) and (21).

Once $\dot{\phi}_{h,\text{arm}}$ is known, the solution of equation (19) is

$$\dot{\phi}_{h,\text{wrist}} = -\mathbf{J}_3^{-1}\left[\mathbf{J}_2\dot{\phi}_{h,\text{arm}}\right] \tag{22}$$

Equation (22) formally represents the solution of equation (19), but simple expressions are derived in appendix D to expedite calculation of $\dot{\phi}_{h,\text{wrist}}$ and to deal with the singularity of $\mathbf{J}_3$. Finally, the complete homogeneous solution is

$$\dot{\phi}_h = \left\{ \begin{array}{c} \dot{\phi}_{h,\text{arm}} \\ \hline \dot{\phi}_{h,\text{wrist}} \end{array} \right\} \tag{23}$$

The solutions of equations (13), (14), (18), and (19) together with equations (17), (23), and (3) thus reduce the problem of computing an optimized solution to equation (1) to the problem of inverting two 3 by 3 matrices—$\check{\mathbf{J}}_1$ in equations (15) and (21) and $\mathbf{J}_3$ in equations (16) and (22). *However, it is not always possible to find an invertible* $\check{\mathbf{J}}_1$, *nor is it always possible to invert* $\mathbf{J}_3$. The method outlined in this section for generating an optimized solution to equation (1) is used only if an invertible $\check{\mathbf{J}}_1$ exists and $\mathbf{J}_3$ is also invertible. Cases in which Dubey's method cannot be used are discussed later.

Determining an Invertible $\check{\mathbf{J}}_1$

The matrix $\mathbf{J}_1$ for the LTM expressed in the (X_2,Y_2,Z_2) axis system is

$$\mathbf{J}_1 = \begin{bmatrix} -C_4S_3C_2l_{WE} & -S_4l_{WE} & -C_4S_3l_{WE} & -S_4C_3l_{WE} \\ C_2l_{ES} + (C_4C_3C_2 - S_4S_2)l_{WE} & 0 & C_4C_3l_{WE} & -S_4S_3l_{WE} \\ -C_4S_3S_2l_{WE} & -l_{ES} - C_4C_3l_{WE} & 0 & -C_4l_{WE} \end{bmatrix} \tag{24}$$

as derived in appendix E. The lengths of the elbow-to-shoulder link (l_{ES}) and the wrist-to-elbow link (l_{WE}) are shown in table I. Table II lists the determinants and associated singularities for each of the four possible 3 by 3 submatrices ($\check{\mathbf{J}}_1$) that can be formed by deleting a column from $\mathbf{J}_1$. Any submatrix $\check{\mathbf{J}}_1$ can always be inverted as long as its determinant is not zero (which occurs at its singularities). *Although shown in table II, the singularity conditions* $|\theta_3| = 180°$ *and* $|\theta_4| = 180°$ *are not considered physically realizable and are ignored.* In this paper, mutually exclusive partitions of the motion of θ_4 are used to decide which column of $\mathbf{J}_1$ to delete. These partitions are (1) $|\theta_4| \neq 0°$ and $|\theta_4| \neq 90°$; (2) $|\theta_4| = 0°$; and (3) $|\theta_4| = 90°$.

The equalities and inequalities in the following discussion are treated in a strict sense. But, on a computer, these equalities and inequalities must be defined in terms of regions. Appropriate sizes for the regions are discussed in appendix F.

Partition (1): $|\theta_4| \neq 0°$ and $|\theta_4| \neq 90°$

Notice in table II that after column 1 of $\mathbf{J}_1$ is deleted the remaining $\check{\mathbf{J}}_1$ can always be inverted as long as $|\theta_4|$ is not 0° or 90°. Therefore, if $|\theta_4|$ is neither 0° nor 90°, the index m used in forming the particular and homogeneous solutions is chosen as $m = 1$ (i.e., $\dot{\phi}_{p,\text{arm}}[1] = 0$ and $\dot{\phi}_{h,\text{arm}}[1] = 1$).

Partition (2): $|\theta_4| = 0°$

If $|\theta_4| = 0°$, then neither the elimination of column 1 nor column 3 from $\mathbf{J}_1$ will result in an invertible $\check{\mathbf{J}}_1$. However, it is possible to eliminate column 2 to produce an invertible $\check{\mathbf{J}}_1$ if $|\theta_2| \neq 90°$ and $|\theta_3| \neq 0°$. Therefore, when $|\theta_4| = 0°$, if $|\theta_2| \neq 90°$ and $|\theta_3| \neq 0°$, the index m used in forming the particular and homogeneous solutions is chosen as $m = 2$ (i.e., $\dot{\phi}_{p,\text{arm}}[2] = 0$ and $\dot{\phi}_{h,\text{arm}}[2] = 1$). If $|\theta_2| = 90°$ or $|\theta_3| = 0°$ then it is not possible to form an invertible $\check{\mathbf{J}}_1$ from $\mathbf{J}_1$.

Partition (3): $|\theta_4| = 90°$

If $|\theta_4| = 90°$, then neither the elimination of column 1, column 2, nor column 4 from $\mathbf{J}_1$ will result in an invertible $\check{\mathbf{J}}_1$. However, it is possible to eliminate column 3 to produce an invertible $\check{\mathbf{J}}_1$ if $|\theta_3| \neq 90°$ and $-l_{ES}C_2 \neq l_{WE}(C_4C_3C_2 - S_4S_2)$.

Since $|\theta_4| = 90°$, $-l_{ES}C_2 \neq l_{WE}(C_4C_3C_2 - S_4S_2)$ simplifies to $l_{ES}C_2 \neq \text{sign}(S_4)l_{WE}S_2$ where the sign function is defined as:

$$\text{sign}(x) = \left\{ \begin{matrix} +1 & (x \geq 0) \\ -1 & (x < 0) \end{matrix} \right\} \tag{25}$$

where x is a general argument. Geometrically, the equality condition $l_{ES}C_2 = \text{sign}(S_4)l_{WE}S_2$ holds when the arm lies in the plane of Z_0 and X_1 with the wrist located on Z_0, as shown in figure 3. As discussed in a later section, it is more convenient to describe the inequality condition $l_{ES}C_2 \neq \text{sign}(S_4)l_{WE}S_2$ in terms of the shoulder joint angle θ_2. Toward this end, the angle between the elbow-to-shoulder link and the line-of-sight distance from the shoulder to the wrist (l_{WS}) when $|\theta_4| = 90°$ is called μ and is defined to be positive when $\theta_4 = 90°$ (as in fig. 3). Mathematically, $l_{ES}C_2 \neq \text{sign}(S_4)l_{WE}S_2$ if and only if $|\theta_2 + \mu| \neq 90°$:

$$\sin\mu = \frac{\text{sign}(S_4)l_{WE}}{\sqrt{l_{ES}^2 + l_{WE}^2}} \tag{26}$$

$$\cos\mu = \frac{l_{ES}}{\sqrt{l_{ES}^2 + l_{WE}^2}} \tag{27}$$

(Note that $|\mu|$ is constant, and in this paper, $|\mu| = \arctan(20/23) = 41.01°$.) Then,

$$\begin{aligned} \cos(\theta_2 + \mu) &= C_2\cos\mu - S_2\sin\mu \\ &= \frac{l_{ES}C_2 - \text{sign}(S_4)l_{WE}S_2}{\sqrt{l_{ES}^2 + l_{WE}^2}} \end{aligned} \tag{28}$$

Therefore, the condition $l_{ES}C_2 \neq \text{sign}(S_4)l_{WE}S_2$ is equivalent to the condition $\cos(\theta_2 + \mu) \neq 0$ or

$$|\theta_2 + \mu| \neq 90° \tag{29}$$

When $|\theta_4| = 90°$, if $|\theta_3| \neq 90°$ and $|\theta_2 + \mu| \neq 90°$, the index m used in forming the particular and homogeneous solutions is chosen as $m = 3$ (i.e., $\dot{\phi}_{p,\text{arm}}[3] = 0$ and $\dot{\phi}_{h,\text{arm}}[3] = 1$). If $|\theta_3| = 90°$ or $|\theta_2 + \mu| = 90°$, then it is not possible to form an invertible $\check{\mathbf{J}}_1$ from $\mathbf{J}_1$.

Figure 4 is a flowchart which uses the logic just described to determine which column to eliminate from $\mathbf{J}_1$ to form an invertible $\check{\mathbf{J}}_1$ (or which component to set to 0 and 1 when forming the particular and homogeneous solutions, respectively). Equality conditions are shown in the figure for simplicity, but singularity regions are defined when using the logic in a computer program (appendix F). The flowchart also indicates when it is not possible to form an invertible $\check{\mathbf{J}}_1$ and identifies the associated special solution to use for the arm joint angle rates (each special solution is discussed in a later section).

Determining the Invertibility of $\mathbf{J}_3$

The Jacobian submatrix $\mathbf{J}_3$ expressed in the hand axis system is derived in appendix D as

$$\mathbf{J}_3 = \begin{bmatrix} -C_7C_6 & S_7 & 0 \\ S_7C_6 & C_7 & 0 \\ -S_6 & 0 & 1 \end{bmatrix} \tag{30}$$

The determinant of $\mathbf{J}_3$ is easily calculated from equation (30) as $-\cos\theta_6$. Hence, $\mathbf{J}_3$ is invertible as long as

$$|\theta_6| \neq 90° \tag{31}$$

Optimizing $\dot{\theta}_{\text{arm}}$ When $\mathbf{J}_3$ Is Not Invertible

Even when $\mathbf{J}_3$ is singular, it may still be possible to find six independent joint angle rates from among the components of $\dot{\phi}_{\text{arm}}$ and $\dot{\phi}_{\text{wrist}}$, so that Dubey's method could be applied. But this solution would involve inverting a 6 by 6 submatrix of $\mathbf{J}$ (after it was determined). An alternate solution—optimizing only $\dot{\theta}_{\text{arm}}$ when $\mathbf{J}_1$ has full rank and $\mathbf{J}_3$ is singular—is used in this paper.

A region about the singularity of $\mathbf{J}_3$ is defined as

$$||\theta_6| - 90°| < \delta_6 \tag{32}$$

where δ_6 is a small specified positive angle (the minimum value for δ_6 is given in appendix F). When an invertible $\check{\mathbf{J}}_1$ exists, but θ_6 is inside this singularity region, only the arm joint angle rates are optimized:

$$\dot{\theta} = \left\{ \begin{array}{c} \dot{\theta}_{\text{opt,arm}} \\ \hline \dot{\theta}_{\text{wrist}} \end{array} \right\} = \left\{ \begin{array}{c} \dot{\phi}_{p,\text{arm}} - \dfrac{\dot{\phi}_{p,\text{arm}} \cdot \dot{\phi}_{h,\text{arm}}}{\dot{\phi}_{h,\text{arm}} \cdot \dot{\phi}_{h,\text{arm}}} \dot{\phi}_{h,\text{arm}} + k\nabla \text{H}_{\text{arm}} \\ \hline \dot{\theta}_{\text{wrist}} \end{array} \right\} \tag{33}$$

where $\dot{\phi}_{p,\text{arm}}$ and $\dot{\phi}_{h,\text{arm}}$ are assembled from equations (15) and (21), along with $\dot{\phi}_{p,\text{arm}}[m] = 0$ and $\dot{\phi}_{h,\text{arm}}[m] = 1$. Using the method outlined in appendix D, $\dot{\theta}_{\text{wrist}}$ in equation (33) is solved from equation (D2) with the substitution $\dot{\theta}_{\text{arm}} = \dot{\theta}_{\text{opt,arm}}$:

$$\omega - \mathbf{J}_2 \dot{\theta}_{\text{opt,arm}} = \mathbf{J}_3 \dot{\theta}_{\text{wrist}} \tag{34}$$

Computing Joint Angle Rates When Dubey's Method Does Not Apply

In this paper, Dubey's method does not apply when an invertible $\check{\mathbf{J}}_1$ does not exist. Instead, special solutions for the arm and wrist joint angle rates are formed from the two equations (see eq. (D2)):

$$\mathbf{V} = \mathbf{J}_1 \dot{\theta}_{\text{arm}} \tag{35}$$

$$\omega - \mathbf{J}_2 \dot{\theta}_{\text{arm}} = \mathbf{J}_3 \dot{\theta}_{\text{wrist}} \tag{36}$$

The wrist joint angle rates are calculated by the method outlined in appendix D (regardless of whether $\mathbf{J}_3$ is invertible or not). Special solutions for $\dot{\theta}_{\text{arm}}$ are discussed in the following section.

Special Solutions for $\dot{\theta}_{\text{arm}}$ When an Invertible $\check{\mathbf{J}}_1$ Does Not Exist

There are four sets of configurations of the arm for which Dubey's method does not apply because an invertible $\check{\mathbf{J}}_1$ does not exist (see fig. 4):

1. $|\theta_4| = 0°$ and $|\theta_3| = 0°$
2. $|\theta_4| = 0°$ and $|\theta_2| = 90°$
3. $|\theta_4| = 90°$ and $|\theta_3| = 90°$
4. $|\theta_4| = 90°$ and $|\theta_2 + \mu| = 90°$

In these configurations, the arm cannot physically produce a component of the commanded translational velocity vector $\mathbf{V}$, as shown later.

Special solutions for $\dot{\boldsymbol{\theta}}_{\text{arm}}$ are used in singularity regions defined around these four conditions. The singularity regions are

$$|\theta_4| < \delta_4 \text{ and } |\theta_3| < \delta_3 \tag{37}$$

$$|\theta_4| < \delta_4 \text{ and } ||\theta_2| - 90°| < \delta_2 \tag{38}$$

$$||\theta_4| - 90°| < \delta_4 \text{ and } ||\theta_3| - 90°| < \delta_3 \tag{39}$$

$$||\theta_4| - 90°| < \delta_4 \text{ and } ||\theta_2 + \mu| - 90°| < \delta_2 \tag{40}$$

where δ_2, δ_3, and δ_4 are small specified positive angles, and μ is defined by equations (26) and (27). Minimum values for δ_2, δ_3, and δ_4 are given in appendix F.

For discussion purposes in the sections that follow, joints 2 and 4 are described as the shoulder and elbow yaw joints, respectively, and joints 1 and 3 are described as the shoulder and elbow pitch joints, respectively. (See fig. 2.) Motion produced by $\dot{\theta}_2$ or $\dot{\theta}_4$ is referred to as yaw motion of the arm, and motion produced by $\dot{\theta}_1$ or $\dot{\theta}_3$ is referred to as pitch motion of the arm.

The four special solutions developed in the following sections are by no means the only ones possible nor may they be the best. However, in the tests performed with a 3-D graphics model of the LTM and a six-axis joystick controller, they do seem to produce reasonable responses of the arm. Further experimentation is needed to better evaluate the usefulness of the special solutions and to determine any modifications or refinements which would be beneficial.

Special Solution 1: Full Extension via Elbow Pitch and Elbow Yaw

Special solution 1 applies when the robot arm is at or near full extension, when $\theta_3 = 0°$ and $\theta_4 = 0°$ (for example, as shown in fig. 2). When the arm is fully extended, joints 2 and 4 can only translate the robot hand in either the same or exactly opposite directions; this is also true for joints 1 and 3. Mathematically, substituting equation (24), with $\theta_3 = \theta_4 = 0°$, into equation (35) yields

$$\begin{Bmatrix} V_{X2} \\ V_{Y2} \\ V_{Z2} \end{Bmatrix} = \begin{bmatrix} 0 & 0 & 0 & 0 \\ C_2(l_{ES} + l_{WE}) & 0 & l_{WE} & 0 \\ 0 & -(l_{ES} + l_{WE}) & 0 & -l_{WE} \end{bmatrix} \dot{\boldsymbol{\theta}}_{\text{arm}} \tag{41}$$

where the components of $\mathbf{V}$ are subscripted to denote the (X_2,Y_2,Z_2) axis system. The row of zeros in equation (41) means that it is not possible to produce V_{X2}. Therefore, there are not enough independent arm joints to apply Dubey's method, and special solution 1 is used.

Overview of Proposed Solution

A scheme to control a six-degree-of-freedom robot arm with a single-jointed elbow in the vicinity of full extension was devised in reference 6. This scheme is extended here to encompass the more complex situation of a double-jointed elbow. Special solution 1 is activated and deactivated as the arm moves in and out of the singularity region defined by equation (37). The pitching joint rates $\dot{\theta}_1$ and $\dot{\theta}_3$ are used as a pair to extend (thrust) the robot arm as far as possible, so that the hand (at wrist) travels along the line of sight from the shoulder to the wrist. The yawing joint rates $\dot{\theta}_2$ and $\dot{\theta}_4$ have the same function. When the arm is fully extended, thrust motion of the hand stops. The extended arm can be maneuvered like a turret at the shoulder, with $\dot{\theta}_1$ doing the pitching and $\dot{\theta}_2$ doing the rotating (yawing). For now, only the pair of yawing joints are used to retract the arm in the singularity region. When the arm is commanded to retract, the elbow bend (in yaw) is opposite to that on entering the singularity region.

Solution for Pitching Joints

Figure 5(a) shows the geometry that is used in deriving equations for $\dot{\theta}_3$ (elbow pitch rate) and $\dot{\theta}_1$ (shoulder pitch rate). Notice that the elbow is not yawed ($\theta_4 = 0°$). Equations based on this geometry are still used even for a slightly yawed elbow.

Hand velocity components V_{T3}, V_{P3}, ***and*** V_{R3}. The translational velocity components V_{T3} (thrust), V_{P3} (pitch), and V_{R3} (rotate or yaw) of the hand relative to the line of sight from the shoulder to the wrist (the dashed line from S to W in fig. 5(a)) are calculated by rotating the commanded velocity vector expressed in the (X_2,Y_2,Z_2) axis system by the angle σ_1 about the Z_2 axis:

$$\begin{Bmatrix} V_{T3} \\ V_{P3} \\ V_{R3} \end{Bmatrix} = \text{Rot}(Z_2,\sigma_1) \begin{Bmatrix} V_{X2} \\ V_{Y2} \\ V_{Z2} \end{Bmatrix}$$

$$= \begin{bmatrix} \cos\sigma_1 & \sin\sigma_1 & 0 \\ -\sin\sigma_1 & \cos\sigma_1 & 0 \\ 0 & 0 & 1 \end{bmatrix} \begin{Bmatrix} V_{X2} \\ V_{Y2} \\ V_{Z2} \end{Bmatrix} \tag{42}$$

The pitching joint angle rates $\dot{\theta}_3$ and $\dot{\theta}_1$ coordinate to produce a velocity along the dashed line that is proportional to V_{T3}, and $\dot{\theta}_1$ is used to produce V_{P3}. (Rotating (yawing) motions are produced by $\dot{\theta}_2$ and are discussed later.)

Expressions for $\cos\sigma_1$ ***and*** $\sin\sigma_1$. From figure 5(a),

$$\cos\sigma_1 = \frac{l_{ES} + l_{WE}C_3}{l_{WS}} \tag{43}$$

$$\sin\sigma_1 = \frac{l_{WE}S_3}{l_{WS}} \tag{44}$$

where (by the law of cosines)

$$l_{WS} = \sqrt{l_{ES}^2 + l_{WE}^2 + 2l_{ES}l_{WE}C_3} \tag{45}$$

The length l_{WS} (wrist to shoulder) varies with θ_3. Physically, the origin of the wrist axis system cannot coincide with the origin of the shoulder axis system, so $l_{WS} \neq 0$. The link lengths l_{ES} (elbow to shoulder) and l_{WE} (wrist to elbow) are constants listed in table I.

Equation for $\dot{\theta}_3$ ***in singularity region.*** The contribution of the elbow pitch rate $\dot{\theta}_3$ in extending the robot arm in response to the commanded thrust velocity V_{T3} is computed as

$$\dot{\theta}_3 = \begin{Bmatrix} -K_3\ V_{T3}\ \text{sign}(\theta_3) & (V_{T3} > 0,\ \theta_3\theta_3^* > 0) \\ 0 & (\text{Otherwise}) \end{Bmatrix} \tag{46}$$

where θ_3^* is the value of θ_3 just before the singularity region was entered, and K_3 is a specified positive constant, which is assumed to be unity in this paper. Equation (46) extends the arm until θ_3 changes sign (i.e., θ_3 passes through 0° but is still approximately 0°) and then freezes θ_3.

Equation for $\dot{\sigma}_1$. The shoulder pitch angle $\dot{\theta}_1$ is used to keep the hand from moving off the line of sight from the shoulder to the wrist by nulling the angular rate $\dot{\sigma}_1$ due to $\dot{\theta}_3$. Differentiate equations (44) and (45) with respect to time and form the two expressions:

$$\dot{\sigma}_1 = \frac{l_{WE}}{\cos\sigma_1}\left(\frac{l_{WS}C_3\dot{\theta}_3 - \dot{l}_{WS}S_3}{l_{WS}^2}\right) \tag{47}$$

$$\dot{l}_{WS} = -\frac{l_{ES} l_{WE} S_3 \dot{\theta}_3}{l_{WS}} \tag{48}$$

With equations (43) and (48), equation (47) is written as

$$\dot{\sigma}_1 = \frac{l_{WE}\dot{\theta}_3}{l_{ES} + l_{WE} C_3} \left(C_3 + \frac{l_{ES} l_{WE} S_3^2}{l_{WS}^2} \right) \tag{49}$$

Equation for $\dot{\rho}_1$. The angular rate $\dot{\rho}_1$ pitches the robot arm in response to an operator's command and is used in computing $\dot{\theta}_1$. The hand at the wrist has a moment arm l_{WS} relative to the shoulder, and the linear pitching rate V_{P3} (commanded) is the product of this moment arm and the angular pitch rate $\dot{\rho}_1$. Thus,

$$\dot{\rho}_1 = \frac{V_{P3}}{l_{WS}} \tag{50}$$

where l_{WS} is defined by equation (45).

Equation for $\dot{\theta}_1$ ***in singularity region.*** The shoulder pitch rate $\dot{\theta}_1$ has two functions in the singularity region: (1) keep the wrist on the dashed line in figure 5(a) as $\dot{\theta}_3$ extends the wrist and (2) allow the operator to pitch the extended arm.

Components of $\dot{\theta}_1$ expressed in the (X_2,Y_2,Z_2) axis system are (see appendix A for transformation matrices)

$$\mathbf{R}_2^1 \mathbf{R}_1^0 \begin{Bmatrix} 0 \\ 0 \\ \dot{\theta}_1 \end{Bmatrix} = \begin{Bmatrix} -S_2\dot{\theta}_1 \\ 0 \\ C_2\dot{\theta}_1 \end{Bmatrix} \tag{51}$$

These components are shown in figure 5(a). The component $-S_2\dot{\theta}_1$ produces an unwanted yaw velocity of the wrist, but this yaw velocity is later nulled by subtracting it from the commanded yaw velocity. The component $C_2\dot{\theta}_1$ is used to pitch the line of sight with rate $\dot{\rho}_1$ and to null the rate $\dot{\sigma}_1$:

$$C_2\dot{\theta}_1 = \dot{\rho}_1 - \dot{\sigma}_1 \tag{52}$$

or

$$\dot{\theta}_1 = \frac{\dot{\rho}_1 - \dot{\sigma}_1}{C_2} \tag{53}$$

where $\dot{\sigma}_1$ and $\dot{\rho}_1$ are given by equations (49) and (50), respectively. Since equation (53) is singular when $|\theta_2| = 90°$, it is used only when θ_2 is outside a region defined around $|\theta_2| = 90°$:

$$\dot{\theta}_1 = \begin{cases} 0 & \| \theta_2| - 90°| < \lambda_2) \\ \dfrac{\dot{\rho}_1 - \dot{\sigma}_1}{C_2} & \text{(Otherwise)} \end{cases} \tag{54}$$

where λ_2 is a positive angle. When $60° \leq |\theta_2| \leq 120°$, half or less of $\dot{\theta}_1$ is in the direction of $\dot{\rho}_1 - \dot{\sigma}_1$ (eq. (52)). This was the criterion used to choose λ_2 in equation (54). Thus, $\lambda_2 = 30°$.

Subtracting Unwanted Yaw Component Due to $\dot{\theta}_1$

From figure 5(a), the moment arm for the component $-S_2\dot{\theta}_1$ is $S_3 l_{WE}$ and the unwanted yaw velocity due to $\dot{\theta}_1$ is therefore $-S_2 S_3 l_{WE}\dot{\theta}_1$. This yaw component (which is parallel to the Z_2 axis) is subtracted from the commanded velocity V_{Z2}:

$$\tilde{V}_{Z2} = V_{Z2} - (-S_2 S_3 l_{WE}\dot{\theta}_1) \tag{55}$$

The adjusted commanded velocity component $\tilde{V}_{Z2}$ is used instead of V_{Z2} when solutions for the yawing joints, $\dot{\theta}_2$ and $\dot{\theta}_4$, are computed.

Solutions for Yawing Joints

Figure 5(b) shows the geometry that is used in forming equations for $\dot{\theta}_4$ (elbow yaw rate) and $\dot{\theta}_2$ (shoulder yaw rate). Notice that the elbow is not pitched ($\theta_3 = 0°$). Equations based on this geometry are still used even for a slightly pitched elbow.

Hand velocity components V_{T4}, V_{P4}, ***and*** V_{R4}. The translational velocity components V_{T4}, V_{P4}, and V_{R4} relative to the line of sight to the wrist (the dashed line in fig. 5(b)) are calculated by rotating the adjusted commanded velocity vector by the angle σ_2 about the Y_2 axis:

$$\begin{Bmatrix} V_{T4} \\ V_{P4} \\ V_{R4} \end{Bmatrix} = \mathrm{Rot}(Y_2, \sigma_2) \begin{Bmatrix} V_{X2} \\ V_{Y2} \\ V_{Z2} \end{Bmatrix}$$

$$= \begin{bmatrix} \cos\sigma_2 & 0 & -\sin\sigma_2 \\ 0 & 1 & 0 \\ \sin\sigma_2 & 0 & \cos\sigma_2 \end{bmatrix} \begin{Bmatrix} V_{X2} \\ V_{Y2} \\ V_{Z2} \end{Bmatrix} \tag{56}$$

The rotating (yawing) joint angle rates $\dot{\theta}_4$ and $\dot{\theta}_2$ coordinate to produce a velocity of the wrist along the dashed line in figure 5(b) that is proportional to V_{T4}. The shoulder rotate (yaw) rate $\dot{\theta}_2$ is used to produce V_{R4}. (Recall that $\dot{\theta}_1$ is used to produce a commanded pitch velocity.)

Expressions for $\cos\sigma_2$ ***and*** $\sin\sigma_2$. From figure 5(b),

$$\cos\sigma_2 = \frac{l_{ES} + l_{WE}C_4}{l_{WS}} \tag{57}$$

$$\sin\sigma_2 = \frac{l_{WE}S_4}{l_{WS}} \tag{58}$$

where (by the law of cosines)

$$l_{WS} = \sqrt{l_{ES}^2 + l_{WE}^2 + 2l_{ES}l_{WE}C_4} \tag{59}$$

The length l_{WS} varies with θ_4. Physically, the origin of the wrist axis system cannot coincide with the origin of the shoulder axis system; therefore, $l_{WS} \neq 0$.

Equation for $\dot{\theta}_4$ ***in singularity region.*** The equation for elbow yaw rate $\dot{\theta}_4$ to extend and retract the arm in proportion to commanded thrust velocity V_{T4} is

$$\dot{\theta}_4 = \begin{cases} 0 & (V_{T4} \geq 0,\ \theta_4\theta_4^* \leq 0) \\ -K_4\ V_{T4}\ \mathrm{sign}(\theta_4) & (\text{Otherwise}) \end{cases} \tag{60}$$

where θ_4^* is the value of θ_4 just before the singularity region was entered, and K_4 is a specified positive constant, which is assumed unity in this paper. Equation (60) extends the arm until the sign of θ_4 changes, which means that θ_4 passes through 0° but is still approximately 0°. The arm holds this extension (but is still free to move in pitch or yaw) until a negative V_{T4} is commanded to retract the arm, whereupon the arm retracts by yawing the elbow in a direction opposite to that with which it entered the singularity region. If an elbow bend does not suit the operator, he simply straightens and retracts the arm again.

Equation for $\dot{\sigma}_2$. The shoulder yaw angle $\dot{\theta}_2$ is used to keep the hand from moving off the line of sight from the shoulder to the wrist by nulling the angular rate $\dot{\sigma}_2$ due to $\dot{\theta}_4$. Differentiate equations (58) and (59) with respect to time and form the two expressions:

$$\dot{\sigma}_2 = \frac{l_{WE}}{\cos\sigma_2}\left(\frac{l_{WS}C_4\dot{\theta}_4 - \dot{l}_{WS}S_4}{l_{WS}^2}\right) \tag{61}$$

$$\dot{l}_{WS} = -\frac{l_{ES} l_{WE} S_4 \dot{\theta}_4}{l_{WS}} \tag{62}$$

With equations (57) and (62), equation (61) is then written as

$$\dot{\sigma}_2 = \frac{l_{WE}\dot{\theta}_4}{l_{ES} + l_{WE} C_4} \left(C_4 + \frac{l_{ES} l_{WE} S_4^2}{l_{WS}^2} \right) \tag{63}$$

Equation for $\dot{\rho}_2$. The angular rate $\dot{\rho}_2$ yaws the robot arm in response to an operator's command and is used in computing $\dot{\theta}_2$. The wrist has a moment arm l_{WS} relative to the shoulder, and the linear pitching rate V_{R4} (commanded) is the product of this moment arm and the angular pitch rate $\dot{\rho}_2$. Thus,

$$\dot{\rho}_2 = -\frac{V_{R4}}{l_{WS}} \tag{64}$$

where l_{WS} is defined in equation (59). Note that the minus sign is needed in equation (64) due to the assigned direction for positive ρ_2 (fig. 5(b)).

Equation for $\dot{\theta}_2$ ***in singularity region.*** The shoulder yaw rate $\dot{\theta}_2$ has two functions in the singularity region: (1) keep the wrist on the dashed line in figure 5(b) as $\dot{\theta}_4$ extends the hand (null $\dot{\sigma}_2$) and (2) allow the operator to yaw the arm according to $\dot{\rho}_2$. Consequently,

$$\dot{\theta}_2 = \dot{\rho}_2 - \dot{\sigma}_2 \tag{65}$$

where $\dot{\sigma}_2$ and $\dot{\rho}_2$ are given by equations (63) and (64), respectively.

Flowchart for Special Solution 1

The joints θ_2 and θ_4 play exactly the same role as the shoulder and elbow joints, respectively, in reference 6. The elbow yaw rate $\dot{\theta}_4$ is calculated by equation (60). When positive thrust is commanded, $\dot{\theta}_4$ extends the arm until θ_4 changes sign (crosses 0°), and then θ_4 is frozen (i.e., $\dot{\theta}_4 = 0$). When a negative thrust is commanded, $\dot{\theta}_4$ retracts the arm. The shoulder yaw rate $\dot{\theta}_2$ is calculated by equation (65). The elbow pitch rate $\dot{\theta}_3$ is calculated by equation (46) to extend the robot arm when positive thrust is commanded. The shoulder pitch rate $\dot{\theta}_1$ is calculated by equation (54). Figure 6 is a flowchart describing special solution 1.

Special Solution 2: Full Extension via Elbow Yaw, at ±90° Shoulder Yaw

Special solution 2 applies near the singular configuration $|\theta_2| = 90°$ and $\theta_4 = 0°$ (for example, as shown in fig. 7). In this configuration, the hand velocities produced by $\dot{\theta}_1$, $\dot{\theta}_2$, and $\dot{\theta}_4$ are all collinear. Mathematically, substitute equation (24), with $|\theta_2| = 90°$ and $\theta_4 = 0°$, into equation (35) and transform the result into (X_3, Y_3, Z_3) coordinates to get

$$\begin{Bmatrix} V_{X3} \\ V_{Y3} \\ V_{Z3} \end{Bmatrix} = \mathbf{R}_3^2 \begin{bmatrix} 0 & 0 & -S_3 l_{WE} & 0 \\ 0 & 0 & C_3 l_{WE} & 0 \\ -\text{sign}(S_2) S_3 l_{WE} & -(l_{ES} + C_3 l_{WE}) & 0 & -l_{WE} \end{bmatrix} \dot{\boldsymbol{\theta}}_{\text{arm}}$$

$$= \begin{bmatrix} 0 & 0 & 0 & 0 \\ \text{sign}(S_2) S_3 l_{WE} & l_{ES} + C_3 l_{WE} & 0 & l_{WE} \\ 0 & 0 & l_{WE} & 0 \end{bmatrix} \begin{Bmatrix} \dot{\theta}_1 \\ \dot{\theta}_2 \\ \dot{\theta}_3 \\ \dot{\theta}_4 \end{Bmatrix} \tag{66}$$

where $\mathbf{R}_3^2$ is the transpose of $\mathbf{R}_2^3$ (see appendix A). The row of zeros in the matrix in equation (66) means that it is not possible to produce V_{X3}. Therefore, there are not enough independent arm joints to apply Dubey's method, and special solution 2 is used.

Overview of Proposed Solution

When the arm enters the singularity region defined by equation (38), the commanded velocity V_{X3} is ignored. The shoulder yaw rate $\dot{\theta}_2$ is used to produce the commanded velocity V_{Y3}, and the elbow pitch rate $\dot{\theta}_3$ is used to produce the commanded velocity V_{Z3}. The joint angle rates $\dot{\theta}_1$ and $\dot{\theta}_4$ are set to zero.

Computation of the Arm Joint Angle Rates

Figure 7 shows the geometry that is involved in forming special solution 2. Equations are based on this geometry even when $|\theta_2|$ and θ_4 are slightly away from 90° and 0°, respectively. For this solution,

$$\dot{\theta}_1 = \dot{\theta}_4 = 0 \tag{67}$$

Therefore, from equation (66),

$$\dot{\theta}_2 = \frac{V_{Y3}}{l_{ES} + C_3 l_{WE}} \tag{68}$$

and

$$\dot{\theta}_3 = \frac{V_{Z3}}{l_{WE}} \tag{69}$$

Transition Back to Optimized Solution

The operator can move the arm out of the singularity region in a controlled manner by commanding V_{Y3} (i.e., $|\theta_2|$ moves away from 90°). Once outside the singularity region, both special solution 2 and the optimized solution for the entire commanded velocity are calculated. If the sign of the $\dot{\theta}_2$ from the optimized solution matches the sign of $\dot{\theta}_2$ from special solution 2, control switches back to the optimized method and the special solution computation is stopped. If these signs do not match, control with special solution 2 continues. This transition back to the optimization method is used to prevent possible oscillations in the motion of the arm.

Special Solution 3: Both Elbow Joints at ±90°

Special solution 3 applies near the singular configuration $|\theta_3| = 90°$ and $|\theta_4| = 90°$ (for example, as shown in fig. 8). In this configuration, $\dot{\theta}_3$ cannot translate the hand, and the hand velocities produced by $\dot{\theta}_1$ and $\dot{\theta}_4$ are collinear. Mathematically, substituting equation (24), with $|\theta_3| = |\theta_4| = 90°$, into equation (35) yields

$$\begin{Bmatrix} V_{X2} \\ V_{Y2} \\ V_{Z2} \end{Bmatrix} = \begin{bmatrix} 0 & -\text{sign}(S_4) l_{WE} & 0 & 0 \\ C_2 l_{ES} - \text{sign}(S_4) S_2 l_{WE} & 0 & 0 & -\text{sign}(S_3 S_4) l_{WE} \\ 0 & -l_{ES} & 0 & 0 \end{bmatrix} \dot{\boldsymbol{\theta}}_{\text{arm}} \tag{70}$$

The angle μ (shown in fig. 8) was defined in equations (26) and (27), which are written here as

$$\sin \mu = \frac{\text{sign}(S_4) l_{WE}}{l_{WS}} \tag{71}$$

$$\cos \mu = \frac{l_{ES}}{l_{WS}} \tag{72}$$

where

$$l_{WS} = \sqrt{l_{ES}^2 + l_{WE}^2} \tag{73}$$

Rotating the commanded velocity in equation (70) by the angle μ about the Y_2 axis reveals that

$$\begin{Bmatrix} V_{X\mu} \\ V_{Y\mu} \\ V_{Z\mu} \end{Bmatrix} = \mathrm{Rot}(Y_2, \mu) \begin{Bmatrix} V_{X2} \\ V_{Y2} \\ V_{Z2} \end{Bmatrix}$$

$$= \begin{bmatrix} \cos\mu & 0 & -\sin\mu \\ 0 & 1 & 0 \\ \sin\mu & 0 & \cos\mu \end{bmatrix}$$

$$\times \begin{bmatrix} 0 & -\mathrm{sign}(S_4) l_{WE} & 0 & 0 \\ C_2 l_{ES} - \mathrm{sign}(S_4) S_2 l_{WE} & 0 & 0 & -\mathrm{sign}(S_3 S_4) l_{WE} \\ 0 & -l_{ES} & 0 & 0 \end{bmatrix} \dot{\boldsymbol{\theta}}_{\mathrm{arm}}$$

$$= \begin{bmatrix} 0 & 0 & 0 & 0 \\ C_2 l_{ES} - \mathrm{sign}(S_4) S_2 l_{WE} & 0 & 0 & -\mathrm{sign}(S_3 S_4) l_{WE} \\ 0 & -l_{WS} & 0 & 0 \end{bmatrix} \dot{\boldsymbol{\theta}}_{\mathrm{arm}} \tag{74}$$

The row of zeros in the matrix in equation (74) means that it is not possible to produce $V_{X\mu}$. Therefore, there are not enough independent arm joints to apply Dubey's method and special solution 3 is used.

Overview of Proposed Solution

When the arm enters the singularity region defined by equation (39), the commanded velocity $V_{X\mu}$ is ignored. The shoulder yaw rate $\dot{\theta}_2$ is used to produce the commanded velocity $V_{Z\mu}$; and the elbow yaw rate $\dot{\theta}_4$ is used to produce the commanded velocity $V_{Y\mu}$. The pitch rates $\dot{\theta}_1$ and $\dot{\theta}_3$ are set to zero.

Computation of the Arm Joint Angle Rates

Figure 8 shows the geometry that is involved in forming special solution 3. Equations are based on this geometry even when $|\theta_3|$ and $|\theta_4|$ are slightly away from 90°. For this solution,

$$\dot{\theta}_1 = \dot{\theta}_3 = 0 \tag{75}$$

Therefore, from equation (74),

$$\dot{\theta}_2 = \frac{-V_{Z\mu}}{l_{WS}} \tag{76}$$

and

$$\dot{\theta}_4 = \frac{V_{Y\mu}}{-\mathrm{sign}(S_3 S_4) l_{WE}} \tag{77}$$

Transition Back to Optimized Solution

The operator can move the arm out of the singularity region in a controlled manner by commanding $V_{Y\mu}$ (i.e., $|\theta_4|$ moves away from 90°). Once outside the singularity region, both special solution 3 and the optimized solution for the entire commanded velocity are calculated. If the sign of $\dot{\theta}_4$ from the optimized solution matches the sign of $\dot{\theta}_4$ from special solution 3, control switches back to the optimized method and computation of the special solution stops. If these signs do not match, control using special solution 3 continues. This transition back to the optimization method is used to prevent possible oscillations in the motion of the arm.

Special Solution 4: Loss of Shoulder and Elbow Pitch

Special solution 4 applies near the singular configuration $|\theta_4| = 90°$ and $|\theta_2 + \mu| = 90°$ (for example, as shown in fig. 9). In this configuration, neither $\dot{\theta}_1$ nor $\dot{\theta}_3$ can translate the hand (at

the wrist). Mathematically, substituting equation (24), with $|\theta_4| = 90°$ and $|\theta_2 + \mu| = 90°$ (or equivalently, $C_2 l_{ES} = \text{sign}(S_4) S_2 l_{WE}$) into equation (35) yields

$$\begin{Bmatrix} V_{X2} \\ V_{Y2} \\ V_{Z2} \end{Bmatrix} = \begin{bmatrix} 0 & -\text{sign}(S_4) l_{WE} & 0 & -\text{sign}(S_4) C_3 l_{WE} \\ 0 & 0 & 0 & -\text{sign}(S_4) S_3 l_{WE} \\ 0 & -l_{ES} & 0 & 0 \end{bmatrix} \dot{\boldsymbol{\theta}}_{\text{arm}} \tag{78}$$

The velocity component which cannot be produced by the arm in this configuration is determined as follows. Multiply equation (78) by the matrix $\text{Rot}(Y_2, \mu)$ defined in equation (74) and substitute equations (71), (72), and (73) into the result to get

$$\begin{Bmatrix} V_{X\mu} \\ V_{Y\mu} \\ V_{Z\mu} \end{Bmatrix} = \begin{bmatrix} 0 & 0 & 0 & -\text{sign}(S_4) C_3 l_{WE} \cos\mu \\ 0 & 0 & 0 & -\text{sign}(S_4) S_3 l_{WE} \\ 0 & -\text{sign}(S_4) l_{WE} \sin\mu - l_{ES} \cos\mu & 0 & -\text{sign}(S_4) C_3 l_{WE} \sin\mu \end{bmatrix} \dot{\boldsymbol{\theta}}_{\text{arm}}$$

$$= \begin{bmatrix} 0 & 0 & 0 & -\text{sign}(S_4) C_3 l_{WE} \cos\mu \\ 0 & 0 & 0 & -\text{sign}(S_4) S_3 l_{WE} \\ 0 & -l_{WS} & 0 & -\text{sign}(S_4) C_3 l_{WE} \sin\mu \end{bmatrix} \dot{\boldsymbol{\theta}}_{\text{arm}} \tag{79}$$

The second column of the resulting matrix in equation (79) indicates that $\dot{\theta}_2$ can produce a velocity in the Z_μ direction only. Transforming equation (78) into the (X_3,Y_3,Z_3) coordinate system yields

$$\begin{Bmatrix} V_{X3} \\ V_{Y3} \\ V_{Z3} \end{Bmatrix} = \mathbf{R}_3^2 \begin{bmatrix} 0 & -\text{sign}(S_4) l_{WE} & 0 & -\text{sign}(S_4) C_3 l_{WE} \\ 0 & 0 & 0 & -\text{sign}(S_4) S_3 l_{WE} \\ 0 & -l_{ES} & 0 & 0 \end{bmatrix} \dot{\boldsymbol{\theta}}_{\text{arm}}$$

$$= \begin{bmatrix} 0 & -\text{sign}(S_4) C_3 l_{WE} & 0 & -\text{sign}(S_4) l_{WE} \\ 0 & l_{ES} & 0 & 0 \\ 0 & -\text{sign}(S_4) S_3 l_{WE} & 0 & 0 \end{bmatrix} \dot{\boldsymbol{\theta}}_{\text{arm}} \tag{80}$$

The fourth column of the resulting matrix in equation (80) indicates that $\dot{\theta}_4$ can produce a velocity in the X_3 direction only.

Since $\dot{\theta}_2$ can produce a velocity in the Z_μ direction only and $\dot{\theta}_4$ can produce a velocity in the X_3 direction only, the direction of the velocity which cannot be produced in the singularity $|\theta_4| = 90°$ and $|\theta_2 + \mu| = 90°$ is the direction perpendicular to Z_μ and X_3 (i.e., the direction of the cross product of Z_μ and X_3). The angle between X_μ and $Z_\mu \times X_3$ is called ν and is defined as

$$\cos\nu = \frac{-S_3}{\sqrt{S_3^2 + C_3^2 \cos^2\mu}} \tag{81}$$

$$\sin\nu = \frac{C_3 \cos\mu}{\sqrt{S_3^2 + C_3^2 \cos^2\mu}} \tag{82}$$

(The expressions for $\sin\nu$ and $\cos\nu$ are derived by expressing the cross product of Z_μ and X_3 in (X_μ,Y_μ,Z_μ) coordinates, using the dot product of X_μ and $Z_\mu \times X_3$ to define $\cos\nu$, and using the cross product of X_μ and $Z_\mu \times X_3$ to define $\sin\nu$.) Transforming equation (79) into (X_ν,Y_ν,Z_ν) coordinates then yields

$$\begin{Bmatrix} V_{X\nu} \\ V_{Y\nu} \\ V_{Z\nu} \end{Bmatrix} = \mathrm{Rot}(Z_\mu, \nu) \begin{Bmatrix} V_{X\mu} \\ V_{Y\mu} \\ V_{Z\mu} \end{Bmatrix}$$

$$= \begin{bmatrix} \cos\nu & \sin\nu & 0 \\ -\sin\nu & \cos\nu & 0 \\ 0 & 0 & 1 \end{bmatrix} \begin{bmatrix} 0 & 0 & 0 & -\mathrm{sign}(S_4) C_3 l_{WE} \cos\mu \\ 0 & 0 & 0 & -\mathrm{sign}(S_4) S_3 l_{WE} \\ 0 & -l_{WS} & 0 & -\mathrm{sign}(S_4) C_3 l_{WE} \sin\mu \end{bmatrix} \dot{\boldsymbol{\theta}}_{\mathrm{arm}}$$

$$= \begin{bmatrix} 0 & 0 & 0 & -\mathrm{sign}(S_4) l_{WE} (C_3 \cos\mu \cos\nu + S_3 \sin\nu) \\ 0 & 0 & 0 & \mathrm{sign}(S_4) l_{WE} (C_3 \cos\mu \sin\nu - S_3 \cos\nu) \\ 0 & -l_{WS} & 0 & -\mathrm{sign}(S_4) C_3 l_{WE} \sin\mu \end{bmatrix} \dot{\boldsymbol{\theta}}_{\mathrm{arm}} \tag{83}$$

Substituting equations (81) and (82) into equation (83) yields

$$\begin{Bmatrix} V_{X\nu} \\ V_{Y\nu} \\ V_{Z\nu} \end{Bmatrix} = \begin{bmatrix} 0 & 0 & 0 & 0 \\ 0 & 0 & 0 & \mathrm{sign}(S_4) l_{WE} \sqrt{S_3^2 + C_3^2 \cos^2\mu} \\ 0 & -l_{WS} & 0 & -\mathrm{sign}(S_4) C_3 l_{WE} \sin\mu \end{bmatrix} \dot{\boldsymbol{\theta}}_{\mathrm{arm}} \tag{84}$$

The row of zeros in the matrix in equation (84) means that it is not possible to produce the commanded velocity $V_{X\nu}$. Therefore, there are not enough independent arm joints to apply Dubey's method and special solution 4 is used.

Overview of Proposed Solution

When the arm enters the singularity region defined by equation (40) the commanded velocity $V_{X\nu}$ is ignored. The elbow yaw rate $\dot{\theta}_4$ is used to produce $V_{Y\nu}$, and the shoulder yaw rate $\dot{\theta}_2$ is used to produce $V_{Z\nu}$. The pitch joint angle rates $\dot{\theta}_1$ and $\dot{\theta}_3$ are set equal to zero.

Computation of the Arm Joint Angle Rates

Figure 9 shows the geometry that is involved in forming special solution 4. Equations are based on this geometry even when $|\theta_2 + \mu|$ and $|\theta_4|$ are slightly away from 90°. For this solution,

$$\dot{\theta}_1 = \dot{\theta}_3 = 0 \tag{85}$$

Therefore, from equation (84),

$$\dot{\theta}_4 = \frac{V_{Y\nu}}{\mathrm{sign}(S_4) l_{WE} \sqrt{S_3^2 + C_3^2 \cos^2\mu}} \tag{86}$$

and

$$\dot{\theta}_2 = \frac{V_{Z\nu} + \mathrm{sign}(S_4) C_3 l_{WE} \dot{\theta}_4 \sin\mu}{-l_{WS}} \tag{87}$$

Transition Back to Optimized Solution

The operator can move the arm out of the singularity region if the commanded velocity has a component in the $V_{Z\nu}$ direction (i.e., $|\theta_2 + \mu|$ moves away from 90°), or in the $V_{Y\nu}$ direction (i.e., $|\theta_4|$ moves away from 90°). Once outside the singularity region, both special solution 4 and the optimized solution for the entire commanded velocity are calculated. If the sign of $\dot{\theta}_2$ from the optimized solution matches the sign of $\dot{\theta}_2$ from special solution 4 and the sign of $\dot{\theta}_4$ from the optimized solution matches the sign of $\dot{\theta}_4$ from special solution 4, control switches back to the optimized method and calculation of the special solution is stopped. If the signs of the rates do not match, control using special solution 4 is continued. This transition back to the optimization method is used to prevent possible oscillations in the motion of the arm.

RESULTS AND DISCUSSION

A real-time computer simulation was used to evaluate the optimized and special solution resolved rate equations developed in this paper (see appendix F). The current version of the simulation runs on a DEC VAX 11/750 computer and (optionally) interfaces to a GTI POLY 2000 graphics system which animates the motions of a 3-D model of the LTM. An operator used a six-axis joystick to issue velocity commands and watched the motions of the LTM model to assess the equations. For the motions simulated, the robot hand moved as commanded and the special solution equations appeared reasonable.

Time histories of selected simulations of the LTM are presented here to add credence to the resolved rate equations and to examine use of the special solutions for the joint angle rates. The data in this paper were taken at a simulation time step of 1/16 sec.

Using Dubey's Method With Performance Criterion

The joint angle rate solution calculated with Dubey's method is a trade-off between trying to minimize the sum of the squares of the joint angle rates and trying to configure the arm to optimize a performance criterion of joint angles. The trade-off depends on a scalar weighting factor k. As $|k| \rightarrow 0$, preference is given to minimizing the rates.

The effect of different values of k is shown in figures 10, 11, and 12 for an example performance criterion (appendix C). In figure 10, $k = 0$; in figure 11, $k = -1$; and in figure 12, $k = -2$. (Negative values of k mean that the tendency is to minimize the performance criterion.) Minimizing the performance criterion tends to keep θ_2, θ_4, and θ_6 close to 0°, or away from 90° (away from singularities). The initial configuration of the arm and commanded velocity of the hand for figures 10 to 12 are listed in table III(a). The commanded velocity is exactly produced by the movement of the arm in each figure. However, as can be seen by comparing corresponding figures, the time histories of the joint angles and joint angle rates are quite different.

In figure 10, the performance criterion is ignored ($k = 0$) in the computation of a least-squares solution for the joint angle rates. In figures 10(a) and (b), the joint angles θ_2, θ_4, and θ_6 move away from 0°. The index m is 1 throughout the simulation run. The results in figure 10 were verified by a generalized matrix inverse (via singular-value decomposition).

Notice in figures 11 and 12, as k takes on the values -1 and -2, the tendency of θ_2, θ_4, and θ_6 to move away from 0° becomes more pronounced in comparison with figure 10. The index m switches from 1 to 2 and back to 1 in these figures as θ_4 moves through 0° (logic in fig. 4).

As more precedence is given to minimizing the performance criterion of joint angles, the norm of $\dot{\theta}$ increases. This is indicated in figure 13, which shows the effect of k on the time history of $\|\dot{\theta}\|$ for $k = 0$ (fig. 10), $k = -1$ (fig. 11), and $k = -2$ (fig. 12). It should be noted that, in general, the curve for $k = 0$ may not remain below the curves for other values of k, because as the joint angles change, different trajectories are being compared. However, if $k = 0$ is used anywhere on a curve generated for a nonzero value of k, a lower value of $\|\dot{\theta}\|$ will be computed in this vicinity.

Inherent Error in Special Solutions

Four special solutions for arm joint angle rates have been developed as alternatives to using a generalized inverse solution for joint angle rates when the configuration of the arm is such that Dubey's method does not apply. The reason for alternate solutions is that the generalized inverse solution can cause undesirable oscillations of the arm in these configurations and is computationally intensive. Oscillations are avoided by the special solutions, at the expense of allowing an error between the commanded velocity of the hand and that which is actually produced. *It is assumed that a human operator can compensate for this error as time progresses; however, if continuous positional accuracy is an important issue, the special solutions are not applicable.* Some examples of the error produced by the special solutions are presented.

Errors Due to Special Solution 1

Joint angles, joint angle rates, and the actual velocity of the hand for full extension of the arm using a generalized-inverse solution and using special solution 1 are shown in figures 14 and 15, respectively. The initial configuration of the arm and the commanded velocity of the hand for

figures 14 and 15 are listed in table III(b). Oscillations which occur when using a generalized inverse solution at full extension are evident in figure 14. These oscillations are due to the integration time step (1/16 sec) used in numerically integrating the joint angle rates. A reduction in the oscillations will result by decreasing the integration time step. However, use of the generalized inverse very close to arm singularities can result in sluggish arm response and compromised hand velocities.

Special solution 1 eliminates oscillations, and, as shown in figure 15(e), there is very little extraneous motion of the hand. Of the four special solutions developed in this paper, special solution 1 produces the most acceptable response of the arm. The reader should also note that the motion of the elbow upon retraction of the arm (which may be important in avoiding obstacles, for example) can be anticipated by the operator if special solution 1 is used. If further experimentation reveals that it is better to use the elbow pitch joint θ_3 (or a combination of the elbow joints θ_3 and θ_4) instead of the elbow yaw joint θ_4 to retract the arm, special solution 1 can be modified to perform the desired elbow motion. When the generalized inverse is used to retract the arm, the motion of the elbow cannot be anticipated by the operator in most cases.

Errors Due to Special Solutions 2, 3, and 4

Commanding an outward thrust of the hand when the arm is fully extended makes no sense, and thus the consequences of ignoring commanded outward thrust when the arm is fully extended (special solution 1) are slight. On the other hand, ignoring a component of the commanded velocity in other singular regions (special solutions 2, 3, and 4) can produce unfavorable errors in the motion of the arm. Fortunately, using Dubey's method tends to keep the arm out of these singular regions if the arm starts movement far enough away from the regions. This action happens because a least-squares solution for the joint angle rates attempts to keep the arm away from configurations that induce large joint angle rates.

Special solutions 2, 3, and 4 provide the operator with a means of moving the LTM in and out of singularity regions in a controlled manner and without oscillations. The solutions are computed quickly and are applicable for real-time control. However, since they can result in erroneous motion of the arm, the angles δ_2, δ_3, and δ_4—which define the spans of the singularity regions—should be made as small as practical to prevent the control program from switching to the special solutions most of the time. Some examples which characterize the nature of the errors are presented in figures 16 and 17. The initial configuration of the arm and the commanded velocity of the hand for figures 16 and 17 are listed in table III(c).

Figure 16 shows time histories of joint angles, joint angle rates, and actual velocity of the hand for motion of the LTM near the singularity associated with special solution 2 ($|\theta_2| = 90°$ and $\theta_4 = 0°$), but calculated with a generalized inverse solution. Oscillations occur as the arm passes close to the singularity, although components of the actual velocity are still in the correct proportion (the actual velocity of the hand is a scaled version of the commanded velocity due to joint angle rate scaling). Figure 17 corresponds to figure 16, except that special solution 2 is used. The arm does not oscillate, but there is significant error in the actual velocity of the hand when the control program switches to special solution 2, as shown in figure 17(e). (Recall that the component V_{X3} of the commanded velocity is ignored for special solution 2. This component is approximately equal to the commanded velocity V_Z (75 mm/sec) for this simulation.) Once the arm enters the singularity region associated with special solution 2, it remains in the region because the component of the commanded velocity which can move it out of the region—V_X in this case—is zero. An operator can compensate for such errors by simply moving the arm far enough out of the singularity region that control switches back to Dubey's method, and then commanding a different approach path to the point of interest.

Figures 18, 19, and 20 are included here to show how subtle changes in the configuration of the arm in singularity regions can vary the response of the hand. In all three figures, the arm is in the singularity associated with special solution 4 ($|\theta_2 + \mu| = 90°$ and $|\theta_4| = 90°$). Only the initial position of the elbow pitch joint (θ_3) is different in each figure. (For special solution 4, θ_3 does not translate the hand (at the wrist) so that, regardless of the value of θ_3, the hand remains at the same point in the workspace.) The commanded motion of the hand is also identical for the three figures and is expressed in base coordinates. The initial configuration of the arm and commanded velocity of the hand for figures 18, 19, and 20 are listed in table III(d).

In figure 18, the commanded velocity does not have a component in the direction ignored by special solution 4. Therefore, there is very little error in the actual velocity of the hand, as shown in figure 18(e).

Figure 19 is a time history of the response of the arm with conditions identical to those of figure 18, except that the elbow pitch joint is at 45° initially. For this simulation, a portion of the commanded velocity is in the direction which is ignored by special solution 4; thus, there is significant error in the actual velocity of the hand (fig. 19(e)) until control switches back to Dubey's method at 0.45 sec.

Figure 20 is a time history of the response of the arm with conditions identical to those of figures 18 and 19, except that the elbow pitch joint is at 85° initially. In this case, practically all the commanded velocity is in the direction which is ignored by special solution 4; thus, the hand moves very little. Therefore, the operator must command the arm to move in another direction to get it out of the singularity region before the desired motion can be accomplished.

It is emphasized that the special solutions developed in this paper are by no means the only possible approaches for coping with singular configurations of the arm in which Dubey's method does not apply. They are presented here to give a physical interpretation to the problems which occur when the arm reaches the singular configurations and are intended to represent a starting point for controlling the LTM with the assurance that real-time performance can be maintained and that damage to the hardware due to high-frequency oscillations of the arm will not occur.

CONCLUDING REMARKS

A set of optimized resolved rate equations have been developed for real-time control of the seven-degree-of-freedom Laboratory Telerobotic Manipulator (LTM). The equations, which are based on a recent innovative optimization scheme developed at the Oak Ridge National Laboratory, represent a trade-off between two solutions: (1) a least-squares solution for the joint angle rates to produce a commanded velocity of the hand and (2) a solution to minimize joint angle rates while compromisingly configuring the manipulator to satisfy a performance criterion of the joint angles.

A problem with using the scheme to formulate control equations is that it requires selecting a column of the Jacobian matrix so that the remaining six columns (or equivalently, six joint angle rates) are independent. A method for determining quickly which column to select is presented in this paper. But, such a selection is not always possible—in which case the scheme does not apply—and alternate control equations were devised.

A three-dimensional graphics model of the LTM was driven in response to velocity commands from a six-axis hand controller to assess the equations developed in this paper. For the motions simulated, the robot hand moves as commanded and the singularity fixes appear reasonable.

NASA Langley Research Center
Hampton, VA 23665-5225
August 15, 1989

APPENDIX A

MATRICES AND VECTORS ASSOCIATED WITH THE LTM

Homogeneous Transformation Matrices

Homogeneous transformation matrices are commonplace in the description of robotic manipulators. In general, the homogeneous transformation matrix from coordinate system i to coordinate system $i-1$ is (ref. 7)

$$\mathbf{A}_{i-1}^{i} = \begin{bmatrix} \cos\theta_i' & -\cos\alpha_i \sin\theta_i' & \sin\alpha_i \sin\theta_i' & a_i \cos\theta_i' \\ \sin\theta_i' & \cos\alpha_i \cos\theta_i' & -\sin\alpha_i \cos\theta_i' & a_i \sin\theta_i' \\ 0 & \sin\alpha_i & \cos\alpha_i & d_i \\ 0 & 0 & 0 & 1 \end{bmatrix} \tag{A1}$$

which is expressed in terms of Denavit-Hartenberg parameters a_i, d_i, α_i, and θ_i' (in ref. 7, θ_i replaces θ_i'). The three parameters α_i, d_i, and a_i are constants, and θ_i' is the variable joint angle. The rotational part of the transformation matrix $\mathbf{A}_i^{i-1}$ is the upper-left 3×3 submatrix denoted as

$$\mathbf{R}_{i-1}^{i} = \begin{bmatrix} \cos\theta_i' & -\cos\alpha_i \sin\theta_i' & \sin\alpha_i \sin\theta_i' \\ \sin\theta_i' & \cos\alpha_i \cos\theta_i' & -\sin\alpha_i \cos\theta_i' \\ 0 & \sin\alpha_i & \cos\alpha_i \end{bmatrix} \tag{A2}$$

The position vector associated with $\mathbf{A}_{i-1}^{i}$ is

$$\mathbf{p}_i^{i-1} = \begin{Bmatrix} a_i \cos\theta_i' \\ a_i \sin\theta_i' \\ d_i \end{Bmatrix} \tag{A3}$$

which is expressed in axis system $i-1$ and is directed from axis system $i-1$ to axis system i.

The robot's motion is usually expressed in terms of joint angles θ_i that are initially referenced to some initial position. But, the matrix $\mathbf{A}_{i-1}^{i}$ in equation (A1) is expressed in terms of the Denavit-Hartenberg joint angle θ_i'. To switch joint angle descriptions, make the substitution

$$\theta_i' = \theta_i + \beta_i \tag{A4}$$

where β_i is a constant offset bias to account for different starting positions.

Homogeneous Transformation Matrices for the LTM

The home position and axis systems for the LTM are shown in figure 2. Denavit-Hartenberg parameters for the LTM are shown in table I. For this paper, $\theta_i' = \theta_i$, except for the matrix $\mathbf{A}_5^6$, in which $\theta_6' = \theta_6 + 90°$ (i.e., $\beta_6 = 90°$, all others are zero). Note that the parameter d_7, which locates the hand axis system from the wrist, is considered zero in this paper ($l_{HW} = 0$).

Using these parameters and replacing the angles θ' with the angles θ except for θ_6', which is replaced with $\theta_6 + 90°$, the transformation matrices $\mathbf{A}_{i-1}^{i}$ become

$$\mathbf{A}_0^1 = \begin{bmatrix} C_1 & 0 & -S_1 & 0 \\ S_1 & 0 & C_1 & 0 \\ 0 & -1 & 0 & 0 \\ 0 & 0 & 0 & 1 \end{bmatrix} \tag{A5}$$

$$\mathbf{A}_1^2 = \begin{bmatrix} C_2 & 0 & S_2 & l_{ES}C_2 \\ S_2 & 0 & -C_2 & l_{ES}S_2 \\ 0 & 1 & 0 & 0 \\ 0 & 0 & 0 & 1 \end{bmatrix} \tag{A6}$$

$$\mathbf{A}_2^3 = \begin{bmatrix} C_3 & 0 & -S_3 & 0 \\ S_3 & 0 & C_3 & 0 \\ 0 & -1 & 0 & 0 \\ 0 & 0 & 0 & 1 \end{bmatrix} \tag{A7}$$

$$\mathbf{A}_3^4 = \begin{bmatrix} C_4 & 0 & S_4 & l_{WE}C_4 \\ S_4 & 0 & -C_4 & l_{WE}S_4 \\ 0 & 1 & 0 & 0 \\ 0 & 0 & 0 & 1 \end{bmatrix} \tag{A8}$$

$$\mathbf{A}_4^5 = \begin{bmatrix} C_5 & 0 & -S_5 & 0 \\ S_5 & 0 & C_5 & 0 \\ 0 & -1 & 0 & 0 \\ 0 & 0 & 0 & 1 \end{bmatrix} \tag{A9}$$

$$\mathbf{A}_5^6 = \begin{bmatrix} -S_6 & 0 & C_6 & 0 \\ C_6 & 0 & S_6 & 0 \\ 0 & 1 & 0 & 0 \\ 0 & 0 & 0 & 1 \end{bmatrix} \tag{A10}$$

$$\mathbf{A}_6^7 = \begin{bmatrix} C_7 & -S_7 & 0 & 0 \\ S_7 & C_7 & 0 & 0 \\ 0 & 0 & 1 & 0 \\ 0 & 0 & 0 & 1 \end{bmatrix} \tag{A11}$$

where C_i means $\cos\theta_i$ and S_i means $\sin\theta_i$.

Calculation of Hand-to-Base Transformation

Commanded translational velocities in the hand axis system are transformed down to the base axis system of the robot arm when controlling the LTM. Consequently, the transformation matrix from the hand axis system to the base axis system must be calculated each time the joint rates are updated. The hand-to-base transformation (the transformation from axis system seven to axis system zero in fig. 2) is the product of the seven homogeneous matrices. That is,

$$\mathbf{A}_0^7 = \mathbf{A}_0^1\mathbf{A}_1^2\mathbf{A}_2^3\mathbf{A}_3^4\mathbf{A}_4^5\mathbf{A}_5^6\mathbf{A}_6^7 \tag{A12}$$

This same transformation can be calculated in fewer operations as follows.

The rotational part of the matrix $\mathbf{A}_j^i$ is

$$\mathbf{R}_j^i = \left[\begin{array}{c|c|c} X_i & Y_i & Z_i \end{array}\right] \tag{A13}$$

where X_i, Y_i, and Z_i are the axes of coordinate system i expressed in coordinate system j. For example,

$$\mathbf{R}_0^1 = \left[\begin{array}{c|c|c} \hat{X}_1 & \hat{Y}_1 & \hat{Z}_1 \end{array}\right] \tag{A14}$$

where the caret ($\hat{}$) means that the vector is expressed in the base axis system. Therefore, from

equation (A5), the Z_1 axis expressed in base coordinates is

$$\hat{Z}_1 = \begin{Bmatrix} -S_1 \\ C_1 \\ 0 \end{Bmatrix} \tag{A15}$$

Similarly,

$$\mathbf{R}_0^2 = \mathbf{R}_0^1 \mathbf{R}_1^2 = \left[\begin{array}{c|c|c} \hat{X}_2 & \hat{Y}_2 & \hat{Z}_2 \end{array}\right] \tag{A16}$$

Multiplying the rotational parts of the matrices $\mathbf{A}_0^1$ and $\mathbf{A}_1^2$ given by equations (A5) and (A6) and substituting the result into equation (A16) yields the following expressions for the X_2 and Z_2 axes expressed in base coordinates:

$$\hat{X}_2 = \begin{Bmatrix} C_1 C_2 \\ S_1 C_2 \\ -S_2 \end{Bmatrix} \tag{A17}$$

$$\hat{Z}_2 = \begin{Bmatrix} C_1 S_2 \\ S_1 S_2 \\ C_2 \end{Bmatrix} \tag{A18}$$

The X_3 axis expressed in base coordinates is

$$\begin{aligned} \hat{X}_3 &= \mathbf{R}_0^1 \mathbf{R}_1^2 \mathbf{R}_2^3 \begin{Bmatrix} 1 \\ 0 \\ 0 \end{Bmatrix} \\ &= \left[\begin{array}{c|c|c} \hat{X}_2 & \hat{Y}_2 & \hat{Z}_2 \end{array}\right] \begin{Bmatrix} C_3 \\ S_3 \\ 0 \end{Bmatrix} \\ &= C_3 \hat{X}_2 + S_3 \hat{Y}_2 \end{aligned} \tag{A19}$$

However, Y_2 projects totally to Z_1:

$$\mathbf{R}_1^2 Y_2 = \left[\begin{array}{c|c|c} C_2 & 0 & S_2 \\ S_2 & 0 & -C_2 \\ 0 & 1 & 0 \end{array}\right] \begin{Bmatrix} 0 \\ 1 \\ 0 \end{Bmatrix} = \begin{Bmatrix} 0 \\ 0 \\ 1 \end{Bmatrix} = Z_1 \tag{A20}$$

Therefore, expressed in any common axis system, Y_2 and Z_1 are the same. Hence, $\hat{Y}_2 = \hat{Z}_1$, and equation (A19) can be written as

$$\hat{X}_3 = C_3 \hat{X}_2 + S_3 \hat{Z}_1 \tag{A21}$$

where $\hat{X}_2$ is given by equation (A17) and $\hat{Z}_1$ is given by equation (A15). The following coordinate system axes can be calculated in a manner similar to the calculation of $\hat{X}_3$:

$$\hat{Z}_3 = -S_3 \hat{X}_2 + C_3 \hat{Z}_1 \tag{A22}$$

$$\hat{X}_4 = C_4 \hat{X}_3 - S_4 \hat{Z}_2 \tag{A23}$$

$$\hat{Z}_4 = S_4\hat{X}_3 + C_4\hat{Z}_2 \tag{A24}$$

$$\hat{X}_5 = C_5\hat{X}_4 + S_5\hat{Z}_3 \tag{A25}$$

$$\hat{Z}_5 = -S_5\hat{X}_4 + C_5\hat{Z}_3 \tag{A26}$$

$$\hat{X}_6 = -S_6\hat{X}_5 - C_6\hat{Z}_4 \tag{A27}$$

$$\hat{Z}_6 = C_6\hat{X}_5 - S_6\hat{Z}_4 \tag{A28}$$

$$\hat{X}_7 = C_7\hat{X}_6 + S_7\hat{Z}_5 \tag{A29}$$

$$\hat{Y}_7 = -S_7\hat{X}_6 + C_7\hat{Z}_5 \tag{A30}$$

$$\hat{Z}_7 = \hat{Z}_6 \tag{A31}$$

The rotational part of the hand-to-base transformation is formed as

$$\mathbf{R}_0^7 = \left[\begin{array}{c|c|c} \hat{X}_7 & \hat{Y}_7 & \hat{Z}_7 \end{array}\right] \tag{A32}$$

where $\hat{X}_7$, $\hat{Y}_7$, and $\hat{Z}_7$ are calculated by equations (A15), (A17), (A18), and (A21) to (A31).

As seen in figure 2, the X_2 axis is always aligned with the shoulder-to-elbow link of the LTM. Therefore, the position vector from the origin of the base axis system to the origin of the (X_2,Y_2,Z_2) axis system expressed in base coordinates is

$$\hat{\mathbf{p}}_2^0 = l_{ES}\hat{X}_2 \tag{A33}$$

where l_{ES} is length of the elbow-to-shoulder link listed in table I, and $\hat{X}_2$ is calculated from equation (A17). Also, the X_4 axis is always aligned with the wrist-to-elbow link of the LTM. Therefore, the position vector from the origin of the (X_2,Y_2,Z_2) axis system to the origin of the (X_4,Y_4,Z_4) axis system expressed in base coordinates is

$$\hat{\mathbf{p}}_4^2 = l_{WE}\hat{X}_4 \tag{A34}$$

where l_{WE} is length of the wrist-to-elbow link listed in table I, and $\hat{X}_4$ is calculated from equation (A23). The position vector from the base axis system to the (X_4,Y_4,Z_4) axis system expressed in base coordinates is

$$\hat{\mathbf{p}}_4^0 = \hat{\mathbf{p}}_2^0 + \hat{\mathbf{p}}_4^2 \tag{A35}$$

Since in this paper the hand-to-wrist distance (l_{HW} in fig. 2) is zero,

$$\hat{\mathbf{p}}_7^0 = \hat{\mathbf{p}}_6^0 = \hat{\mathbf{p}}_5^0 = \hat{\mathbf{p}}_4^0 \tag{A36}$$

So, from equations (A32) and (A36), the hand-to-base transformation is

$$\mathbf{A}_0^7 = \left[\begin{array}{c|c} \mathbf{R}_0^7 & \hat{\mathbf{p}}_7^0 \\ - & - \\ 0 & 1 \end{array}\right] \tag{A37}$$

Equations (A32) and (A33) to (A36) may be used to compute the hand-to-base transformation matrix more efficiently than equation (A12). *Several of the vectors calculated in this appendix are also needed when computing the Jacobian matrix for the LTM as discussed in appendix D.*

APPENDIX B

EXTENDED APPLICATION OF EQUATIONS

The resolved rate equations in the main text take the robot hand velocity (at wrist) as an input and calculate joint angle rates to produce this commanded velocity. This appendix explains how to use the equations in a more general setting, namely in moving an object relative to some arbitrarily specified axis system. The equations in this appendix are based on the general control structure for one or more robot arms described in reference 8.

Reference Frames

A robot hand and an object (held by the hand) are considered as one composite body; that is, hand and object move as a single body. The object may be the hand itself. An operator specifies the location and orientation of an axis system on the composite body, called the *moving reference frame* (mrf) in reference 8. The relationship between the hand axis system and the mrf remains fixed as the robot hand moves.

An operator also specifies an axis system for his inputs, called the *control reference frame* (crf) in reference 8. Operator inputs represent the commanded velocity of the composite body (mrf), expressed in the crf. The commanded velocity is used to compute the velocity that the hand should have so that the object moves as desired.

The object axis system (mrf) plays no role other than to influence the commanded velocity. For example, in teleoperation, an operator watches the movement of an object as he makes velocity inputs to control its motion. Or, the presently known position of the object axis system may be known and a new position is desired, in which case the commanded velocity is based on a positional error.

Computing Hand Velocity To Move Object

Velocity is commanded in the crf to move the object; but, once issued, this velocity represents the velocity of the composite body (hand and object). For example, when the object rotates about a line in the control reference frame, the composite body rotates about the line with the same rotational velocity as the object. Thus, the hand must also rotate with this commanded velocity. Hence, the velocity that is used to command movement of the object can be used directly to tell the hand how to move. Toward this end, form the matrix

$$\left[\begin{array}{ccc|c} & \mathbf{R}_{\text{hand}}^{crf} & & \mathbf{p}_{crf}^{\text{hand}} \\ - & - - - & - & - - - \\ 0 & 0 & 0 & 1 \end{array}\right] = \mathbf{A}_{\text{hand}}^{crf} = \left[\mathbf{A}_{\text{base}}^{\text{hand}}\right]^{-1} \mathbf{A}_{\text{base}}^{crf} \tag{B1}$$

where the matrix $\mathbf{A}_{\text{base}}^{\text{hand}}$ is a known function of the arm configuration (joint angles), and the matrix $\mathbf{A}_{\text{base}}^{crf}$ is specified by the operator.

Since the hand and object are a composite body,

$$\omega_{\text{hand}} = \mathbf{R}_{\text{hand}}^{crf} \omega_{crf} \tag{B2}$$

where ω_{crf} is the commanded rotational velocity of the object. Then, the translational velocity of the hand is

$$\mathbf{V}_{\text{hand}} = \mathbf{R}_{\text{hand}}^{crf} \mathbf{V}_{crf} - \omega_{\text{hand}} \times \mathbf{p}_{crf}^{\text{hand}} \tag{B3}$$

where $\mathbf{V}_{crf}$ is the commanded translational velocity of the object, and $\mathbf{p}_{crf}^{\text{hand}}$ is the moment arm from the hand to the crf. The translational and rotational hand velocities, $\mathbf{V}_{\text{hand}}$ and ω_{hand}, respectively, computed in equations (B2) and (B3) are used in resolved rate equations to cause the commanded movement of the object with respect to the control reference frame.

APPENDIX C

EXAMPLE PERFORMANCE CRITERION (H(θ))

Suppose the intent is to avoid arm and wrist singularities of the LTM by keeping $|\theta_2|$, $|\theta_4|$, and $|\theta_6|$ away from 90° whenever possible. For this purpose, define the performance criterion $H(\theta)$ as

$$H(\theta) = \frac{1}{2}\left(\sin^2\theta_2 + \sin^2\theta_4 + \sin^2\theta_6\right) \tag{C1}$$

The gradient of the performance criterion is

$$\nabla H = \begin{Bmatrix} \nabla H_{arm} \\ \hline \nabla H_{wrist} \end{Bmatrix} = \begin{Bmatrix} \partial H/\partial\theta_1 \\ \partial H/\partial\theta_2 \\ \partial H/\partial\theta_3 \\ \partial H/\partial\theta_4 \\ \hline \partial H/\partial\theta_5 \\ \partial H/\partial\theta_6 \\ \partial H/\partial\theta_7 \end{Bmatrix} = \begin{Bmatrix} 0 \\ \sin\theta_2\cos\theta_2 \\ 0 \\ \sin\theta_4\cos\theta_4 \\ \hline 0 \\ \sin\theta_6\cos\theta_6 \\ 0 \end{Bmatrix} \tag{C2}$$

To keep $|\theta_2|$, $|\theta_4|$, and $|\theta_6|$ away from 90°, $H(\theta)$ is minimized; i.e., the rate-of-convergence constant k should be negative. Assume $k = -1$. In applying the performance criterion, equation (C2) is used in computing $k\nabla H$ in equation (3), $k\mathbf{J}_1\nabla H_{arm}$ in equation (15), $k\nabla H_{arm}$ and $k\mathbf{J}_3\nabla H_{wrist}$ in equation (16), and $k\nabla H_{arm}$ in equation (33).

The reader should note that when joint angle rates are optimized (with eq. (3) or (33)), the arm may continue to move even when the commanded velocities of the hand are zero. Motion will occur if a configuration of the arm can be reached which minimizes $H(\theta)$ *without moving the hand.* This action may not be desirable. To ensure that the arm does not move when the commanded velocity of the hand is zero, the rate-of-convergence constant is assigned as follows:

$$k = \begin{Bmatrix} 0 & (|\mathbf{V}| < \delta_V \text{ and } |\boldsymbol{\omega}| < \delta_\omega) \\ k & \text{(Otherwise)} \end{Bmatrix} \tag{C3}$$

where δ_V and δ_ω are small positive deadbands. The magnitude of k may also be changed to speed or slow the rate of convergence. However, large values of k can cause oscillations as the robot arm nears the joint configuration which minimizes the performance criterion (ref. 9). The maximum value of k which can be used depends on the integration time step size.

APPENDIX D

COMPUTING J_1, J_3, AND SOLUTIONS OF WRIST EQUATIONS

Joint angle rates of a robot arm cause the hand to move with velocity $\dot{x}$, described by the familiar kinematic equation

$$\dot{\mathbf{x}} = \mathbf{J}\dot{\boldsymbol{\theta}} \tag{D1}$$

If a robot has a three-axis, spherical wrist, and the hand axis system is located at the wrist, equation (D1) can be partitioned as

$$\begin{Bmatrix} \mathbf{V} \\ - \\ \boldsymbol{\omega} \end{Bmatrix} = \left[\begin{array}{c|c} \mathbf{J}_1 & 0 \\ - & - \\ \mathbf{J}_2 & \mathbf{J}_3 \end{array}\right] \begin{Bmatrix} \dot{\boldsymbol{\theta}}_{\text{arm}} \\ \hline \dot{\boldsymbol{\theta}}_{\text{wrist}} \end{Bmatrix} \tag{D2}$$

where $\mathbf{V}$ is the commanded translational velocity of the hand, $\boldsymbol{\omega}$ is the commanded rotational velocity of the hand, $\dot{\boldsymbol{\theta}}_{\text{arm}}$ is a vector of the arm joint angle rates (which translate the hand), and $\dot{\boldsymbol{\theta}}_{\text{wrist}}$ is a vector of the wrist joint angle rates.

For the LTM, $\mathbf{J}_1$ and $\mathbf{J}_2$ are 3 by 4 matrices, and $\mathbf{J}_3$ is a 3 by 3 matrix. The joint angle rate vector $\dot{\boldsymbol{\theta}}_{\text{arm}}$ is a vector of the joint angle rates $\dot{\theta}_1$, $\dot{\theta}_2$, $\dot{\theta}_3$, and $\dot{\theta}_4$; and the joint angle rate vector $\dot{\boldsymbol{\theta}}_{\text{wrist}}$ is a vector of the joint angle rates $\dot{\theta}_5$, $\dot{\theta}_6$, and $\dot{\theta}_7$. A method for real-time computation of an optimized $\dot{\boldsymbol{\theta}}$ is described in the main text. For singular configurations of the arm or wrist in which the optimization method does not apply, special solutions for $\dot{\boldsymbol{\theta}}_{\text{arm}}$ and $\dot{\boldsymbol{\theta}}_{\text{wrist}}$ are presented. Explicit computation of the matrices $\mathbf{J}_1$ and $\mathbf{J}_3$ (which is necessary when using the optimization method) is discussed in this appendix. A general method for solving wrist equations (14), (19), and (34) (when optimizing joint angle rates) and wrist equation (36) (when special solutions are used) is also presented.

Computation of J_1 in Base Axis System

The translational velocity of the robot hand is the vector sum of the translational-velocity contributions from each of the arm joint angle rates. Consequently, the Jacobian submatrix $\mathbf{J}_1$ in equation (D2) has the form:

$$\mathbf{J}_1 = \left[\begin{array}{c|c|c|c} \hat{Z}_0 \times \hat{\mathbf{p}}_7^0 & \hat{Z}_1 \times \hat{\mathbf{p}}_7^1 & \hat{Z}_2 \times \hat{\mathbf{p}}_7^2 & \hat{Z}_3 \times \hat{\mathbf{p}}_7^3 \end{array}\right] \tag{D3}$$

where the caret ($\hat{}$) signifies that the vector is expressed in the base axis system. The position vector $\hat{\mathbf{p}}_7^i$ extends from the origin of axis system i to the origin of axis system 7 (the hand axis system). Physically, $\hat{Z}_i$, whose elements are the first three entries in the third column of the homogeneous transformation matrix $\mathbf{A}_0^i$, is a unit vector directed along the rotational axis of joint $i+1$.

Referring to figure 1, the position vectors $\hat{\mathbf{p}}_7^0$ and $\hat{\mathbf{p}}_7^1$ are equal to the position vector from the base axis system to the (X_4,Y_4,Z_4) axis system:

$$\hat{\mathbf{p}}_7^0 = \hat{\mathbf{p}}_7^1 = \hat{\mathbf{p}}_4^0 \tag{D4}$$

and the position vectors $\hat{\mathbf{p}}_7^2$ and $\hat{\mathbf{p}}_7^3$ are equal to the position vector from the (X_2,Y_2,Z_2) axis system to the (X_4,Y_4,Z_4) axis system:

$$\hat{\mathbf{p}}_7^2 = \hat{\mathbf{p}}_7^3 = \hat{\mathbf{p}}_4^2 \tag{D5}$$

Therefore, the Jacobian submatrix $\mathbf{J}_1$ may be expressed as

$$\mathbf{J}_1 = \left[\begin{array}{c|c|c|c} \hat{Z}_0 \times \hat{\mathbf{p}}_4^0 & \hat{Z}_1 \times \hat{\mathbf{p}}_4^0 & \hat{Z}_2 \times \hat{\mathbf{p}}_4^2 & \hat{Z}_3 \times \hat{\mathbf{p}}_4^2 \end{array}\right] \tag{D6}$$

The position vectors $\hat{\mathbf{p}}_4^0$ and $\hat{\mathbf{p}}_4^2$ are assumed already known from equations (A35) and (A34), respectively, in appendix A. Furthermore, the vector $\hat{Z}_0$ is the first three elements of the third column of the identity matrix $\mathbf{A}_0^0$ (base axis system transformed to itself), and the remaining vectors $\hat{Z}_1$, $\hat{Z}_2$, and $\hat{Z}_3$ in equation (D6) are assumed already known from equations (A15), (A18), and (A22), respectively.

The first column of $\mathbf{J}_1$ is

$$\begin{Bmatrix} \mathbf{J}_1[1,1] \\ \mathbf{J}_1[2,1] \\ \mathbf{J}_1[3,1] \end{Bmatrix} = \hat{Z}_0 \times \hat{\mathbf{p}}_4^0 = \begin{Bmatrix} 0 \\ 0 \\ 1 \end{Bmatrix} \times \hat{\mathbf{p}}_4^0 = \begin{Bmatrix} -\hat{\mathbf{p}}_4^0[y] \\ \hat{\mathbf{p}}_4^0[x] \\ 0 \end{Bmatrix} \tag{D7}$$

The second column of $\mathbf{J}_1$ is

$$\begin{Bmatrix} \mathbf{J}_1[1,2] \\ \mathbf{J}_1[2,2] \\ \mathbf{J}_1[3,2] \end{Bmatrix} = \hat{Z}_1 \times \hat{\mathbf{p}}_4^0 = \begin{Bmatrix} -S_1 \\ C_1 \\ 0 \end{Bmatrix} \times \hat{\mathbf{p}}_4^0 = \begin{Bmatrix} C_1\hat{\mathbf{p}}_4^0[z] \\ S_1\hat{\mathbf{p}}_4^0[z] \\ -C_1\hat{\mathbf{p}}_4^0[x] - S_1\hat{\mathbf{p}}_4^0[y] \end{Bmatrix} \tag{D8}$$

The third column of $\mathbf{J}_1$ is

$$\begin{Bmatrix} \mathbf{J}_1[1,3] \\ \mathbf{J}_1[2,3] \\ \mathbf{J}_1[3,3] \end{Bmatrix} = \hat{Z}_2 \times \hat{\mathbf{p}}_4^2 = \begin{Bmatrix} \hat{Z}_2[y]\ \hat{\mathbf{p}}_4^2[z] - \hat{Z}_2[z]\ \hat{\mathbf{p}}_4^2[y] \\ \hat{Z}_2[z]\ \hat{\mathbf{p}}_4^2[x] - \hat{Z}_2[x]\ \hat{\mathbf{p}}_4^2[z] \\ \hat{Z}_2[x]\ \hat{\mathbf{p}}_4^2[y] - \hat{Z}_2[y]\ \hat{\mathbf{p}}_4^2[x] \end{Bmatrix} \tag{D9}$$

The fourth column of $\mathbf{J}_1$ is

$$\begin{Bmatrix} \mathbf{J}_1[1,4] \\ \mathbf{J}_1[2,4] \\ \mathbf{J}_1[3,4] \end{Bmatrix} = \hat{Z}_3 \times \hat{\mathbf{p}}_4^2 = \begin{Bmatrix} \hat{Z}_3[y]\ \hat{\mathbf{p}}_4^2[z] - \hat{Z}_3[z]\ \hat{\mathbf{p}}_4^2[y] \\ \hat{Z}_3[z]\ \hat{\mathbf{p}}_4^2[x] - \hat{Z}_3[x]\ \hat{\mathbf{p}}_4^2[z] \\ \hat{Z}_3[x]\ \hat{\mathbf{p}}_4^2[y] - \hat{Z}_3[y]\ \hat{\mathbf{p}}_4^2[x] \end{Bmatrix} \tag{D10}$$

Equations (D7) to (D10) are used to calculate the Jacobian submatrix $\mathbf{J}_1$ when solving equations (13) and (18) in the main text.

Computation of $\mathbf{J}_3$ in Hand Axis System

The rotational velocity of the hand contributed by the wrist is the vector sum of the three wrist joint velocities. Therefore, in equation (D2), the columns of $\mathbf{J}_3$ are the axes of rotation of the wrist joints:

$$\mathbf{J}_3 = \left[\begin{array}{c|c|c} Z_4 & Z_5 & Z_6 \end{array}\right] \tag{D11}$$

When expressed in the hand axis system, the rotational axes of the wrist are

$$Z_4 = \mathbf{R}_7^6\mathbf{R}_6^5\mathbf{R}_5^4 \begin{Bmatrix} 0 \\ 0 \\ 1 \end{Bmatrix} \tag{D12}$$

$$Z_5 = \mathbf{R}_7^6\mathbf{R}_6^5 \begin{Bmatrix} 0 \\ 0 \\ 1 \end{Bmatrix} \tag{D13}$$

$$Z_6 = \mathbf{R}_7^6 \begin{Bmatrix} 0 \\ 0 \\ 1 \end{Bmatrix} \tag{D14}$$

(See appendix A for the required rotational transformation matrices.) Expanding equations (D12) to (D14) and substituting the results into equation (D11) yield

$$\mathbf{J}_3 = \begin{bmatrix} -C_7C_6 & S_7 & 0 \\ S_7C_6 & C_7 & 0 \\ -S_6 & 0 & 1 \end{bmatrix} \tag{D15}$$

Equation (D15) is used to compute $k\mathbf{J}_3\nabla\mathrm{H}_{\mathrm{wrist}}$ in equation (16) in the main text.

Solving Wrist Equations (14), (19), (34), and (36)

Wrist equations (14), (19), (34), and (36) are all of the form

$$\boldsymbol{\gamma} - \mathbf{J}_2\dot{\boldsymbol{\Theta}}_{\mathrm{arm}} = \mathbf{J}_3\dot{\boldsymbol{\Theta}}_{\mathrm{wrist}} \tag{D16}$$

where $\boldsymbol{\gamma}$ and $\dot{\boldsymbol{\Theta}}_{\mathrm{arm}}$ are known and a solution is sought for $\dot{\boldsymbol{\Theta}}_{\mathrm{wrist}}$. In equation (14), $\boldsymbol{\gamma}$ corresponds to $\boldsymbol{\omega} - k\mathbf{J}_3\nabla\mathrm{H}_{\mathrm{wrist}}$, $\dot{\boldsymbol{\Theta}}_{\mathrm{arm}}$ corresponds to $\dot{\boldsymbol{\phi}}_{p,\mathrm{arm}} + k\nabla\mathrm{H}_{\mathrm{arm}}$, and $\dot{\boldsymbol{\Theta}}_{\mathrm{wrist}}$ corresponds to $\dot{\boldsymbol{\phi}}_{p,\mathrm{wrist}}$. In equation (19), $\boldsymbol{\gamma}$ is 0, $\dot{\boldsymbol{\Theta}}_{\mathrm{arm}}$ corresponds to $\dot{\boldsymbol{\phi}}_{h,\mathrm{arm}}$, and $\dot{\boldsymbol{\Theta}}_{\mathrm{wrist}}$ corresponds to $\dot{\boldsymbol{\phi}}_{h,\mathrm{wrist}}$. In equation (34), $\boldsymbol{\gamma}$ corresponds to $\boldsymbol{\omega}$, $\dot{\boldsymbol{\Theta}}_{\mathrm{arm}}$ corresponds to $\dot{\boldsymbol{\theta}}_{\mathrm{opt,arm}}$, and $\dot{\boldsymbol{\Theta}}_{\mathrm{wrist}}$ corresponds to $\dot{\boldsymbol{\theta}}_{\mathrm{wrist}}$. In equation (36), $\boldsymbol{\gamma}$ corresponds to $\boldsymbol{\omega}$, $\dot{\boldsymbol{\Theta}}_{\mathrm{arm}}$ corresponds to $\dot{\boldsymbol{\theta}}_{\mathrm{arm}}$, and $\dot{\boldsymbol{\Theta}}_{\mathrm{wrist}}$ corresponds to $\dot{\boldsymbol{\theta}}_{\mathrm{wrist}}$. In equations (14) and (19), $\mathbf{J}_3$ is invertible, and in equations (34) and (36), $\mathbf{J}_3$ is not invertible. A general method for computing a solution of equation (D16) (and, therefore, solutions of eqs. (14), (19), (34), and (36)), regardless of the invertibility of $\mathbf{J}_3$, is presented.

$\mathbf{J}_2\dot{\boldsymbol{\Theta}}_{\mathrm{arm}}$ in Hand Axis System

In equation (D2), the contribution of the arm joint angle rates to the rotational velocity of the hand is $\mathbf{J}_2\dot{\boldsymbol{\theta}}_{\mathrm{arm}}$. This contribution is the vector sum of the rotational velocities of the arm joints. Thus,

$$\begin{aligned}
\mathbf{J}_2\dot{\boldsymbol{\theta}}_{\mathrm{arm}} &= \left[\begin{array}{c|c|c|c} \mathbf{R}_7^0 Z_0 & \mathbf{R}_7^1 Z_1 & \mathbf{R}_7^2 Z_2 & \mathbf{R}_7^3 Z_3 \end{array}\right] \dot{\boldsymbol{\theta}}_{\mathrm{arm}} \\
&= \mathbf{R}_7^0 \begin{Bmatrix} 0 \\ 0 \\ \dot{\theta}_1 \end{Bmatrix} + \mathbf{R}_7^1 \begin{Bmatrix} 0 \\ 0 \\ \dot{\theta}_2 \end{Bmatrix} + \mathbf{R}_7^2 \begin{Bmatrix} 0 \\ 0 \\ \dot{\theta}_3 \end{Bmatrix} + \mathbf{R}_7^3 \begin{Bmatrix} 0 \\ 0 \\ \dot{\theta}_4 \end{Bmatrix} \\
&= \mathbf{R}_7^5\mathbf{R}_3^5 \left\{ \mathbf{R}_3^2 \left[\mathbf{R}_2^1 \left(\mathbf{R}_1^0 \begin{Bmatrix} 0 \\ 0 \\ \dot{\theta}_1 \end{Bmatrix} + \begin{Bmatrix} 0 \\ 0 \\ \dot{\theta}_2 \end{Bmatrix} \right) + \begin{Bmatrix} 0 \\ 0 \\ \dot{\theta}_3 \end{Bmatrix} \right] + \begin{Bmatrix} 0 \\ 0 \\ \dot{\theta}_4 \end{Bmatrix} \right\}
\end{aligned} \tag{D17}$$

Equation (D17) simply transforms the rotational rates of the arm joints to the hand axis system. The term $\mathbf{J}_2\dot{\boldsymbol{\Theta}}_{\mathrm{arm}}$ in equation (D16) (analogous to $\mathbf{J}_2\dot{\boldsymbol{\theta}}_{\mathrm{arm}}$) is therefore expressed:

$$\mathbf{J}_2\dot{\boldsymbol{\Theta}}_{\mathrm{arm}} = \mathbf{R}_7^5\mathbf{R}_3^5 \left\{ \mathbf{R}_3^2 \left[\mathbf{R}_2^1 \left(\mathbf{R}_1^0 \begin{Bmatrix} 0 \\ 0 \\ \dot{\Theta}_1 \end{Bmatrix} + \begin{Bmatrix} 0 \\ 0 \\ \dot{\Theta}_2 \end{Bmatrix} \right) + \begin{Bmatrix} 0 \\ 0 \\ \dot{\Theta}_3 \end{Bmatrix} \right] + \begin{Bmatrix} 0 \\ 0 \\ \dot{\Theta}_4 \end{Bmatrix} \right\} \tag{D18}$$

Equation (D18) is expanded by using two temporary vectors, $\boldsymbol{\gamma}_3$ and $\boldsymbol{\gamma}_5$. First, let

$$\boldsymbol{\gamma}_3 = \begin{Bmatrix} -C_3S_2\dot{\Theta}_1 + S_3\dot{\Theta}_2 \\ -C_2\dot{\Theta}_1 - \dot{\Theta}_3 \\ S_3S_2\dot{\Theta}_1 + C_3\dot{\Theta}_2 + \dot{\Theta}_4 \end{Bmatrix} \tag{D19}$$

which takes rotational rates $\dot{\Theta}_1$, $\dot{\Theta}_2$, $\dot{\Theta}_3$, and $\dot{\Theta}_4$ to axis system 3. Next, let

$$\gamma_5 = \begin{Bmatrix} C_5C_4\gamma_3[x] + C_5S_4\gamma_3[y] + S_5\gamma_3[z] \\ -S_4\gamma_3[x] + C_4\gamma_3[y] \\ -S_5C_4\gamma_3[x] - S_5S_4\gamma_3[y] + C_5\gamma_3[z] \end{Bmatrix} \tag{D20}$$

which takes γ_3 to axis system 5. Finally, compute $\mathbf{J}_2\dot{\boldsymbol{\Theta}}_{\text{arm}}$ as

$$\mathbf{J}_2\dot{\boldsymbol{\Theta}}_{\text{arm}} = \begin{Bmatrix} -C_7S_6\gamma_5[x] + C_7C_6\gamma_5[y] + S_7\gamma_5[z] \\ S_7S_6\gamma_5[x] - S_7C_6\gamma_5[y] + C_7\gamma_5[z] \\ C_6\gamma_5[x] + S_6\gamma_5[y] \end{Bmatrix} \tag{D21}$$

which takes γ_5 to the hand axis system.

Components of $\dot{\boldsymbol{\Theta}}_{\text{wrist}}$

Once $\mathbf{J}_2\dot{\boldsymbol{\Theta}}_{\text{arm}}$ is calculated, the $\dot{\boldsymbol{\Theta}}_{\text{wrist}}$ is computed by inverting $\mathbf{J}_3$:

$$\dot{\boldsymbol{\Theta}}_{\text{wrist}} = \mathbf{J}_3^{-1}\boldsymbol{\Gamma} \tag{D22}$$

where

$$\boldsymbol{\Gamma} = \boldsymbol{\gamma} - \mathbf{J}_2\dot{\boldsymbol{\Theta}}_{\text{arm}} \tag{D23}$$

The expression for the submatrix $\mathbf{J}_3$ shown in equation (D15) is easily inverted as

$$\mathbf{J}_3^{-1} = \frac{-1}{C_6}\begin{bmatrix} C_7 & -S_7 & 0 \\ -S_7C_6 & -C_7C_6 & 0 \\ C_7S_6 & -S_7S_6 & -C_6 \end{bmatrix} \tag{D24}$$

Therefore, equation (D22) can be written as the three simple scalar equations:

$$\dot{\Theta}_5 = \frac{-C_7\Gamma_x + S_7\Gamma_y}{C_6} \tag{D25}$$

$$\dot{\Theta}_6 = S_7\Gamma_x + C_7\Gamma_y \tag{D26}$$

$$\dot{\Theta}_7 = \Gamma_z + S_6\dot{\Theta}_5 \tag{D27}$$

Notice that equation (D25) has a singularity at $|\theta_6| = 90°$, which implies the same for matrix $\mathbf{J}_3$. To prevent a division by zero in equation (D25), the assignment

$$C_6 = K_6 \operatorname{sign}(C_6) \tag{D28}$$

is made whenever

$$|C_6| < K_6 \tag{D29}$$

where K_6 is an arbitrary small number (assumed 10^{-5} in this paper (ref. 10)). Rate scaling must also be employed to avoid large commanded wrist joint angle rates when using this approach.

APPENDIX E

ANALYTIC EXPRESSION FOR $\mathbf{J}_1$ IN (X_2,Y_2,Z_2) AXIS SYSTEM

From appendix D, the columns of the Jacobian submatrix $\mathbf{J}_1$ for the LTM are

$$\mathbf{J}_1 = \left[Z_0 \times \mathbf{p}_4^0 \;\middle|\; Z_1 \times \mathbf{p}_4^0 \;\middle|\; Z_2 \times \mathbf{p}_4^2 \;\middle|\; Z_3 \times \mathbf{p}_4^2 \right] \tag{E1}$$

As a convenience in the development of special solutions for singular arm configurations, $\mathbf{J}_1$ is expressed in the (X_2,Y_2,Z_2) axis system—which means the vectors Z_0, Z_1, Z_2, Z_3, $\mathbf{p}_4^0$, and $\mathbf{p}_4^2$ in equation (E1) are expressed in the (X_2,Y_2,Z_2) axis system. These vectors are (see appendix A for the necessary rotational transformation matrices)

$$Z_0 = \mathbf{R}_2^1 \mathbf{R}_1^0 \begin{Bmatrix} 0 \\ 0 \\ 1 \end{Bmatrix} = \begin{Bmatrix} -S_2 \\ 0 \\ C_2 \end{Bmatrix} \tag{E2}$$

$$Z_1 = \mathbf{R}_2^1 \begin{Bmatrix} 0 \\ 0 \\ 1 \end{Bmatrix} = \begin{Bmatrix} 0 \\ 1 \\ 0 \end{Bmatrix} \tag{E3}$$

$$Z_2 = \begin{Bmatrix} 0 \\ 0 \\ 1 \end{Bmatrix} \tag{E4}$$

$$Z_3 = \mathbf{R}_2^3 \begin{Bmatrix} 0 \\ 0 \\ 1 \end{Bmatrix} = \begin{Bmatrix} -S_3 \\ C_3 \\ 0 \end{Bmatrix} \tag{E5}$$

$$\mathbf{p}_2^0 = l_{ES} X_2 = \begin{Bmatrix} l_{ES} \\ 0 \\ 0 \end{Bmatrix} \tag{E6}$$

$$\mathbf{p}_4^2 = l_{WE} X_4 = l_{WE} \mathbf{R}_2^3 \mathbf{R}_3^4 \begin{Bmatrix} 1 \\ 0 \\ 0 \end{Bmatrix} = \begin{Bmatrix} C_4 C_3 l_{WE} \\ C_4 S_3 l_{WE} \\ -S_4 l_{WE} \end{Bmatrix} \tag{E7}$$

$$\mathbf{p}_4^0 = \mathbf{p}_2^0 + \mathbf{p}_4^2 = \begin{Bmatrix} l_{ES} + C_4 C_3 l_{WE} \\ C_4 S_3 l_{WE} \\ -S_4 l_{WE} \end{Bmatrix} \tag{E8}$$

Taking the appropriate cross products in equation (E1) gives the expression for $\mathbf{J}_1$ in the (X_2,Y_2,Z_2) axis system:

$$\mathbf{J}_1 = \begin{bmatrix} -C_4 S_3 C_2 l_{WE} & -S_4 l_{WE} & -C_4 S_3 l_{WE} & -S_4 C_3 l_{WE} \\ C_2 l_{ES} + (C_4 C_3 C_2 - S_4 S_2) l_{WE} & 0 & C_4 C_3 l_{WE} & -S_4 S_3 l_{WE} \\ -C_4 S_3 S_2 l_{WE} & -l_{ES} - C_4 C_3 l_{WE} & 0 & -C_4 l_{WE} \end{bmatrix} \tag{E9}$$

APPENDIX F

COMPUTER PROGRAM FOR RESOLVED RATE CONTROL OF THE LTM

A computer program which controls the LTM by using the optimization and special-solution resolved rate equations developed in the main text is described in a stepwise manner in this section. The commanded translational and rotational velocities of the hand are read as inputs (from a joystick, for example), and the joint angle rates necessary to produce the commanded velocities are calculated. These joint angle rates are then integrated and sent as joint angle commands to the servo controllers of the LTM. The process of reading operator inputs, calculating joint angle rates, integrating the rates, and sending the updated (desired) joint angles to the servo controllers is repeated in a continuous loop. The time between successive reads of the operator inputs (i.e., the time to complete one iteration of the loop) is denoted Δt.

Since joint angles are integrated over the time interval Δt, the angles δ_2, δ_3, δ_4, and δ_6, which determine the span of the singularity regions of special solutions, cannot have arbitrarily small values. Minimum values for these deltas are

$$\delta_{\min}[i] = \dot{\theta}_{\max}[i]\ \Delta t \tag{F1}$$

where $\dot{\theta}_{\max}[i]$ is the physical maximum (absolute value) joint angle rate which can be produced by joint i, and $\delta_{\min}[i]$ is the minimum value for δ_i. In this paper, $\dot{\theta}_{\max}[i] = 30$ deg/sec for $i = 1$ to 7, and $\Delta t = 1/16$ sec. The angles δ_2, δ_3, δ_4, and δ_6 are assumed to be 2.0°—slightly larger than their minimum values (30/16 or 1.875°).

Given that the LTM is in a known configuration $\theta(t)$ at time t, the steps necessary to calculate the next set of desired joint angles $\theta(t + \Delta t)$ at time $t + \Delta t$ are

Step 1: Calculate the hand-to-base transformation $\mathbf{A}_0^7$ and the Jacobian submatrix $\mathbf{J}_1$, expressed in base coordinates, as outlined in appendixes A and D.

Step 2: Calculate $\mathbf{V}$ and $\boldsymbol{\omega}$, which are the translational and rotational velocities, respectively, of the hand axis system, expressed in the hand axis system, as discussed in appendix B, unless these are already known as operator commands in the hand axis system. Transform $\mathbf{V}$ to base coordinates with $\mathbf{A}_0^7$ that was calculated in step 1.

Step 3: Use the logic outlined in figure 4 to determine which column of $\mathbf{J}_1$ (column m), if any, can be eliminated to form an invertible $\check{\mathbf{J}}_1$ (the equality conditions in fig. 4 should be replaced with the singularity regions defined in equations (37) to (40)). If an invertible $\check{\mathbf{J}}_1$ exists, proceed to step 4. If a singularity region has been entered, set a special solution flag to indicate that a special solution is being used. Then, calculate $\dot{\boldsymbol{\theta}}_{\text{arm}}$ using the appropriate special solution, calculate $\dot{\boldsymbol{\theta}}_{\text{wrist}}$ from equation (36) as discussed in appendix D, and go to step 8.

Step 4: If a performance criterion of joint angles is to be satisfied, calculate the gradient of the performance criterion times the weighting factor $k\nabla\text{H}$ (see appendix C for an example). Also calculate $k\mathbf{J}_1\nabla\text{H}_{\text{arm}}$ and $k\mathbf{J}_3\nabla\text{H}_{\text{wrist}}$ with the $\mathbf{J}_1$ calculated in step 1 and the expression for $\mathbf{J}_3$ (in hand coordinates) in equation (30).

Step 5: Assemble the particular and homogeneous solutions for the arm joint angle rates from equations (15) and (21) with $\dot{\phi}_{p,\text{arm}}[m] = 0$ and $\dot{\phi}_{h,\text{arm}}[m] = 1$. Cramer's rule or any other convenient method may be used to calculate $\check{\dot{\phi}}_{p,\text{arm}}$ and $\check{\dot{\phi}}_{h,\text{arm}}$.

Step 6: If $\mathbf{J}_3$ is near its singularity (eq. (32)), optimize the arm joint angle rates only and calculate the wrist joint angle rates required to produce the commanded rotational velocity of the hand (eqs. (33) and (34)). If $\mathbf{J}_3$ is not near its singularity, calculate the particular and homogeneous solutions for the wrist joint angle rates from equations (14) and (19), as discussed in appendix D, and calculate the optimized solution for the joint angle rates using equation (3).

Step 7: Check the condition of the special solution flag. If the special solution flag is not set, proceed to step 8. If the special solution flag is set, the arm has left one of the singularity regions defined in equations (37), (38), (39), and (40). If special solution 2, 3, or 4 was in use, calculate the arm joint angle rates for this special solution and then compare the appropriate arm joint angle rates of the special solution with the corresponding arm joint angle rates of the optimized solution calculated in step 6. If the signs of the corresponding rates match, reset the special solution flag, discontinue calculation of the special solution, and switch to the optimized solution. (Recall that for special solution 2, the sign of $\dot{\theta}_2$ of the special solution must match the sign of $\dot{\theta}_2$ of the optimized solution; for special solution 3, the sign of $\dot{\theta}_4$ of the special solution must match the sign of $\dot{\theta}_4$ of the optimized solution; and for special solution 4, the signs of $\dot{\theta}_2$ and $\dot{\theta}_4$ of the special solution must match the signs of $\dot{\theta}_2$ and $\dot{\theta}_4$ of the optimized solution, respectively.) If the signs of the corresponding joint angle rates do not match, calculate $\dot{\boldsymbol{\theta}}_{\text{wrist}}$ from equation (36) and continue using the special solution. If special solution 1 was in use, reset the special solution flag, discontinue calculation of the special solution, and immediately switch to the optimized solution.

Step 8: Scale the calculated joint angle rate solution, if necessary, as follows. Using the vector of physical maximum (absolute value) joint angle rates which can be produced by the joints of the robot, $\dot{\boldsymbol{\theta}}_{\max}[i]$, calculate

$$\dot{\epsilon}_i = |\dot{\theta}_i| - \dot{\theta}_{\max}[i] \tag{F2}$$

for $i = 1$ to 7. If all $\dot{\epsilon}_i$'s are less than or equal to zero, the joint angle rates do not need to be scaled. If one or more are greater than zero, find the largest positive element of $\dot{\epsilon}$—denoted $\dot{\epsilon}_j$—and scale the joint angle rates by using the corresponding $\dot{\theta}_j$ and $\dot{\theta}_{\max}[j]$ (ref. 10) as follows:

$$\dot{\theta} = \frac{\dot{\theta}_{\max}[j]}{|\dot{\theta}_j|}\,\dot{\theta} \tag{F3}$$

Equation (F3) sets $\dot{\theta}_j$ to its physical maximum rate (with the proper sign), and proportionally scales the other rates (recall that $\dot{\theta}_{\max}[j]$ is assumed 30 deg/sec for $k = 1$ to 7 in this paper).

Step 9: Integrate the scaled joint angle rates, for example, by using Euler integration,

$$\theta(t + \Delta t) = \dot{\theta}(t)\ \Delta t + \theta(t) \tag{F4}$$

or Adams-Bashforth second-order predictor integration,

$$\theta(t + \Delta t) = \frac{\Delta t}{2}\left(3\dot{\theta}(t) - \dot{\theta}(t - \Delta t)\right) + \theta(t) \tag{F5}$$

Step 10: If all the joint angles $\theta(t + \Delta t)$ are inside their corresponding physical joint angle limits, command the servo controllers of the LTM to move to the calculated joint angle positions, $\theta(t + \Delta t)$, and repeat the loop starting at step 1 with the updated joint angles. If any of the updated angles are outside their limits, do not move from the current position and repeat the loop starting at step 1 with the previous joint angle command ($\theta(t)$).

The steps outlined in this section are not computationally intensive and calculate the optimized solution (when possible) without formally computing the generalized inverse of the Jacobian matrix (which is time consuming).

REFERENCES

1. Whitney, D. E.: The Mathematics of Coordinated Control of Prosthetic Arms and Manipulators. *J. Dyn. Syst., Meas., & Control,* vol. 94, ser. G, no. 4, Dec. 1972, pp. 303–309.
2. Dubey, R. V.; Euler, J. A.; Babcock, S. M.; and Glassell, R. L.: Real-Time Implementation of a Kinematic Optimization Scheme for Seven-Degree-of-Freedom Redundant Robots With Spherical Wrists. *Proceedings of the 1988 American Control Conference,* Volume 2, IEEE Catalog No. 88CH2601-3, American Automatic Control Council, 1988, pp. 1376–1378.
3. Dubey, R. V.; Euler, J. A.; Magness, R. B.; Babcock, S. M.; and Herndon, J. N.: Robotic Control of the Seven-Degree-of-Freedom NASA Laboratory Telerobotic Manipulator. Paper presented at the NASA Conference on Space Telerobotics (Pasadena, California), Jan. 31–Feb. 2, 1989.
4. Liegeois, Alain: Automatic Supervisory Control of the Configuration and Behavior of Multibody Mechanisms. *IEEE Trans. Syst., Man, & Cybern.,* vol. SMC-7, no. 12, Dec. 1977, pp. 868–871.
5. Dubey, R. V.; Euler, J. A.; and Babcock, S. M.: An Efficient Gradient Projection Optimization Scheme for a Seven-Degree-of-Freedom Redundant Robot With Spherical Wrist. *Proceedings 1988 IEEE International Conference on Robotics and Automation,* Volume 1, IEEE Catalog No. 88CH2555-1, Computer Soc. Press, c.1988, pp. 28–36.
6. Barker, L. Keith; Houck, Jacob A.; and Carzoo, Susan W.: *Translational Control of a Graphically Simulated Robot Arm by Kinematic Rate Equations That Overcome Elbow Joint Singularity.* NASA TP-2376, 1984.
7. Fu, K. S.; Gonzalez, R. C.; and Lee, C. S. G.: *Robotics: Control, Sensing, Vision, and Intelligence.* McGraw-Hill, Inc., 1987.
8. Barker, L. K.; and Soloway, D.: Coordination of Multiple Robot Arms. *Proceedings of the Workshop on Space Telerobotics,* Volume II, G. Rodriguez, ed., JPL Publ. 87-13, Vol. II, 1987, pp. 301–306.
9. Euler, J. A.; Dubey, R. V.; Babcock, S. M.; and Hamel, W. R.: A Comparison of Two Real-Time Control Schemes for Redundant Manipulators With Bounded Joint Velocities. *Proceedings 1989 IEEE International Conference on Robotics and Automation,* Volume 1, IEEE Catalog No. 89CH2750-8, IEEE Computer Soc. Press, 1989, pp. 106–112.
10. Barker, L. Keith; Houck, Jacob A.; and Carzoo, Susan W.: *Kinematic Rate Control of Simulated Robot Hand at or Near Wrist Singularity.* NASA TP-2440, 1985.

Table I. Denavit-Hartenberg Parameters for the LTM

Joint i	a_i	d_i	α_i, deg	θ_i'
1	0	0	−90	θ_1
2	$^*l_{ES}$	0	90	θ_2
3	0	0	−90	θ_3
4	$^\dagger l_{WE}$	0	90	θ_4
5	0	0	−90	θ_5
6	0	0	90	$\theta_6 + 90°$
7	0	$^\ddagger l_{HW}$	0	θ_7

$^*l_{ES}$ = Elbow-to-shoulder distance = 23 in. (5842 mm).
$^\dagger l_{WE}$ = Wrist-to-elbow distance = 20 in. (5080 mm).
$^\ddagger l_{HW}$ = Hand-to-wrist distance = 9 in. (2286 mm).
(In the equations in the text, l_{HW} is assumed to be 0.)

Table II. Singularities Associated With the Four $\check{\mathrm{J}}_1$'s Formed by Deleting Column m of J_1

[$|\theta_3| = 180°$ and $|\theta_4| = 180°$ are not physically realizable]

Eliminated column of $\mathbf{J}_1, m$	Determinant of remaining 3 by 3 submatrix of $\mathbf{J}_1$, $\det(\check{\mathbf{J}}_1)$	Singularities
1	$-l_{ES}l_{WE}^2 C_4 S_4$	$\lvert\theta_4\rvert = 0°$ or $90°$ or $180°$
2	$-l_{ES}l_{WE}^2 C_4^2 S_3 C_2$	$\lvert\theta_2\rvert = 90°$ $\lvert\theta_3\rvert = 0°$ or $180°$ $\lvert\theta_4\rvert = 90°$
3	$l_{ES}l_{WE}S_4 C_3[l_{ES}C_2 + l_{WE}(C_4C_3C_2 - S_4S_2)]$	$\lvert\theta_2\rvert = 90°$ and $\lvert\theta_4\rvert = 0°$ or $180°$ $\lvert\theta_3\rvert = 90°$ $\lvert\theta_4\rvert = 0°$ or $180°$ $-l_{ES}C_2 = l_{WE}(C_4C_3C_2 - S_4S_2)$
4	$l_{ES}l_{WE}C_4 S_3[l_{ES}C_2 + l_{WE}(C_4C_3C_2 - S_4S_2)]$	$\lvert\theta_2\rvert = 90°$ and $\lvert\theta_4\rvert = 0°$ or $180°$ $\lvert\theta_3\rvert = 0°$ or $180°$ $\lvert\theta_4\rvert = 90°$ $-l_{ES}C_2 = l_{WE}(C_4C_3C_2 - S_4S_2)$

Table III. Initial Arm Configuration and Commanded Velocities for Figures 10 to 12 and 14 to 20

Initial configuration		Commanded velocity (a)	
(a) Figures 10, 11, and 12			
$\theta_1 = -45°$	$\theta_5 = -45°$	$V_X = 30$ mm/sec	$\omega_X = 10$ deg/sec
$\theta_2 = -45°$	$\theta_6 = -10°$	$V_Y = -30$ mm/sec	$\omega_Y = 15$ deg/sec
$\theta_3 = 45°$	$\theta_7 = 0°$	$V_Z = 0$ mm/sec	$\omega_Z = -10$ deg/sec
$\theta_4 = 10°$			
(b) Figures 14 and 15			
$\theta_1 = 10°$	$\theta_5 = 10°$	$V_X = 0$ mm/sec	$\omega_X = 0$ deg/sec
$\theta_2 = 10°$	$\theta_6 = 10°$	$V_Y = 0$ mm/sec	$\omega_Y = 0$ deg/sec
$\theta_3 = -20°$	$\theta_7 = 0°$	$V_Z = 75$ mm/sec	$\omega_Z = 0$ deg/sec
$\theta_4 = -20°$			
(c) Figures 16 and 17			
$\theta_1 = -45°$	$\theta_5 = 0°$	$V_X = 0$ mm/sec	$\omega_X = 0$ deg/sec
$\theta_2 = 85°$	$\theta_6 = 0°$	$V_Y = -50$ mm/sec	$\omega_Y = 0$ deg/sec
$\theta_3 = -45°$	$\theta_7 = 0°$	$V_Z = 75$ mm/sec	$\omega_Z = 0$ deg/sec
$\theta_4 = 11.5°$			
(d) Figures 18, 19, and 20			
$\theta_1 = 0°$	$\theta_5 = 0°$	$\hat{V}_X = 0$ mm/sec	$\hat{\omega}_X = 0$ deg/sec
$\theta_2 = 48.99°$	$\theta_6 = 0°$	$\hat{V}_Y = 0$ mm/sec	$\hat{\omega}_Y = 0$ deg/sec
[b]$\theta_3 = 0°$	$\theta_7 = 0°$	$\hat{V}_Z = -75$ mm/sec	$\hat{\omega}_Z = 0$ deg/sec
$\theta_4 = 90°$			

[a]Velocities in hand coordinates for parts (a), (b), and (c) and in base coordinates for part (d).
[b]$\theta_3 = 0°$ in figure 18; $\theta_3 = 45°$ in figure 19; $\theta_3 = 85°$ in figure 20.

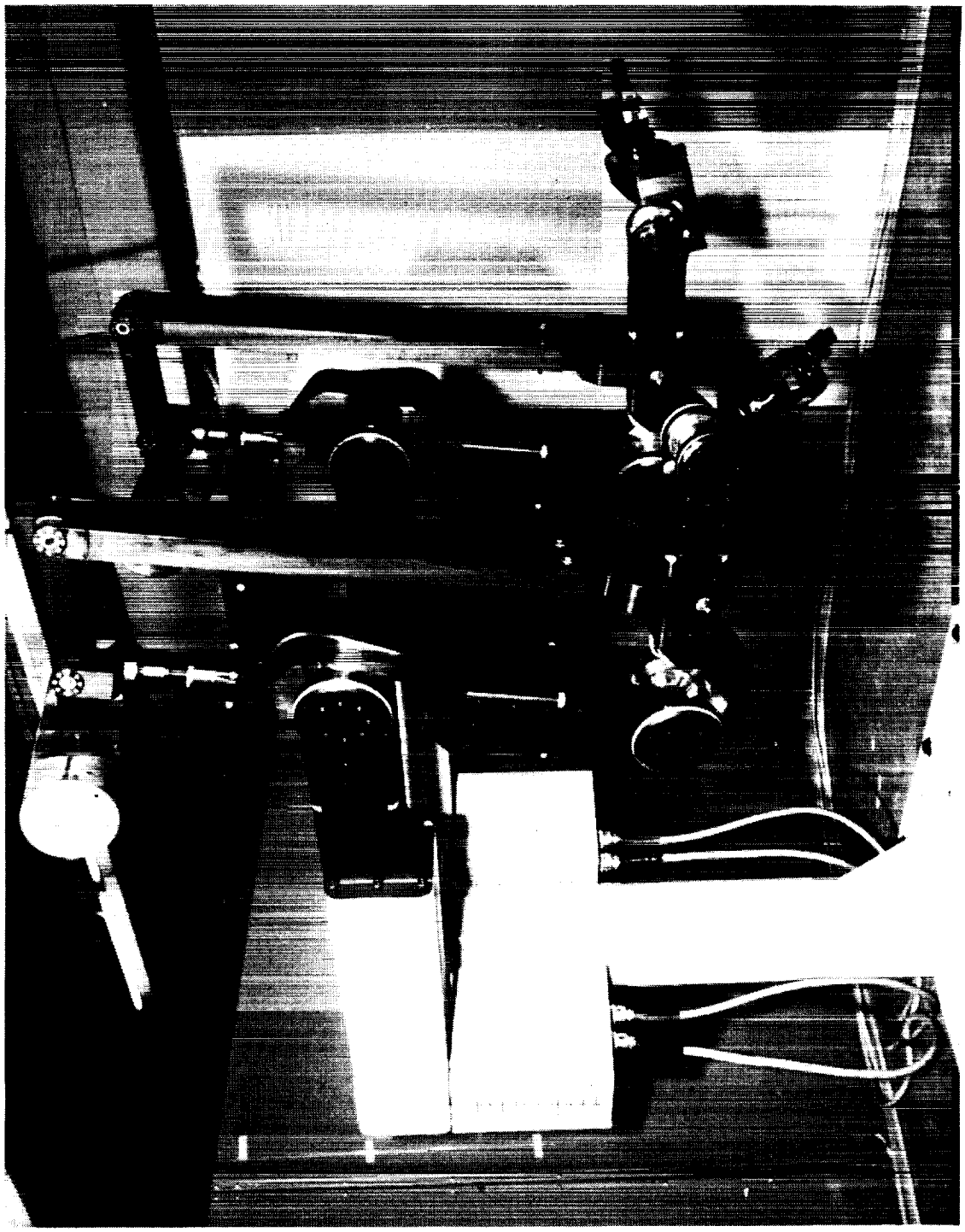

L-89-56

(a) LTM with counterbalancing; each arm has three pitch-yaw joints and wrist-roll joint.

Figure 1. Laboratory Telerobotic Manipulator (LTM).

(b) Pitch-yaw joint.

Figure 1. Concluded.

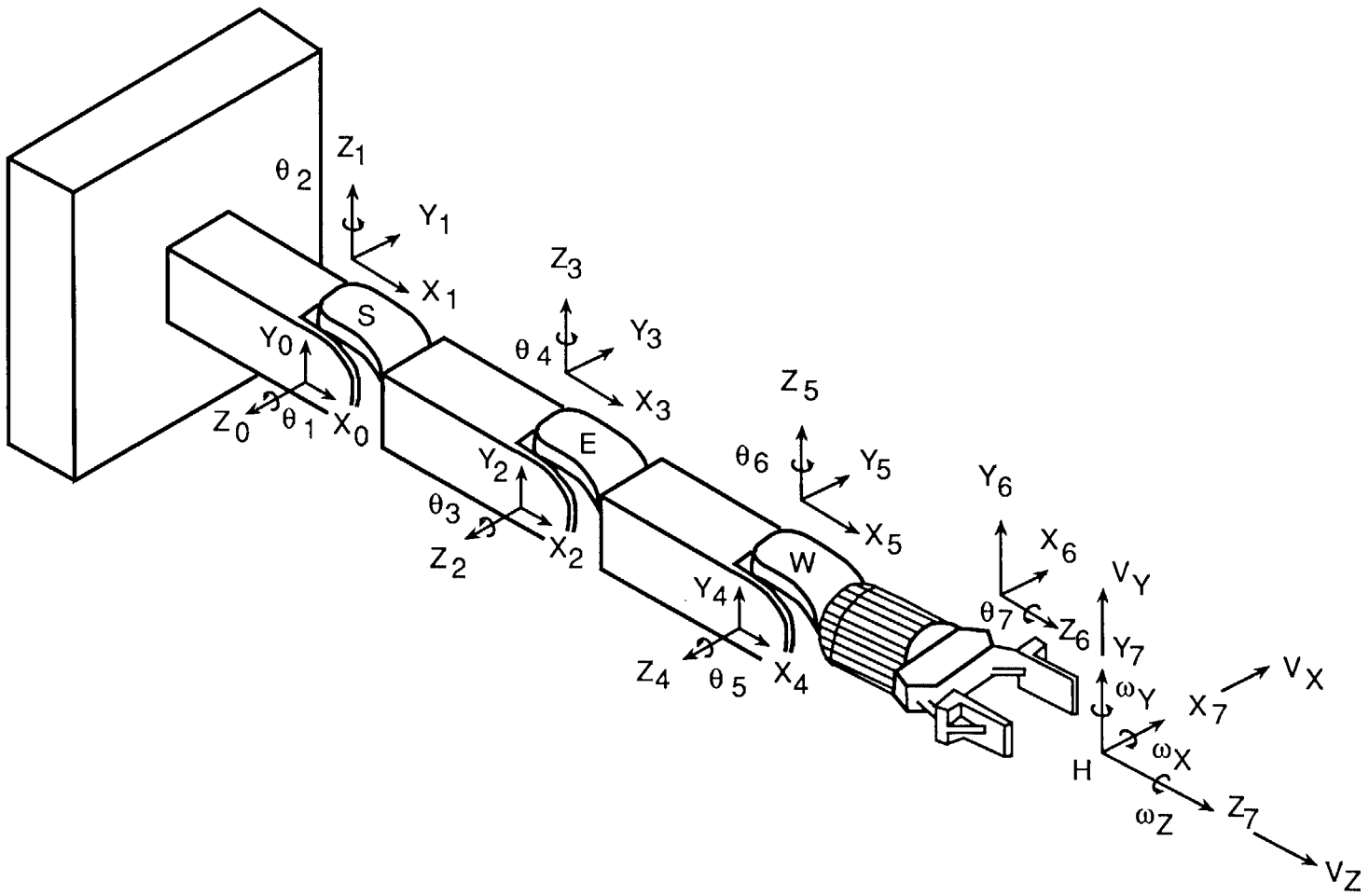

Figure 2. Initial position of robot arm, joint axis systems, and commanded robot hand velocities.

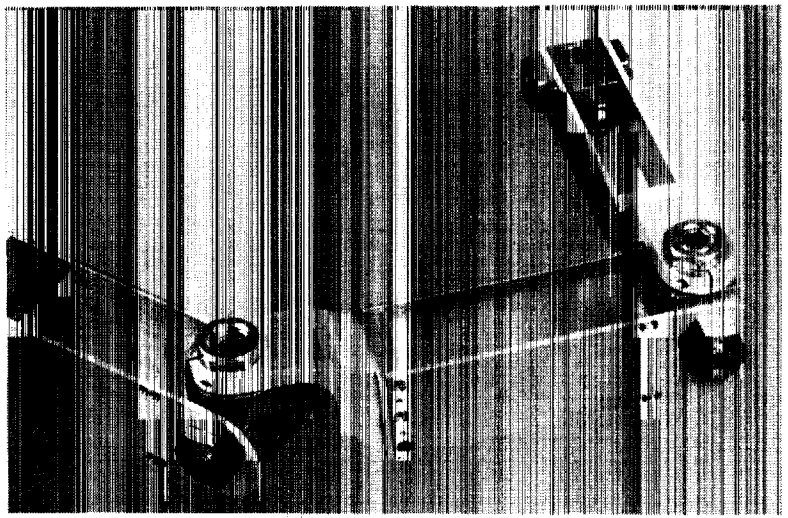

L-89-5107

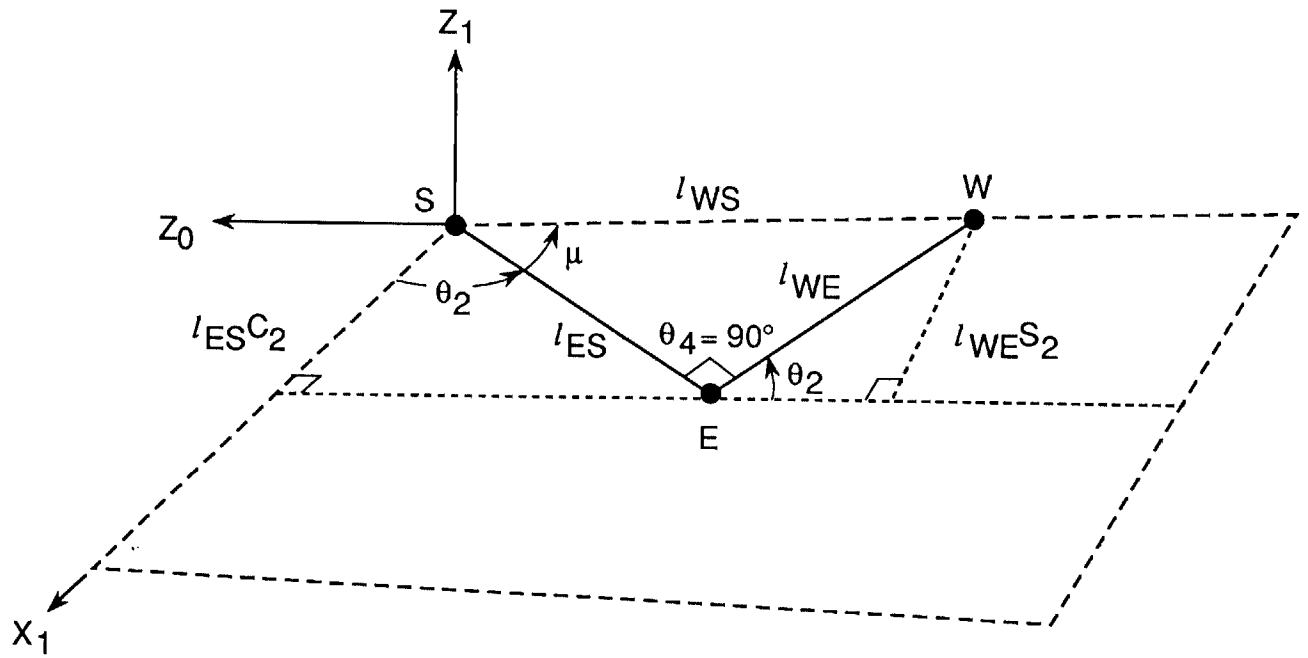

Figure 3. Geometry for robot arm in plane of Z_0 and X_1 with wrist on $-Z_0$. $\theta_4 = 90°$; $\theta_2 + \mu = 90°$.

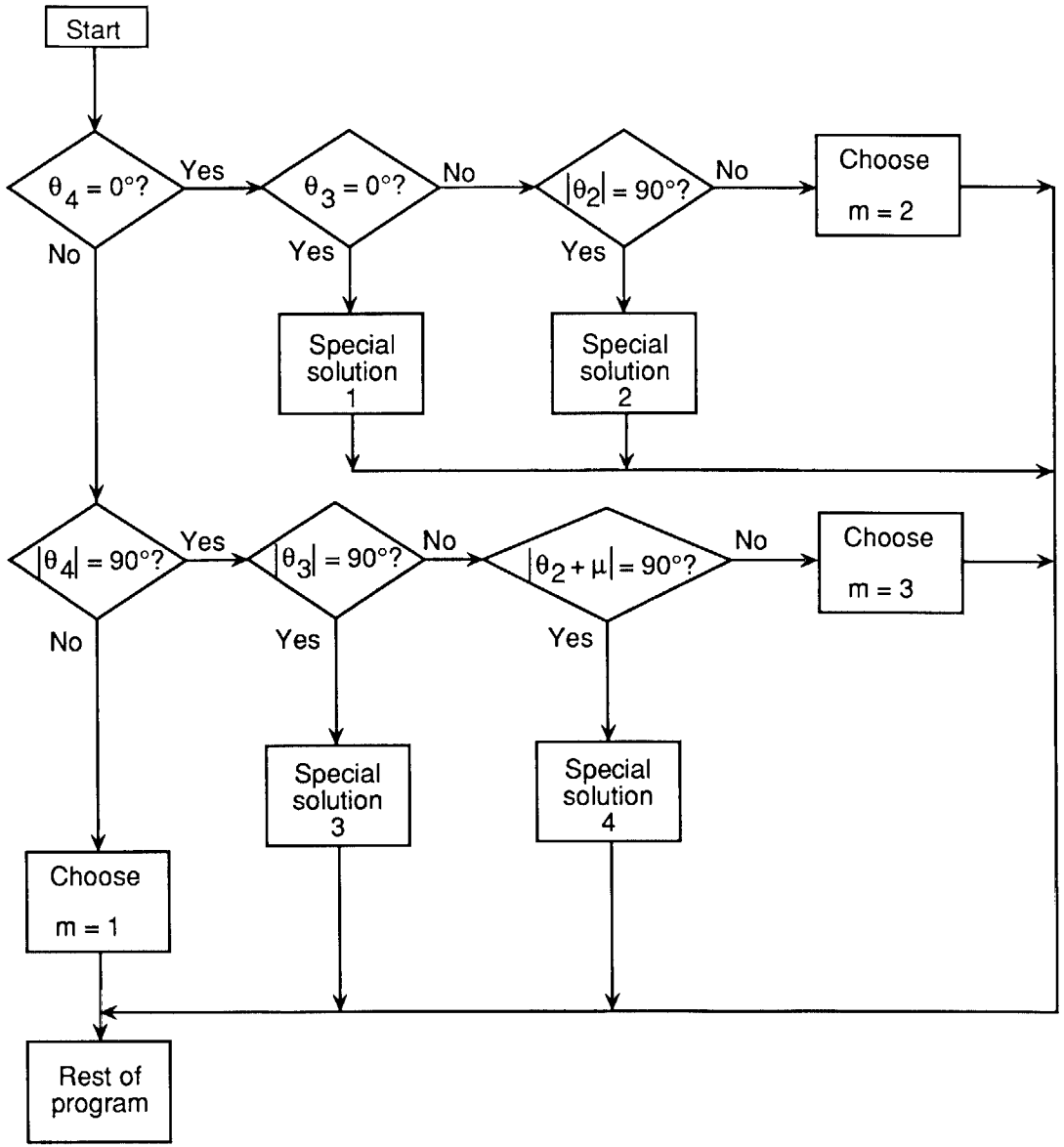

Figure 4. Choosing component m for setting $\dot{\phi}_{p,\mathrm{arm}}[m] = 0$ and $\dot{\phi}_{h,\mathrm{arm}}[m] = 1$ in Dubey's method or identifying special solutions.

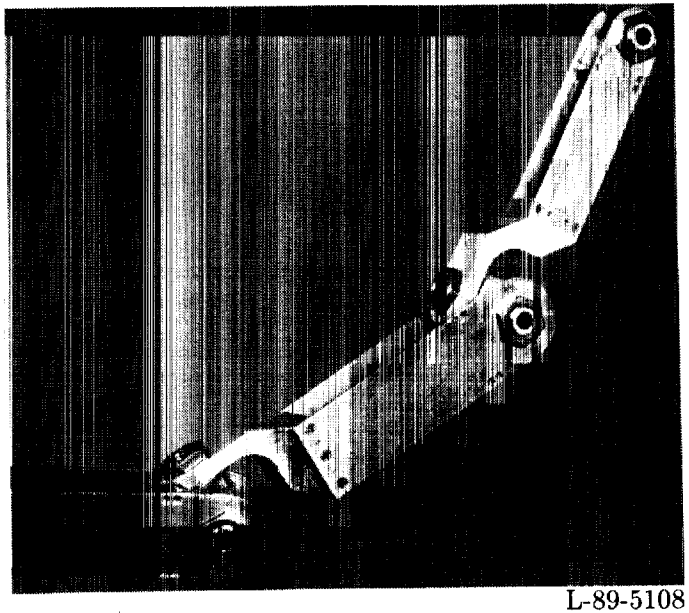

L-89-5108

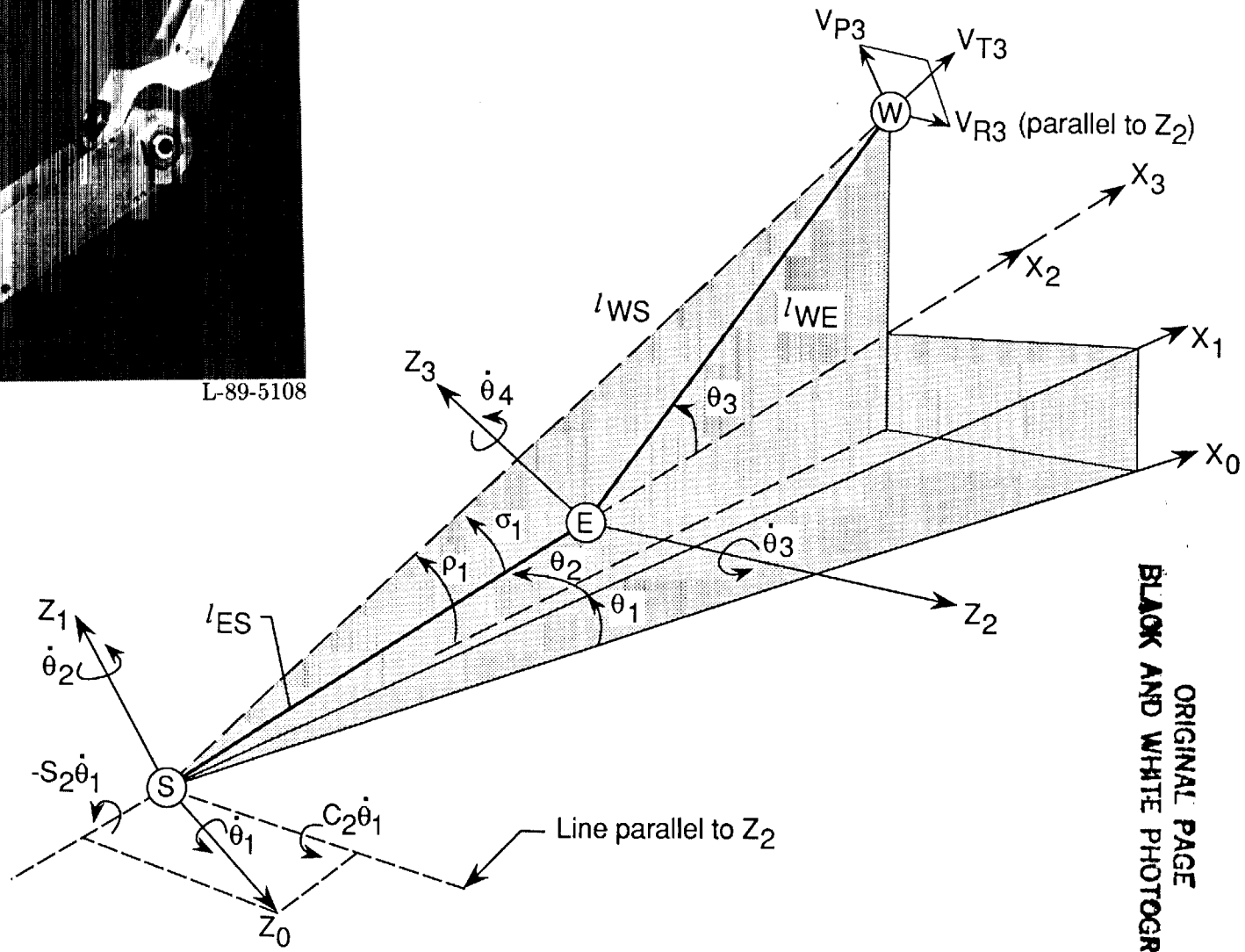

(a) Elbow is not yawed; $\theta_4 = 0°$.

Figure 5. Geometry for special solution 1: full extension via elbow pitch and elbow yaw.

L-89-4719

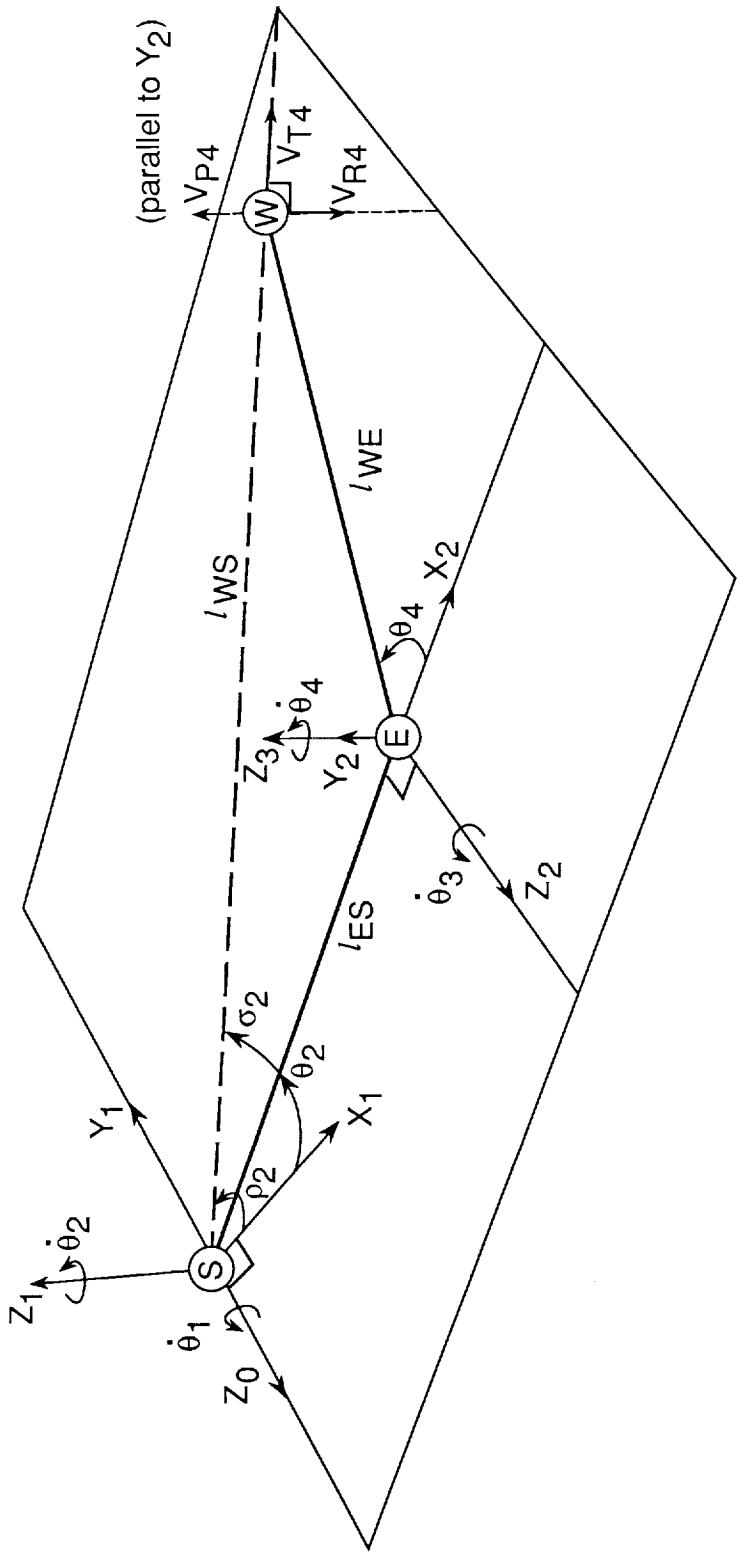

(b) Elbow is not pitched; $\theta_3 = 0°$.

Figure 5. Concluded.

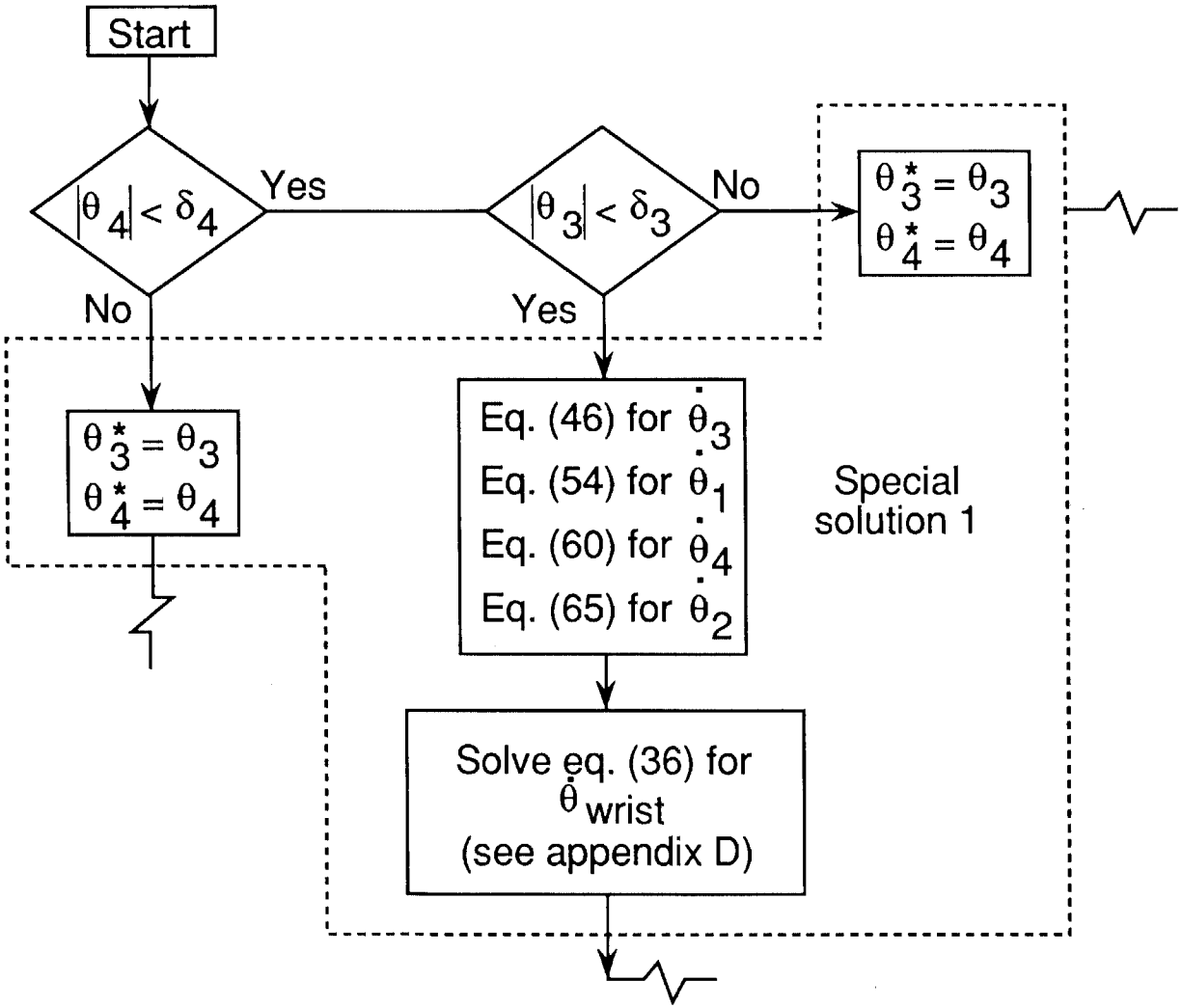

Figure 6. Flowchart for special solution 1.

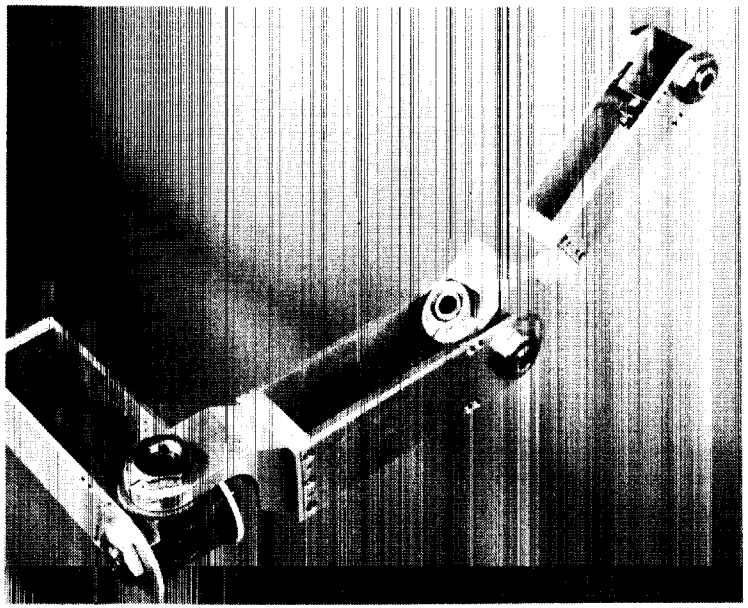

L-89-4720

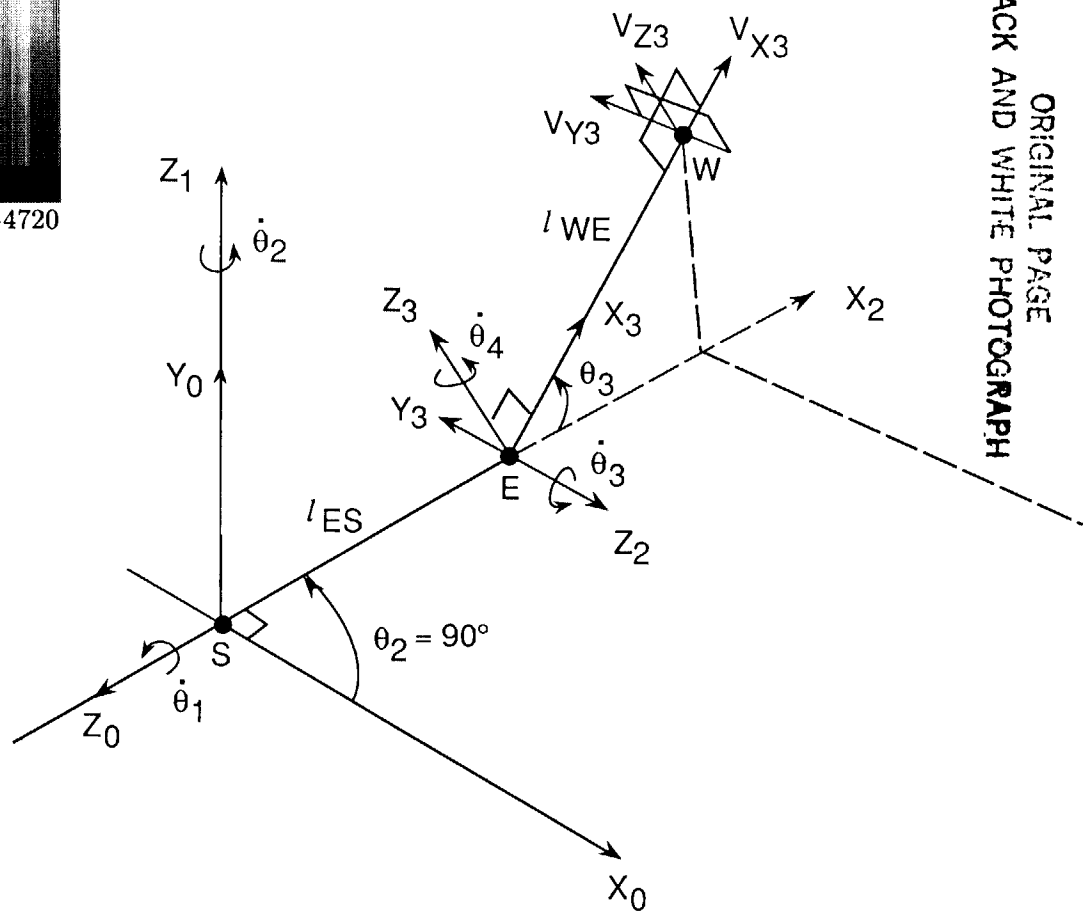

ORIGINAL PAGE
BLACK AND WHITE PHOTOGRAPH

Figure 7. Geometry for special solution 2: full extension via elbow yaw, at ±90° shoulder yaw. $\theta_1 = 0°$.

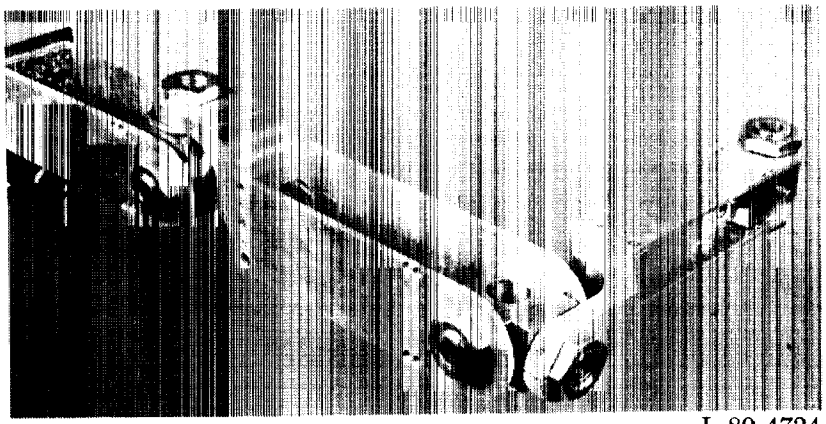

L-89-4724

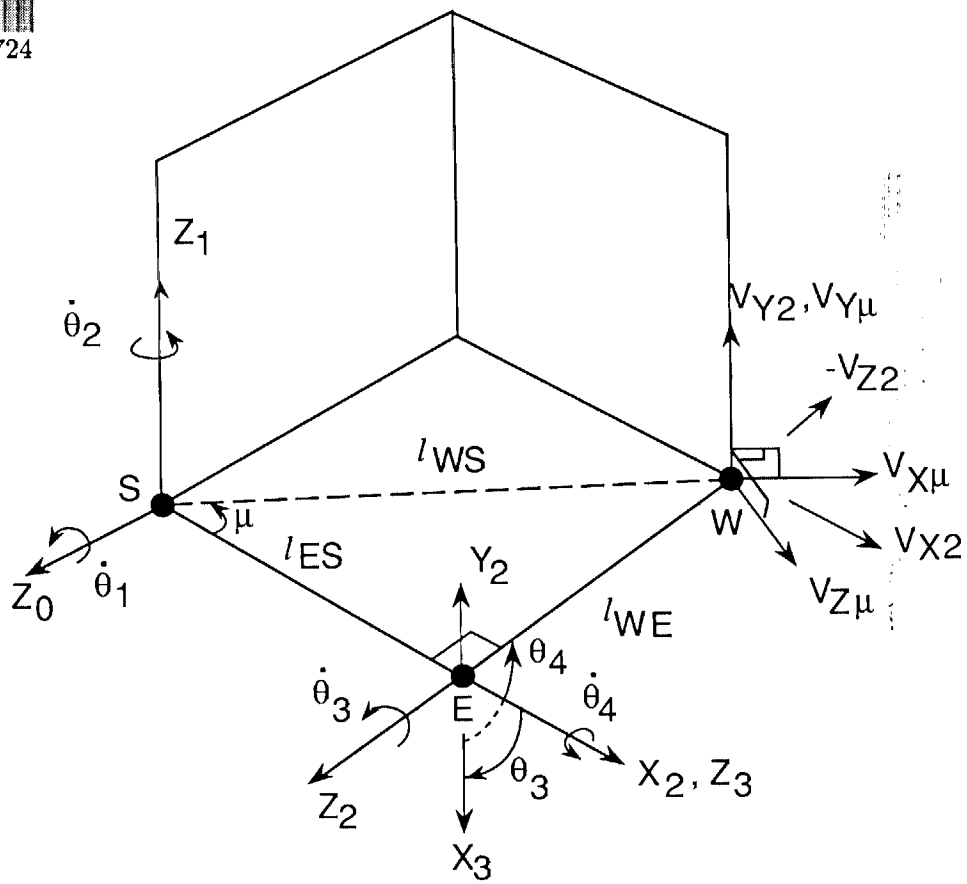

Figure 8. Geometry for special solution 3: both elbow joints at ±90°. $\theta_3 = -90°$; $\theta_4 = 90°$.

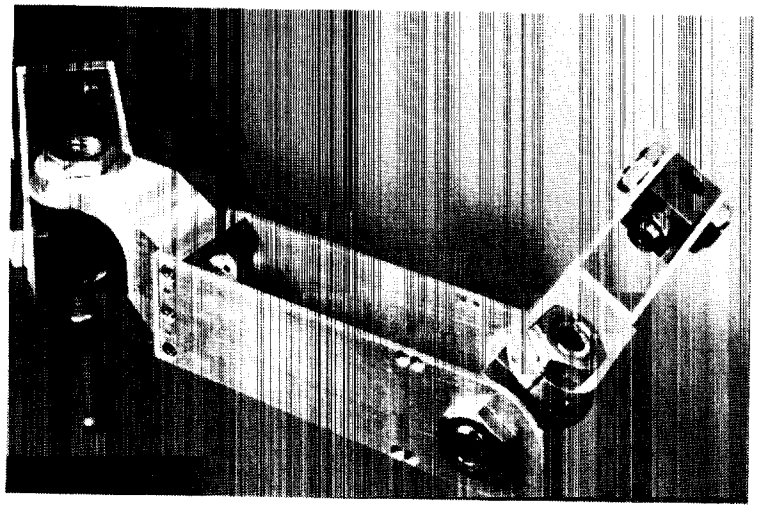

L-89-4722

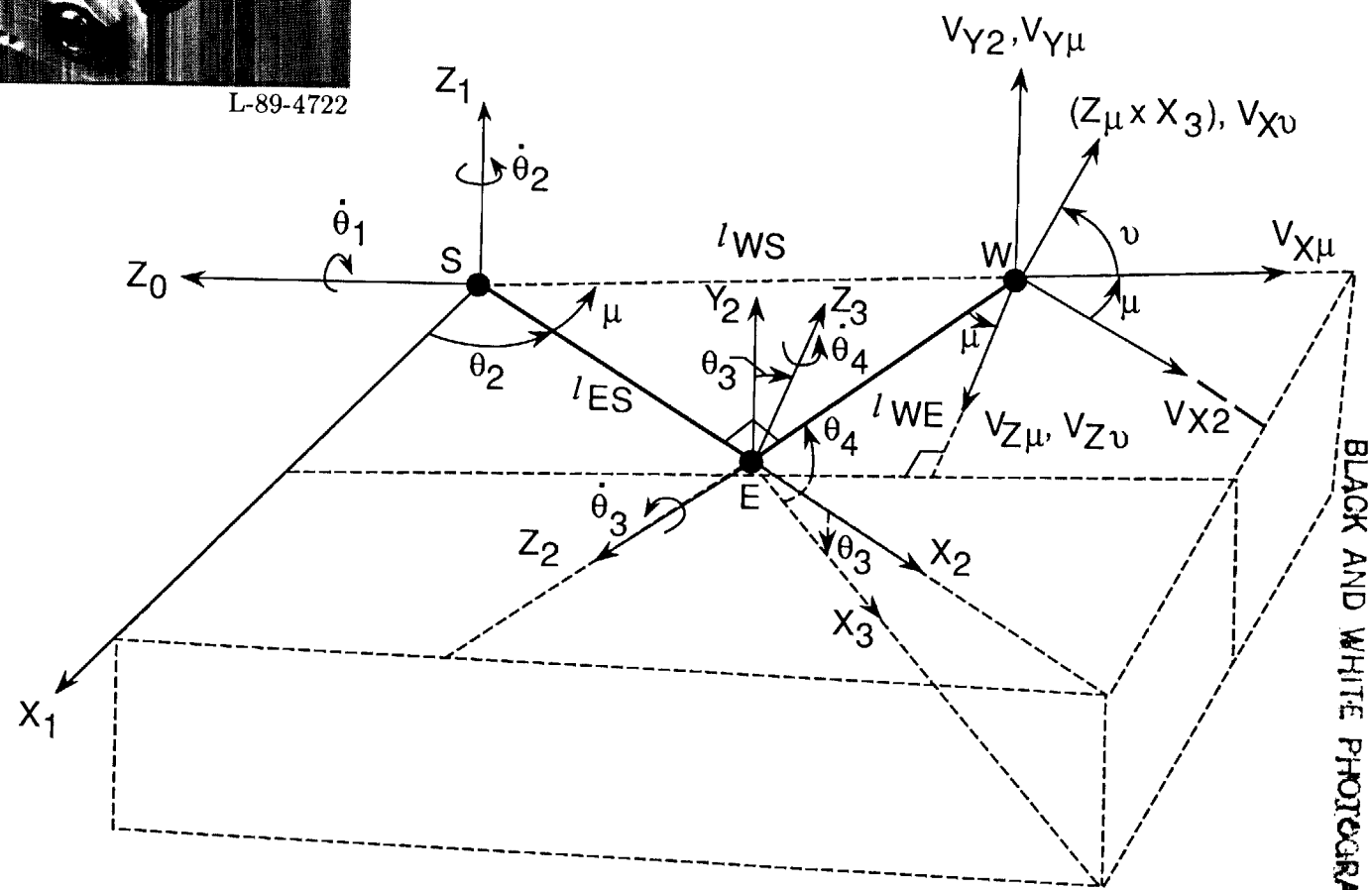

Figure 9. Geometry for special solution 4: loss of shoulder and elbow pitch. $|\theta_4| = 90°$; $|\theta_2 + \mu| = 90°$; $\theta_2 + \mu = 90°$; $\theta_3 = -30°$; $\theta_4 = 90°$.

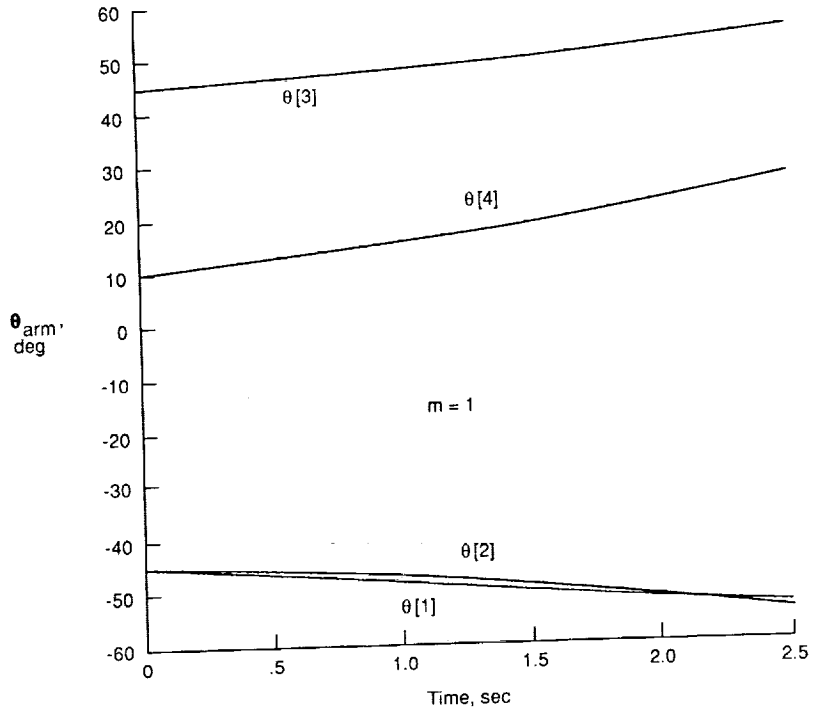

(a) Arm joint angles.

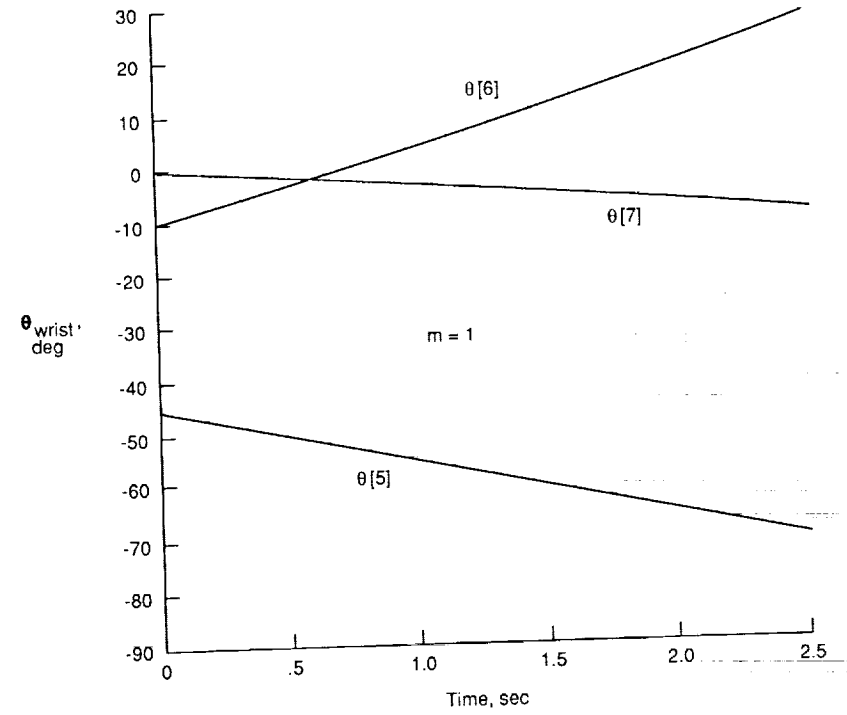

(b) Wrist joint angles.

Figure 10. Motion of arm using Dubey's method with no performance criterion, $k = 0$.

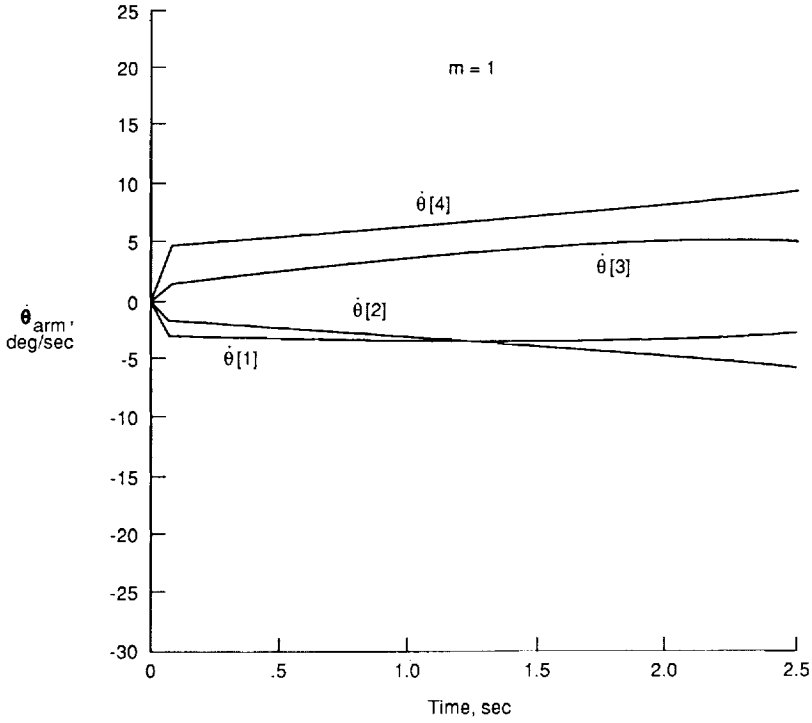

(c) Arm joint angle rates.

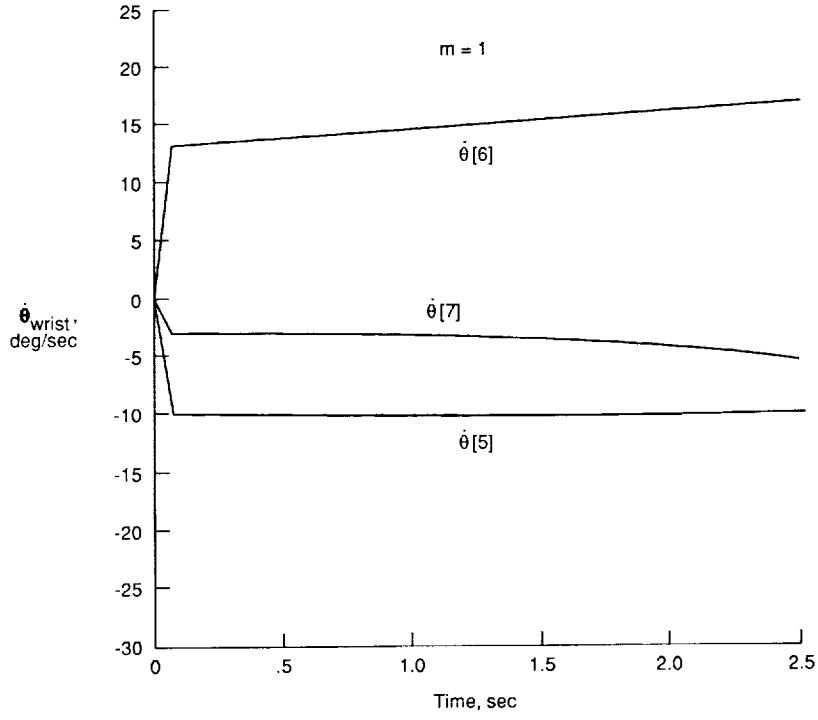

(d) Wrist joint angle rates.

Figure 10. Concluded.

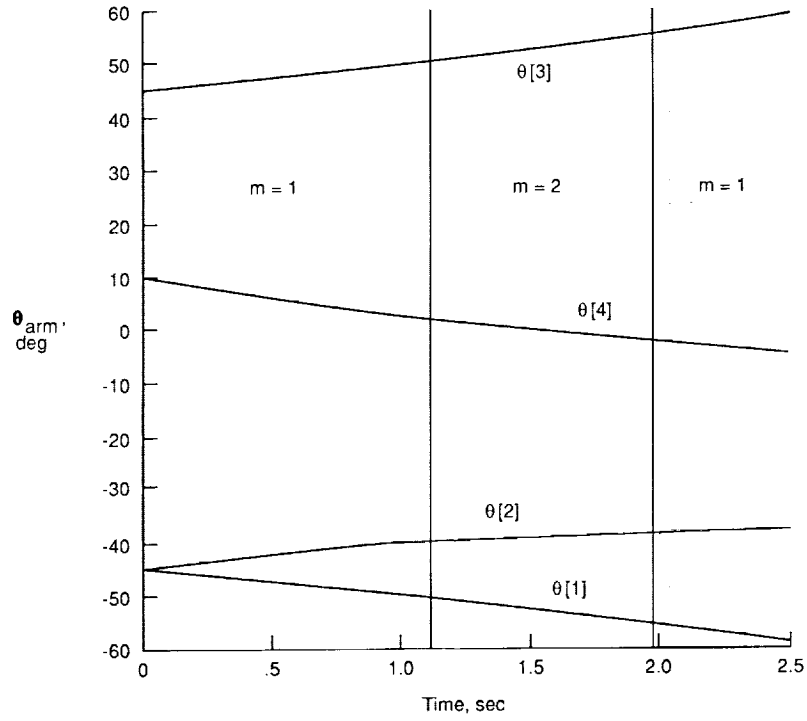

(a) Arm joint angles.

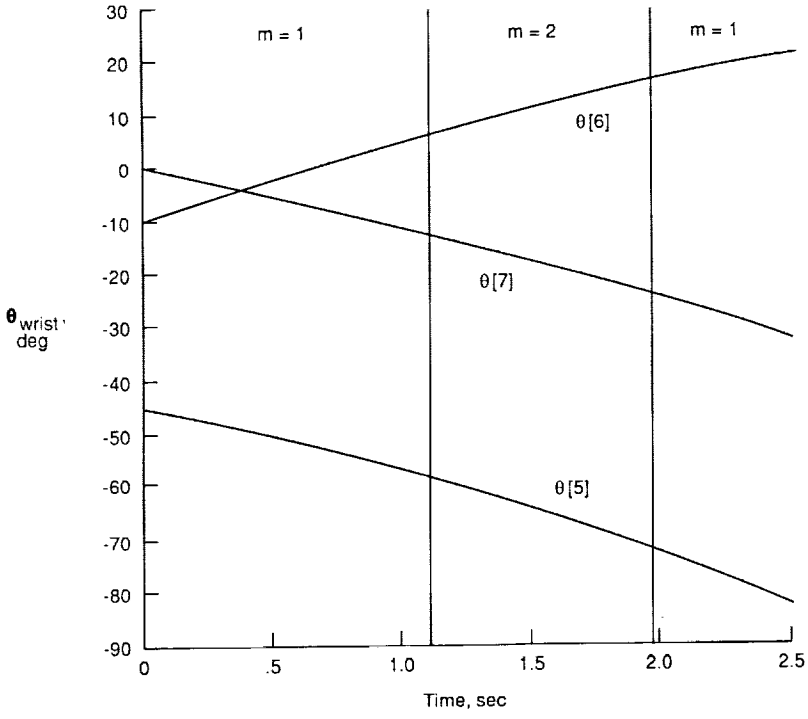

(b) Wrist joint angles.

Figure 11. Motion of arm using Dubey's method and example performance criterion in appendix C with $k = -1$.

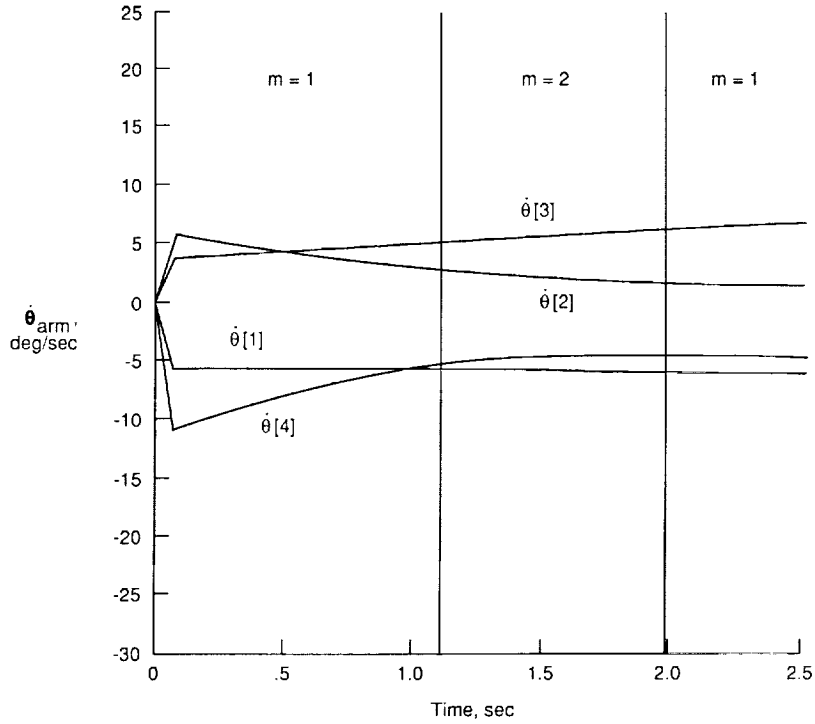

(c) Arm joint angle rates.

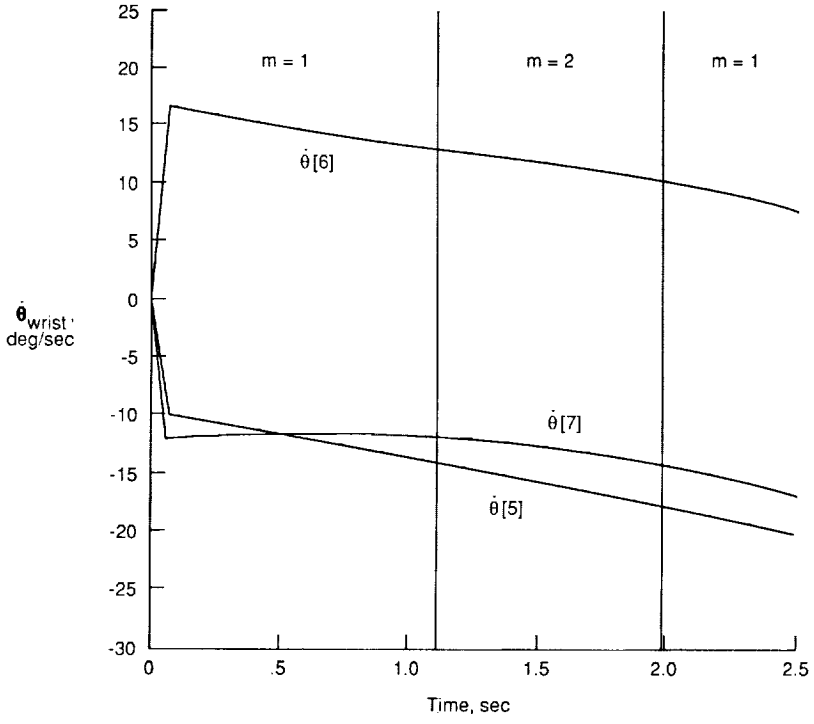

(d) Wrist joint angle rates.

Figure 11. Concluded.

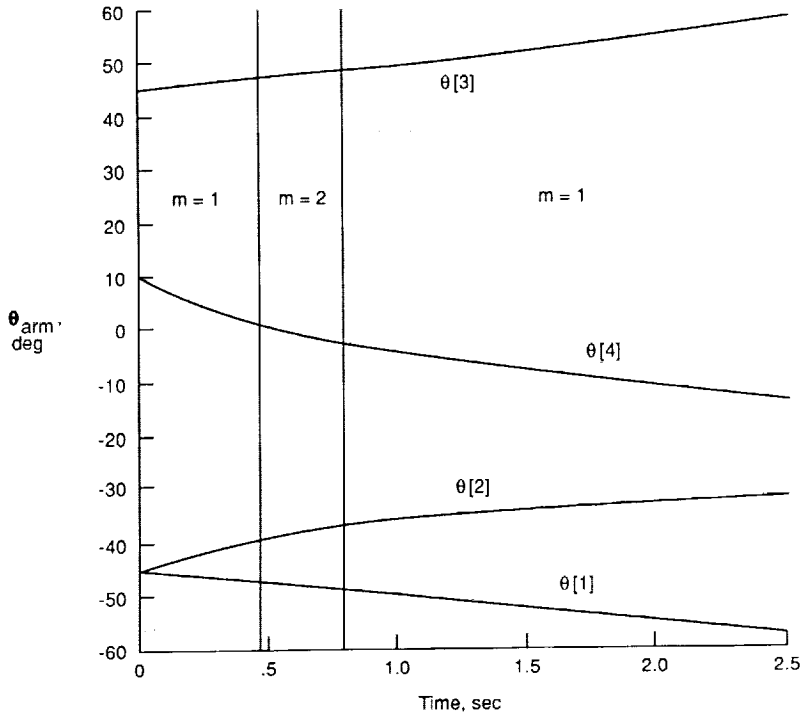

(a) Arm joint angles.

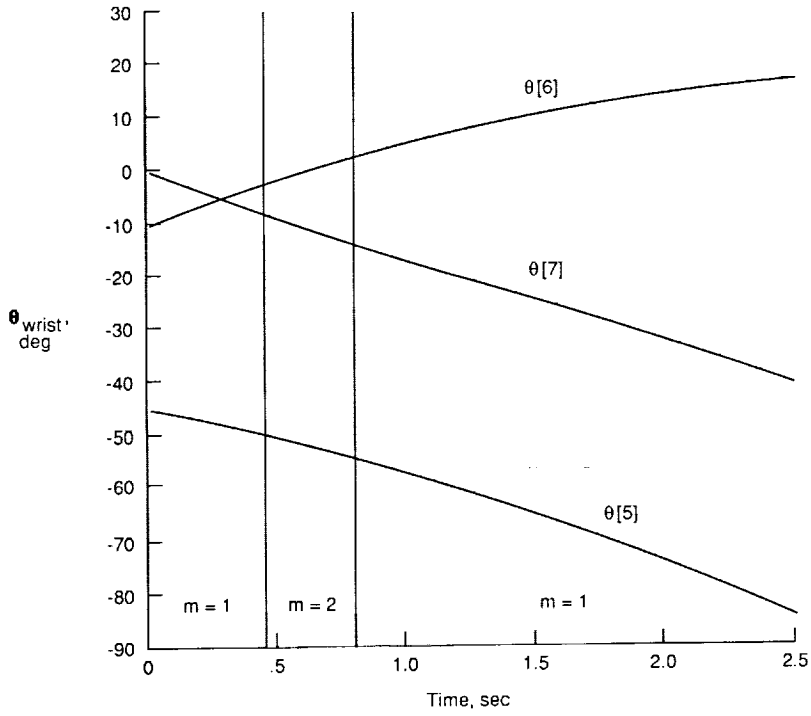

(b) Wrist joint angles.

Figure 12. Motion of arm using Dubey's method and example performance criterion in appendix C with $k = -2$.

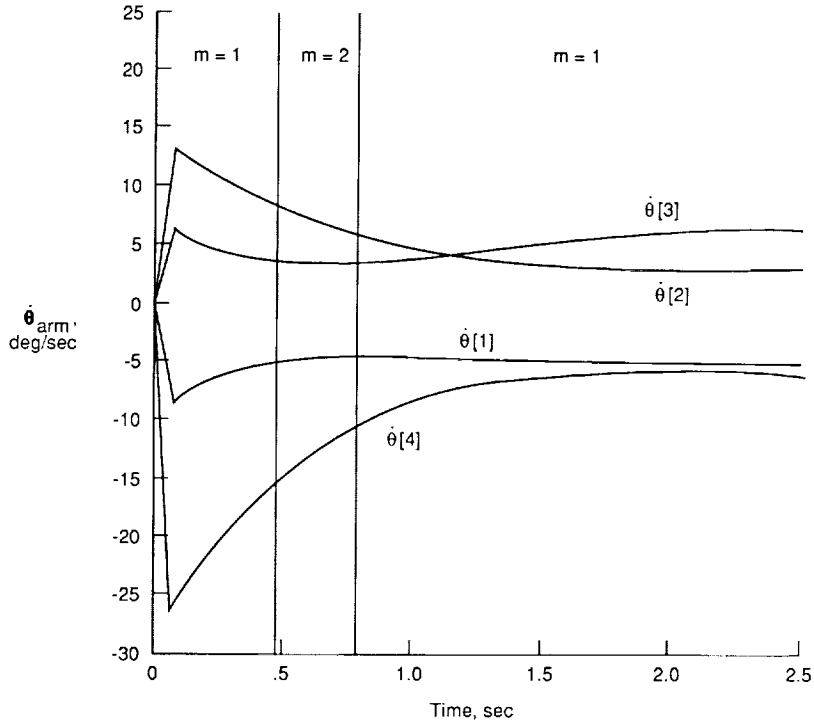

(c) Arm joint angle rates.

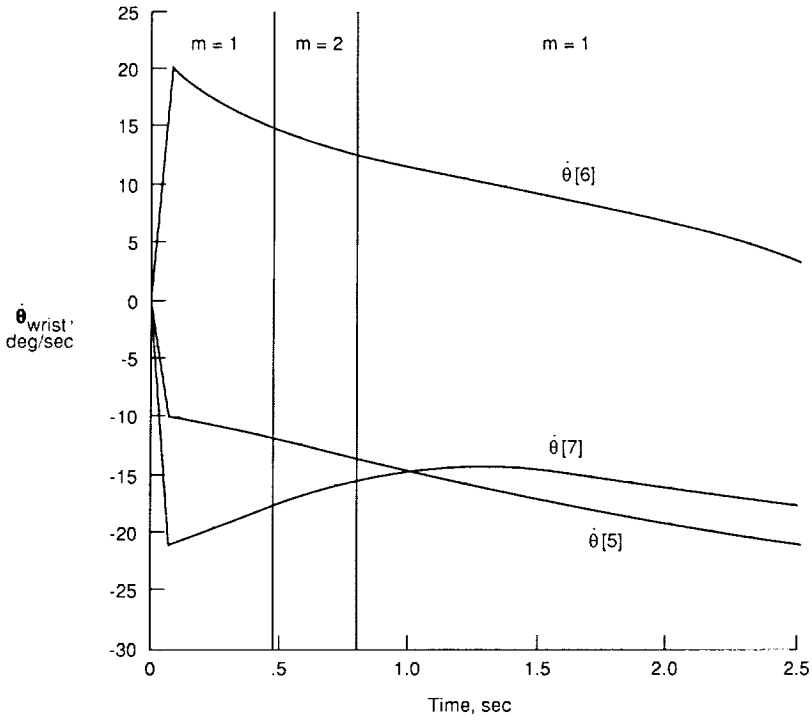

(d) Wrist joint angle rates.

Figure 12. Concluded.

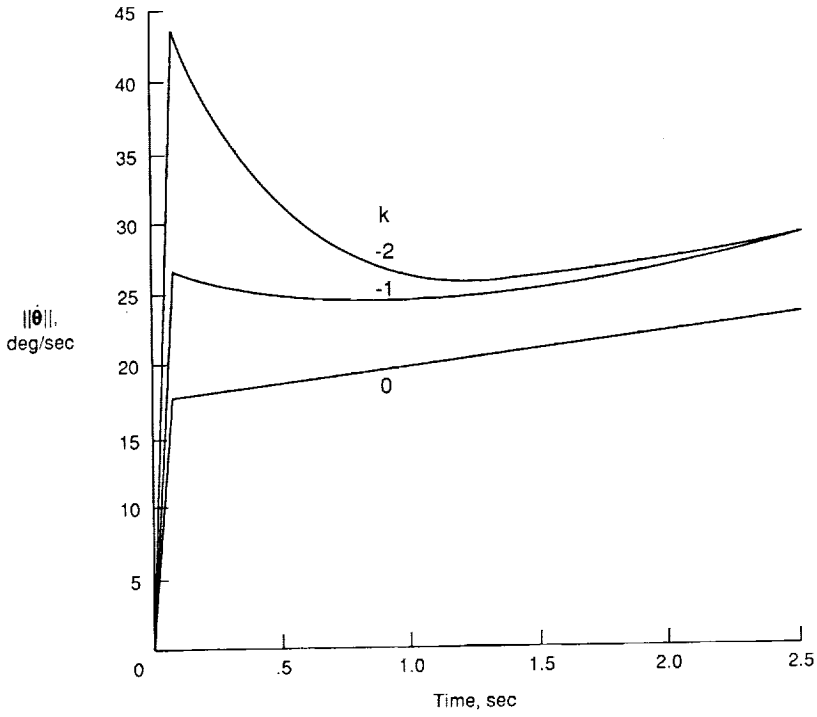

Figure 13. Effect of k on $||\dot{\boldsymbol{\theta}}||$.

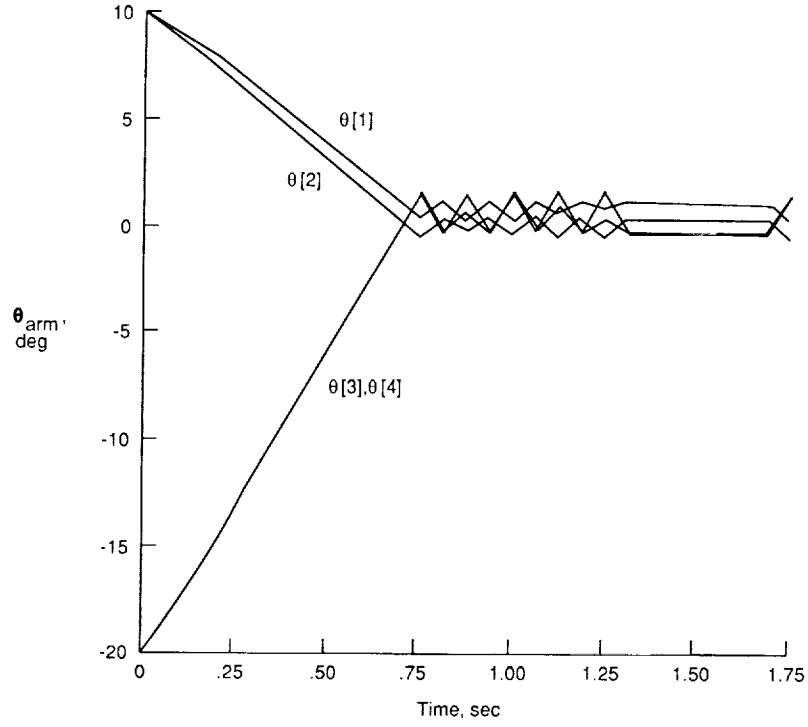

(a) Arm joint angles.

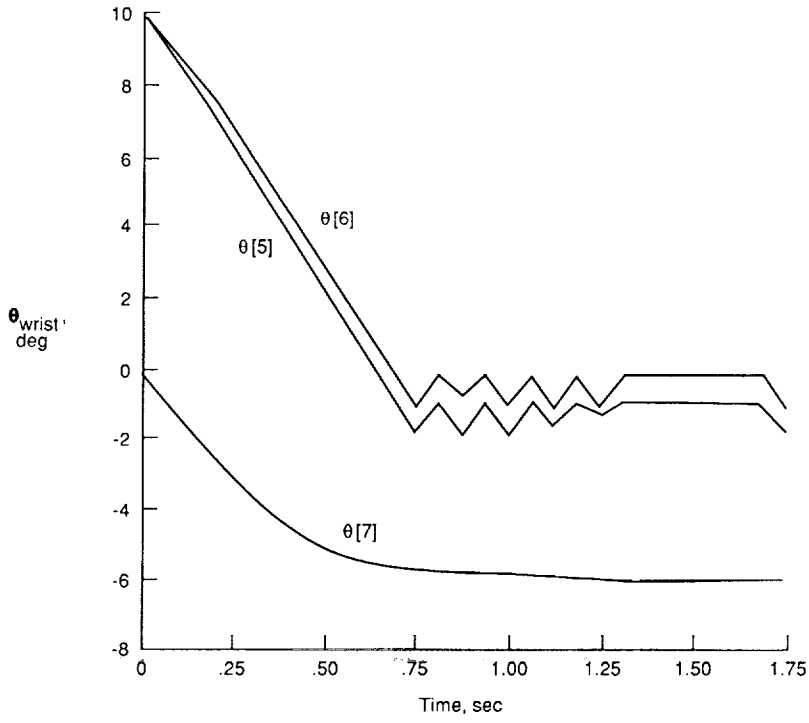

(b) Wrist joint angles.

Figure 14. Full extension of arm using generalized inverse solution.

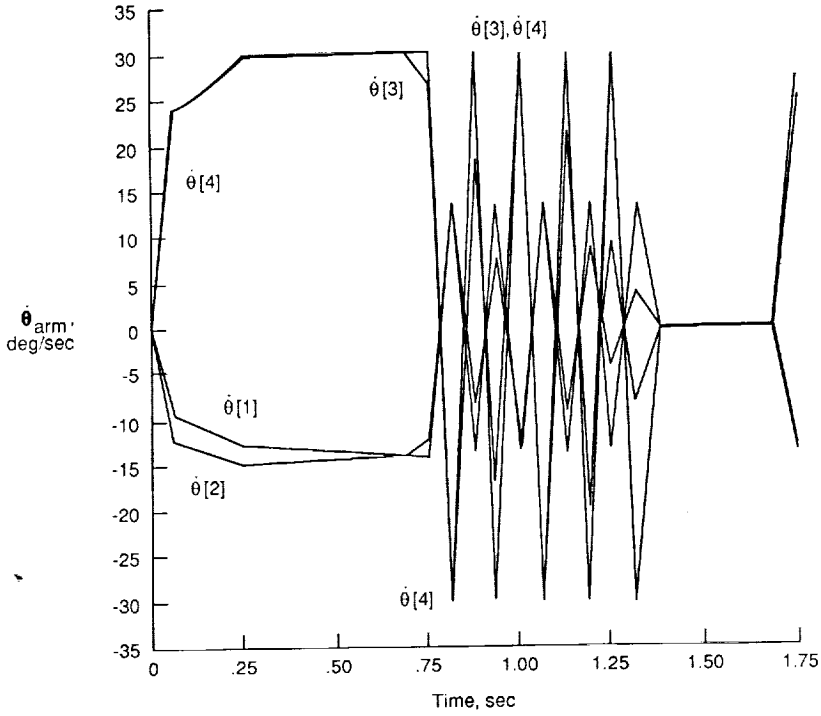

(c) Arm joint angle rates.

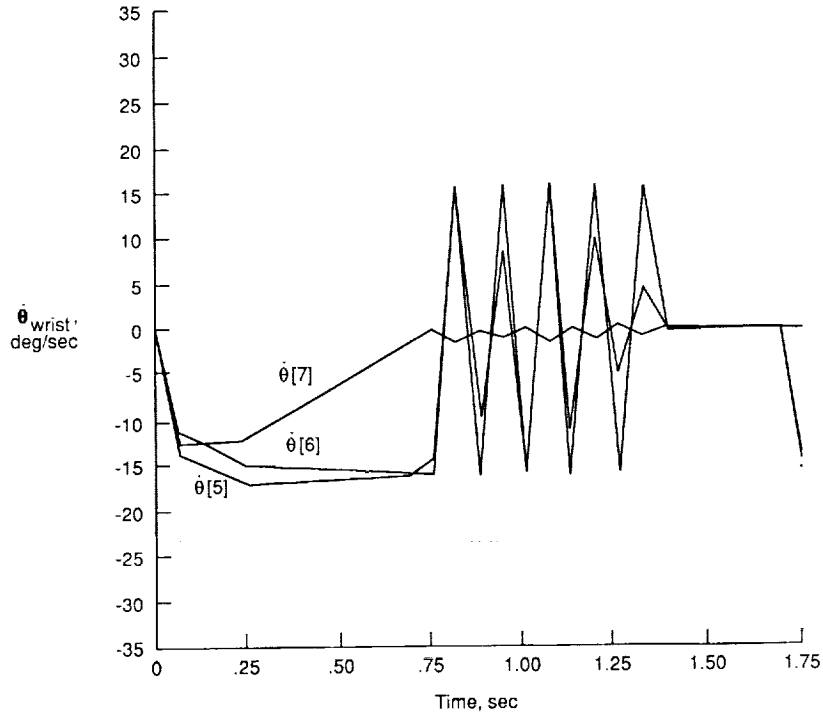

(d) Wrist joint angle rates.

Figure 14. Continued.

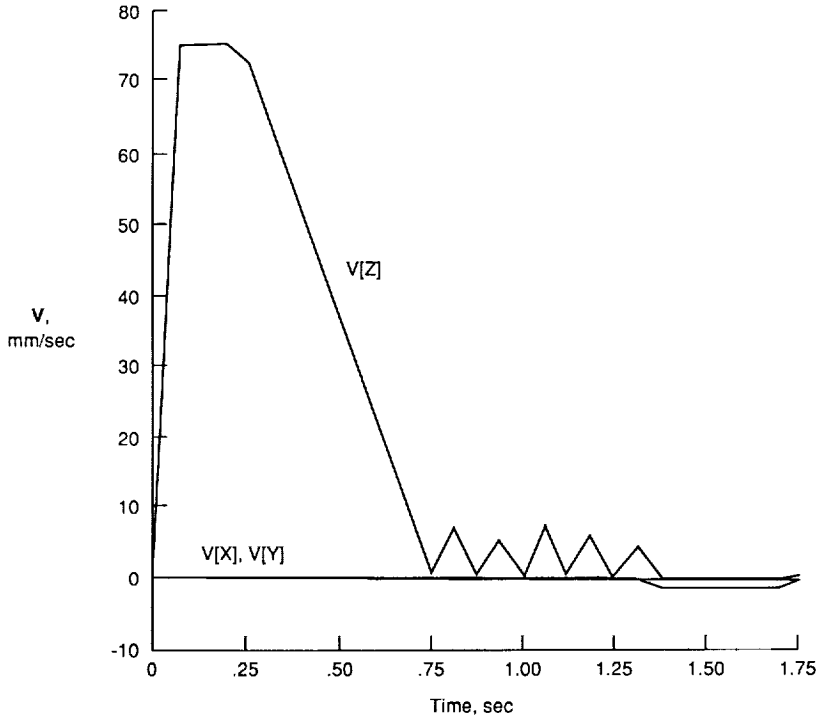

(e) Actual velocity of hand (in hand coordinates).

Figure 14. Concluded.

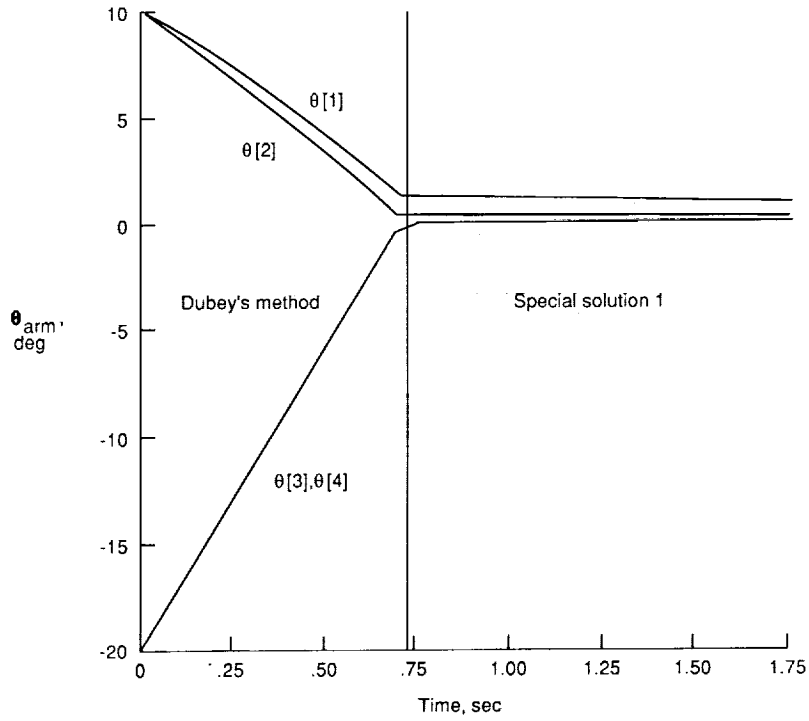

(a) Arm joint angles.

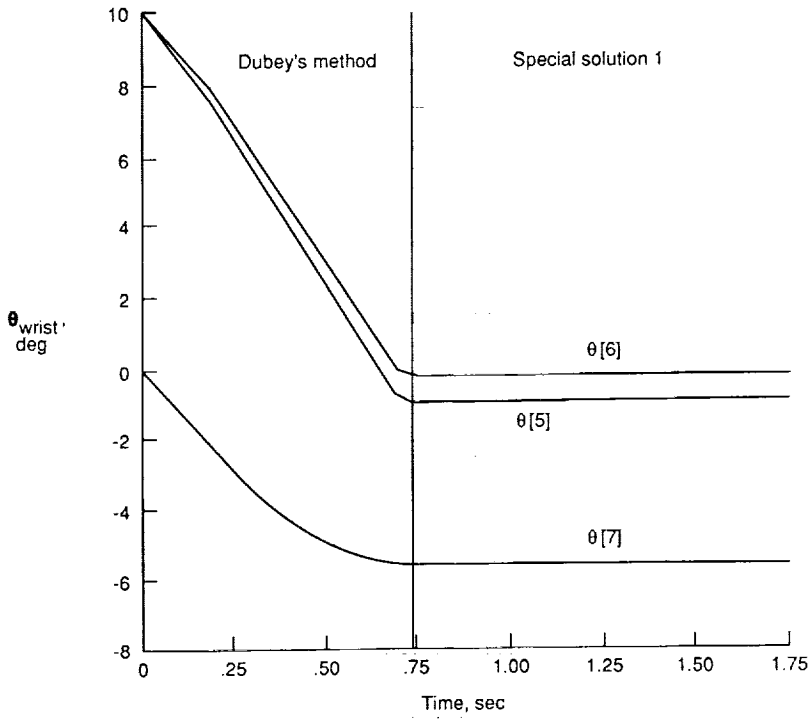

(b) Wrist joint angles.

Figure 15. Full extension of arm using Dubey's method and special solution 1.

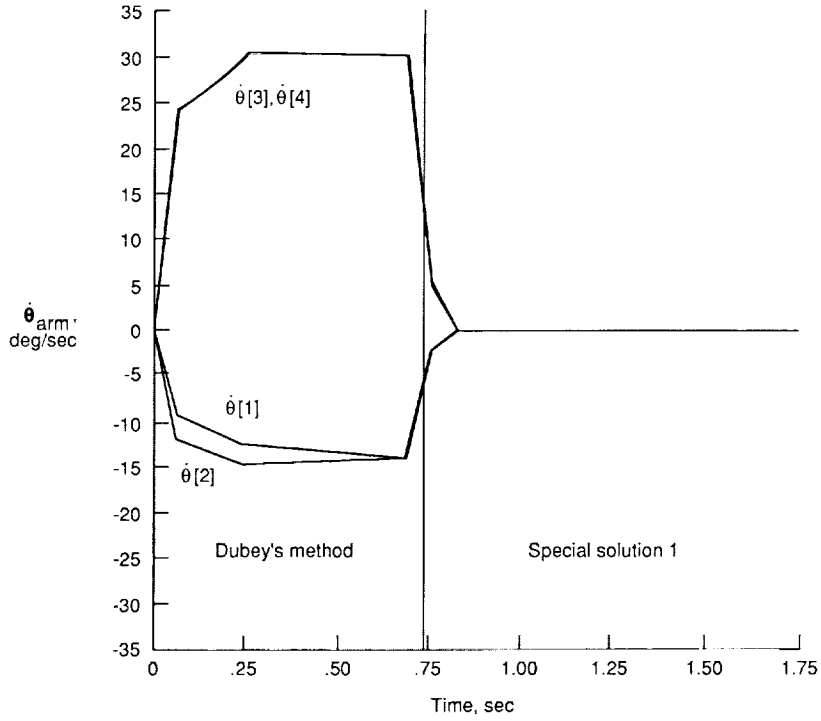

(c) Arm joint angle rates.

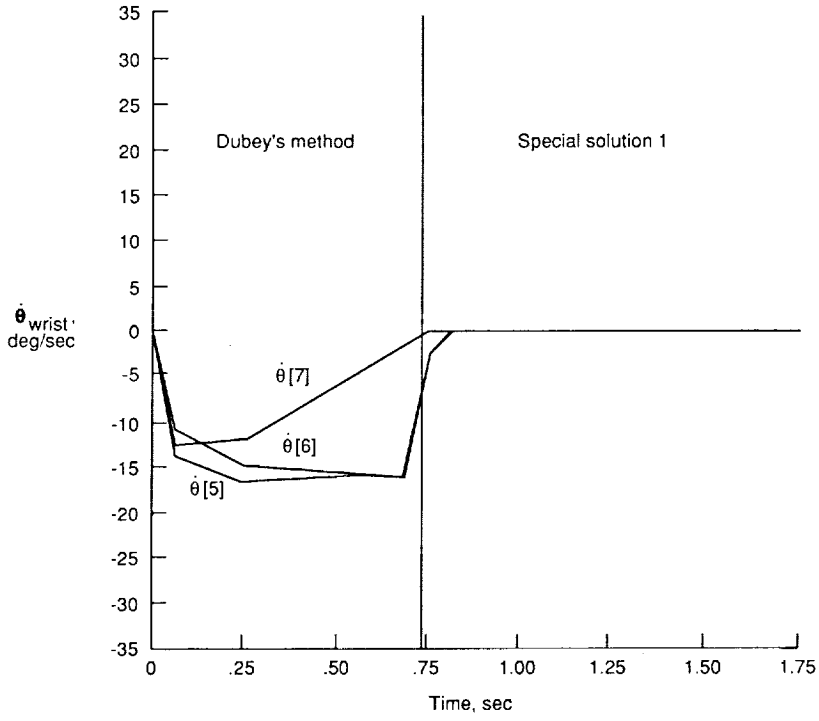

(d) Wrist joint angle rates.

Figure 15. Continued.

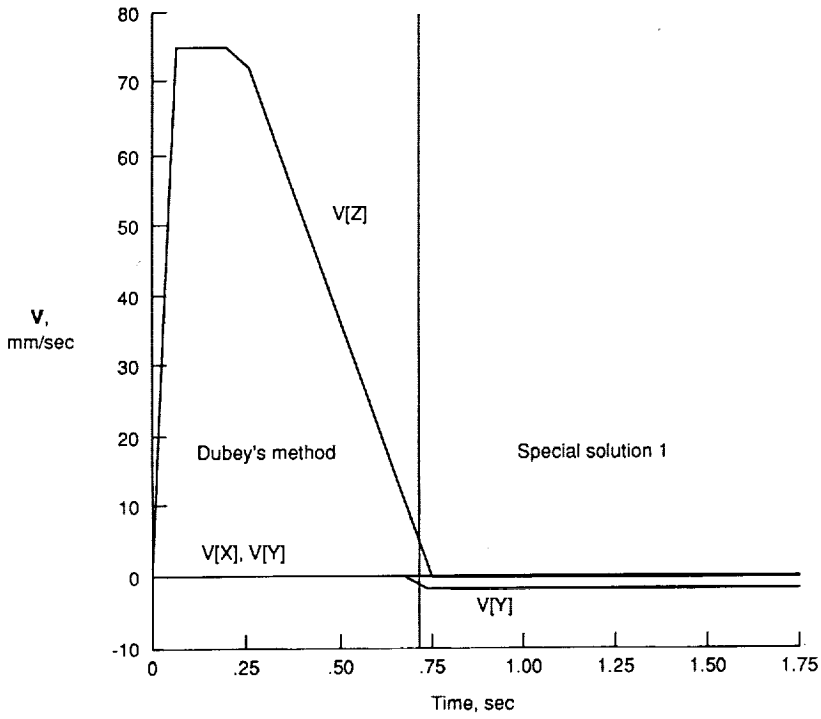

(e) Actual velocity of hand (in hand coordinates).

Figure 15. Concluded.

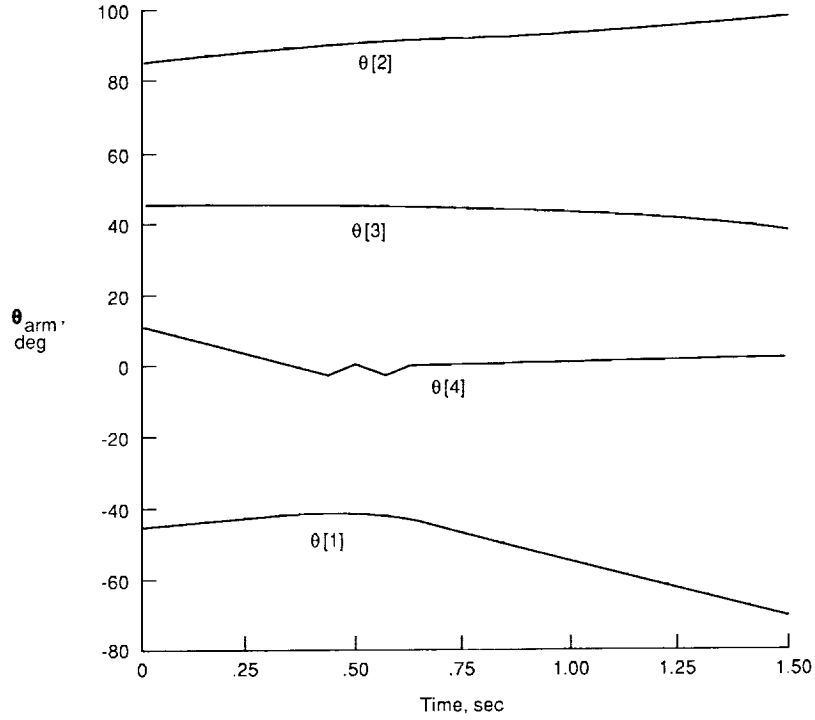

(a) Arm joint angles.

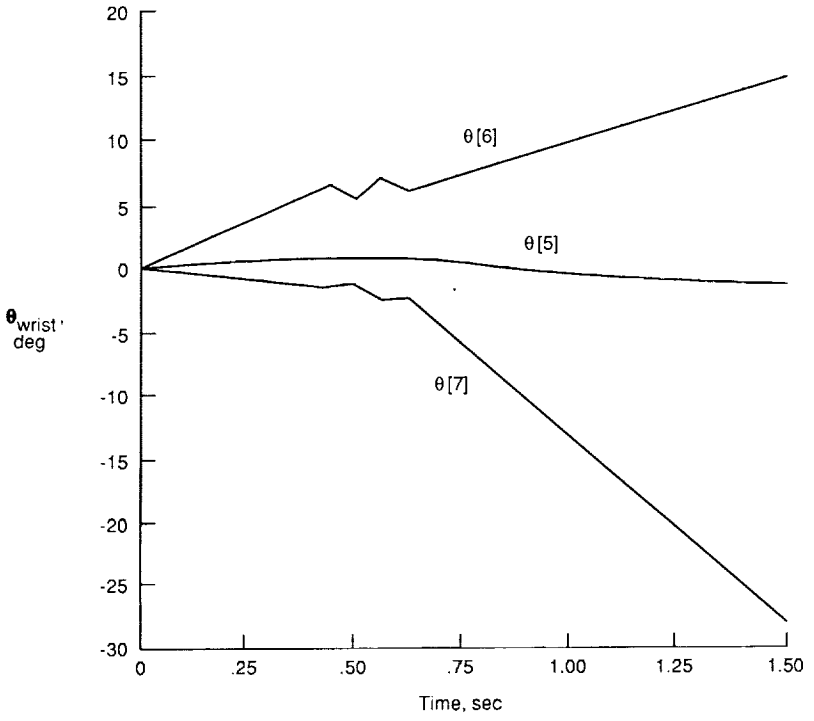

(b) Wrist joint angles.

Figure 16. Motion of arm near the singularity $|\theta_2| = 90°$ and $\theta_4 = 0°$ using generalized inverse solution.

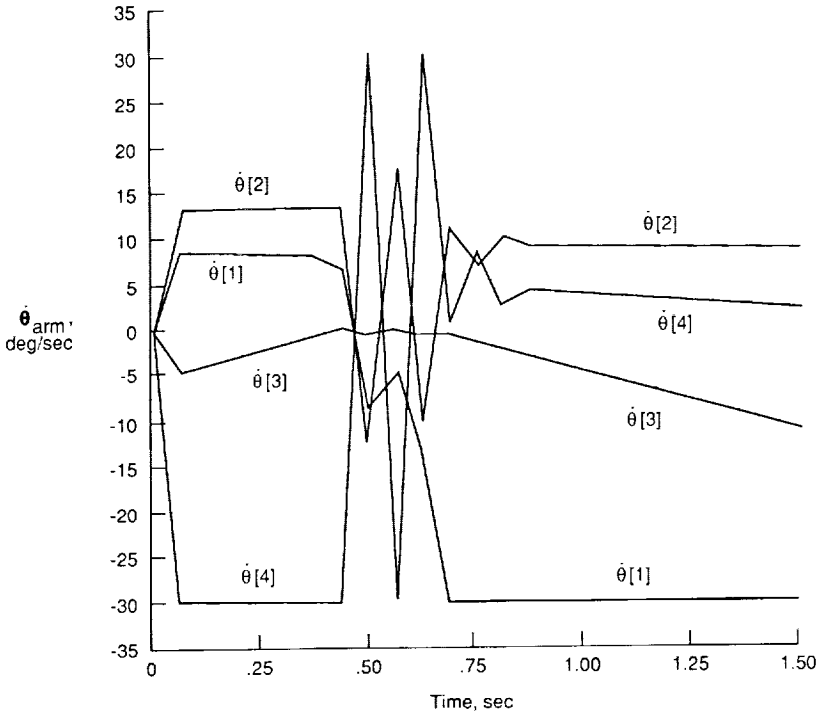

(c) Arm joint angle rates.

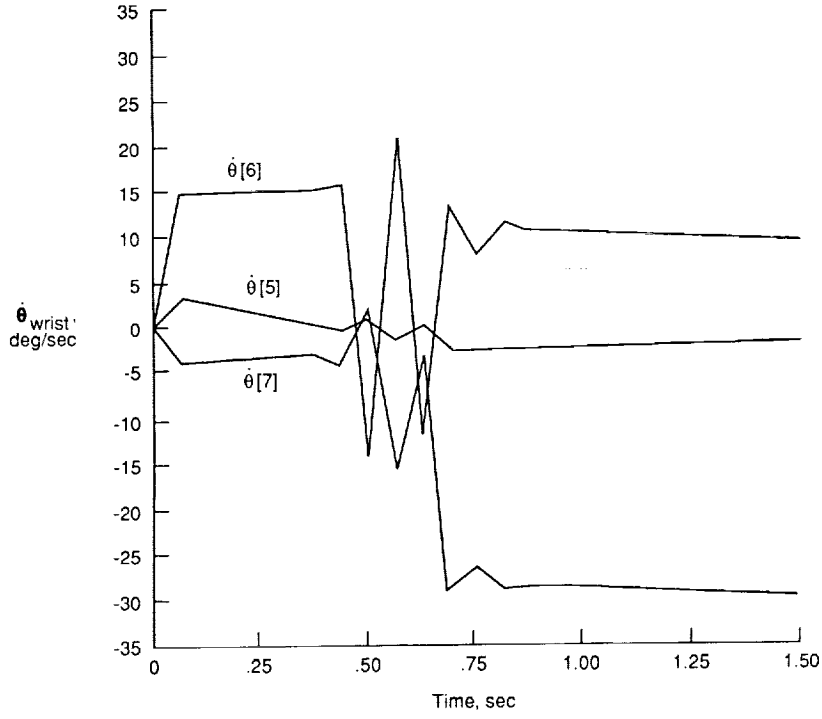

(d) Wrist joint angle rates.

Figure 16. Continued.

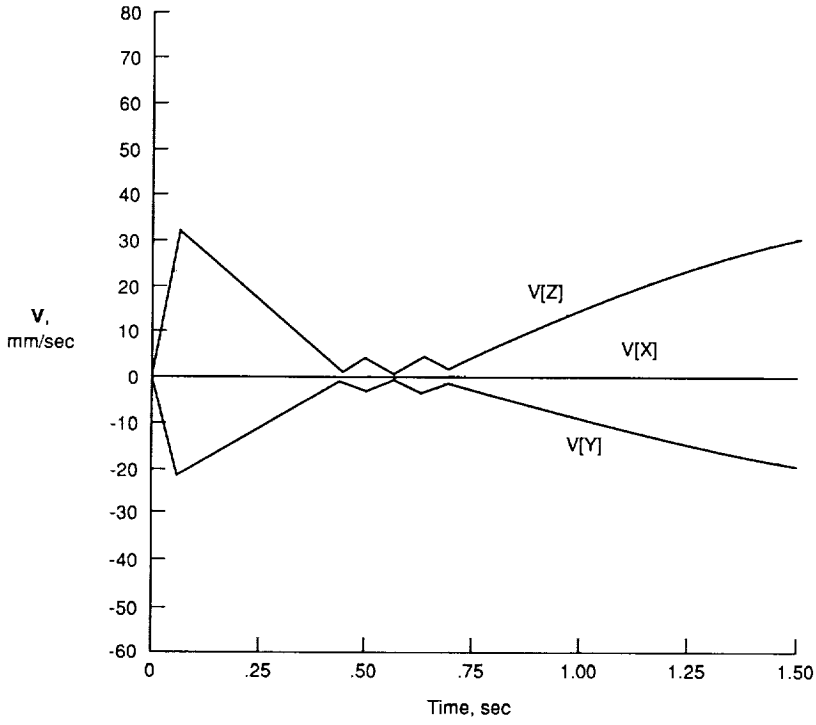

(e) Actual velocity of hand (in hand coordinates).

Figure 16. Concluded.

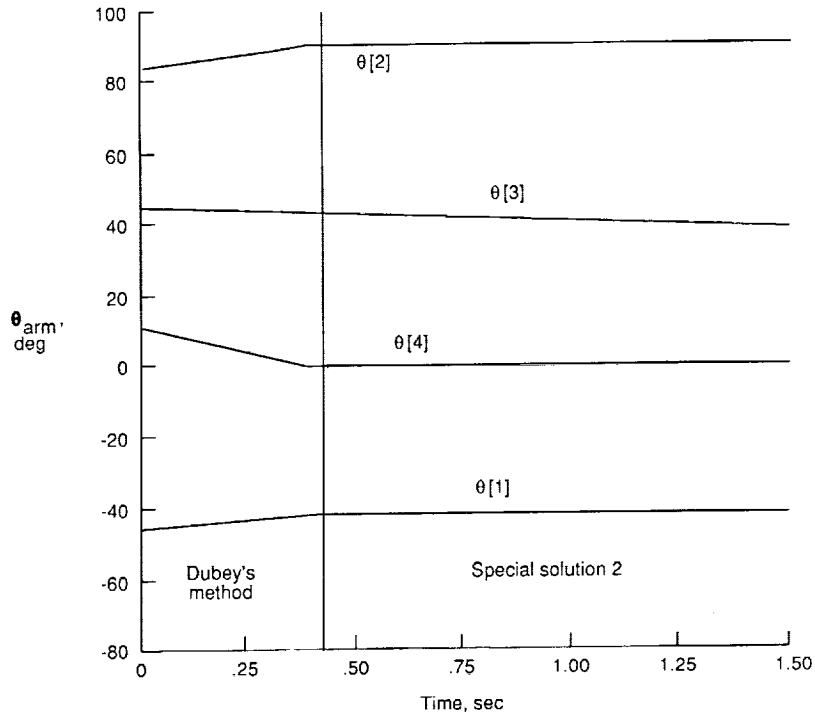

(a) Arm joint angles.

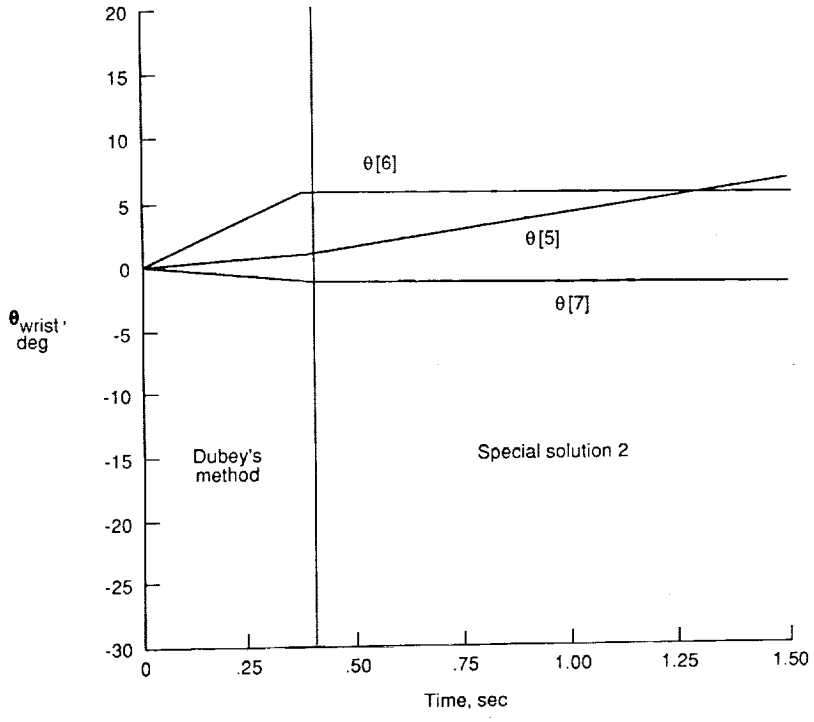

(b) Wrist joint angles.

Figure 17. Motion of arm near the singularity $|\theta_2| = 90°$ and $\theta_4 = 0°$ using Dubey's method and special solution 2.

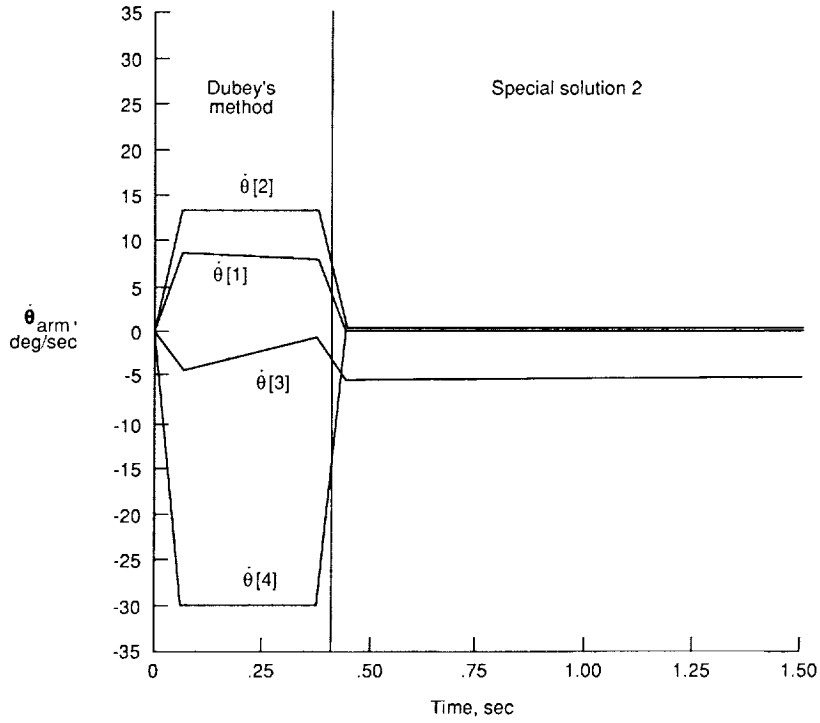

(c) Arm joint angle rates.

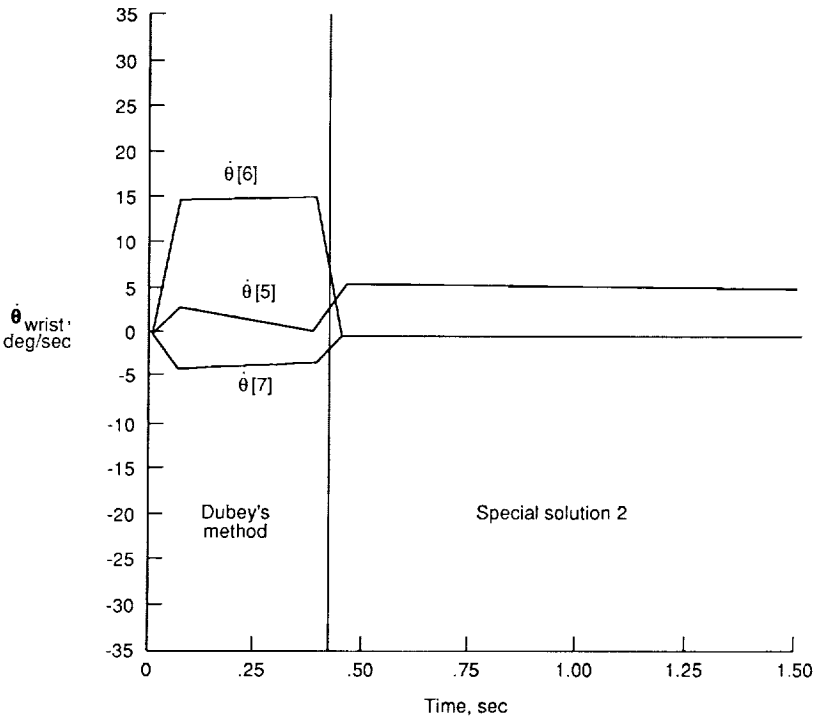

(d) Wrist joint angle rates.

Figure 17. Continued.

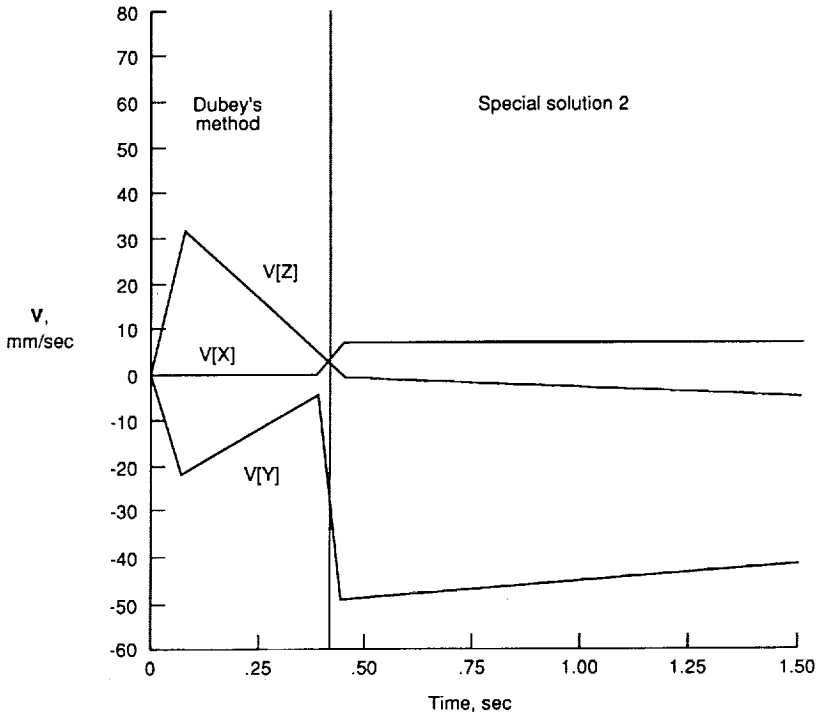

(e) Actual velocity of hand (in hand coordinates).

Figure 17. Concluded.

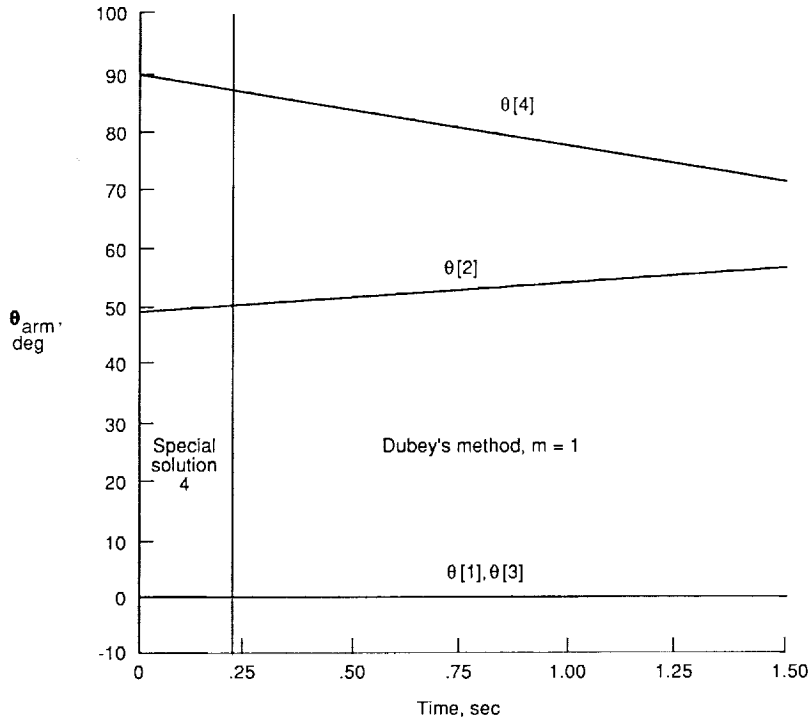

(a) Arm joint angles.

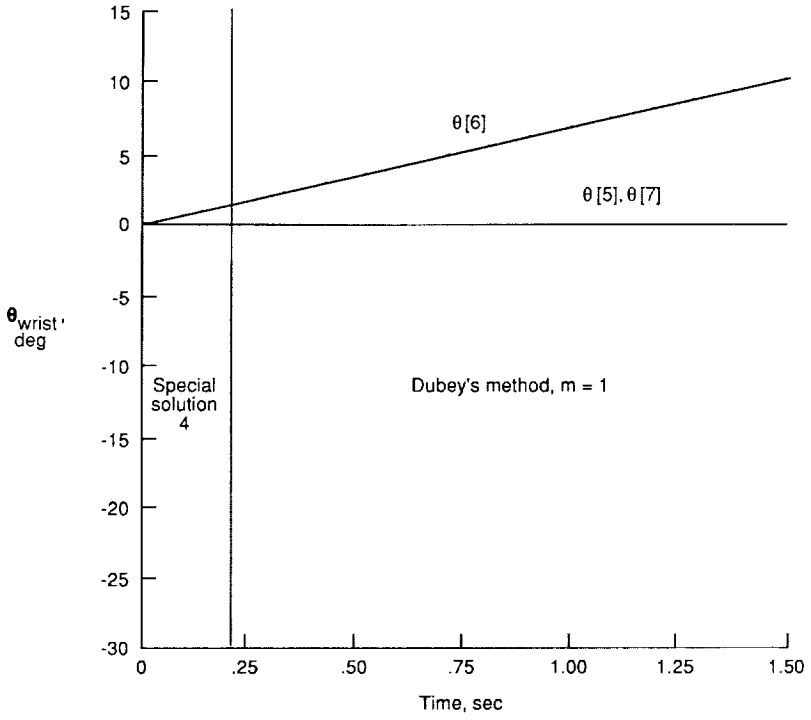

(b) Wrist joint angles.

Figure 18. Motion of arm near the singularity $|\theta_2 + \mu| = 90°$ and $\theta_4 = 0°$ with elbow pitch joint $\theta_3 = 0°$ using special solution 4.

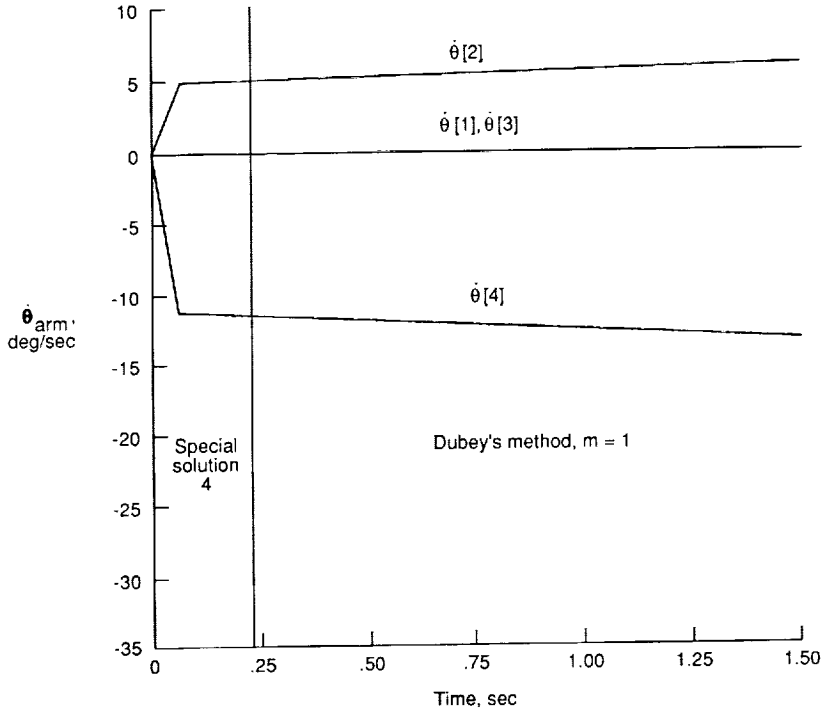

(c) Arm joint angle rates.

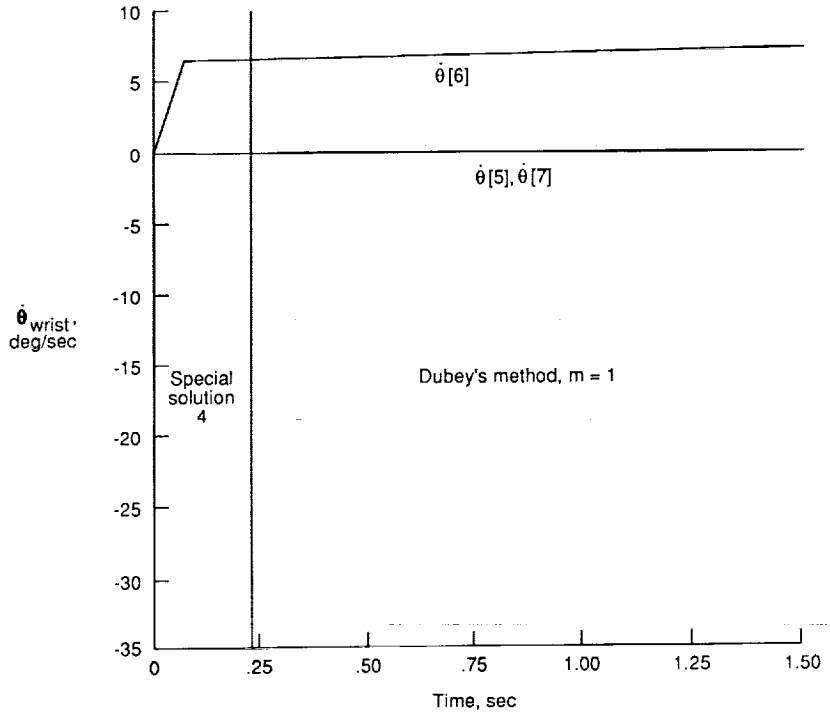

(d) Wrist joint angle rates.

Figure 18. Continued.

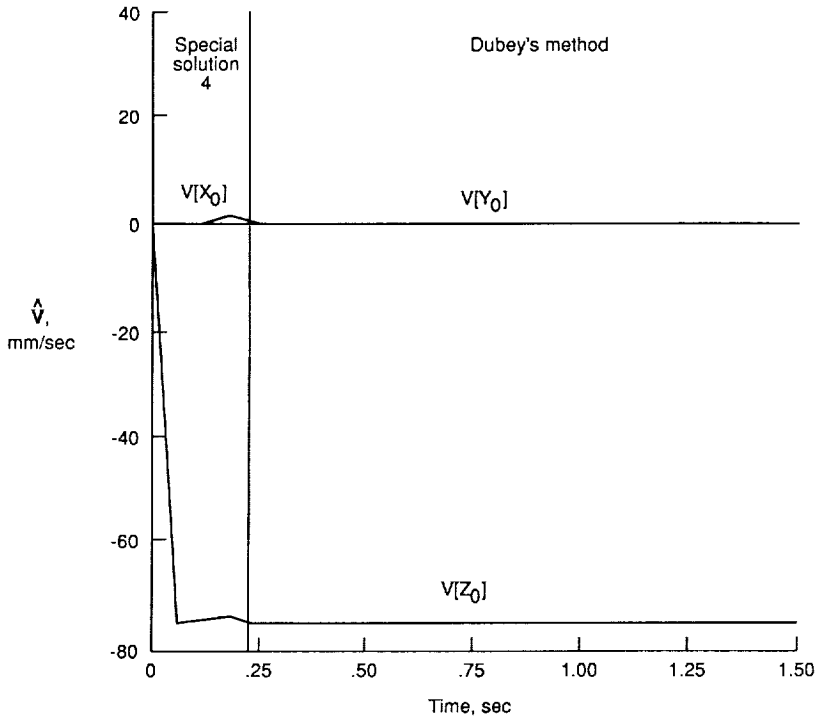

(e) Actual velocity of hand (in base coordinates).

Figure 18. Concluded.

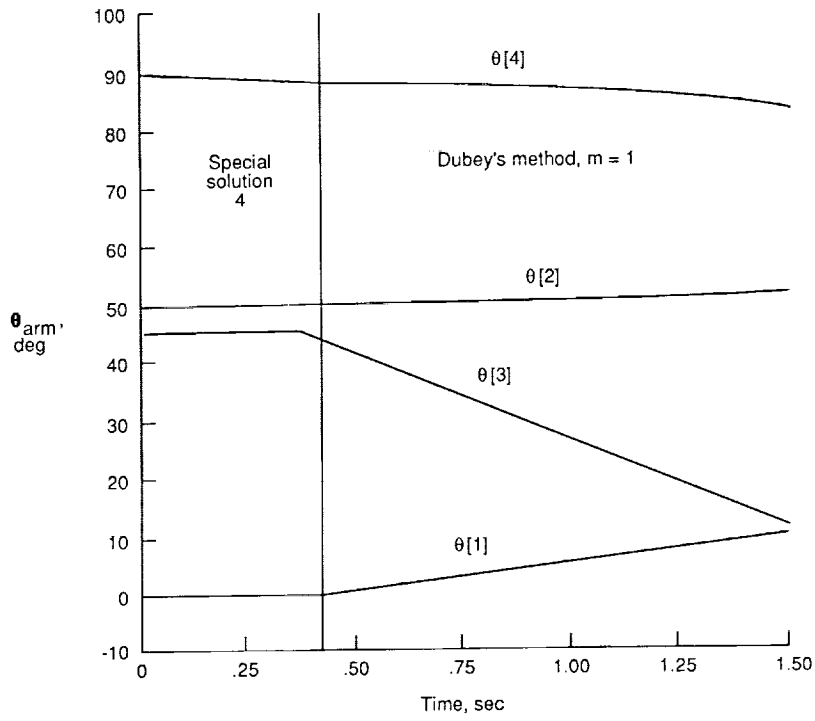

(a) Arm joint angles.

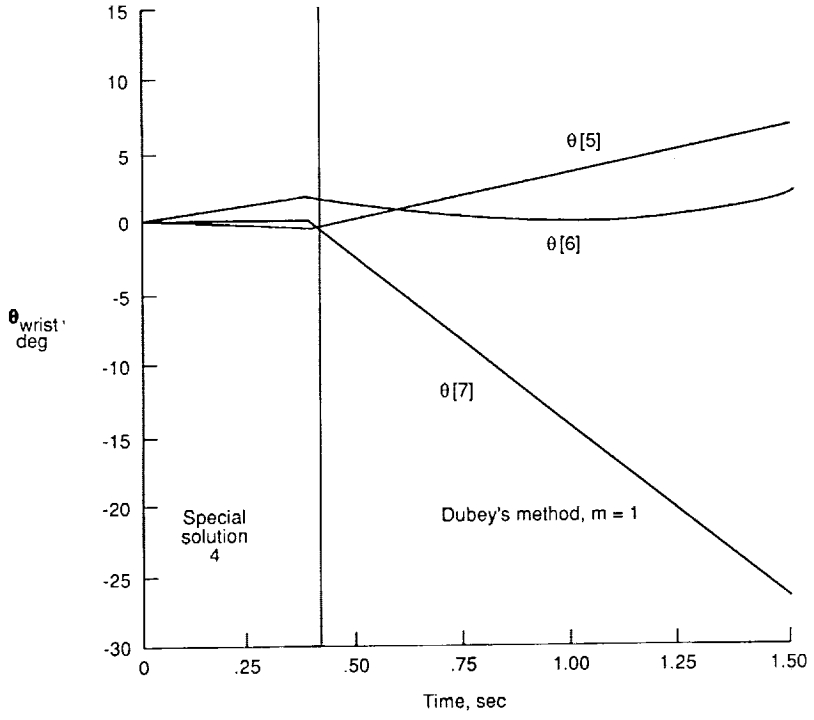

(b) Wrist joint angles.

Figure 19. Motion of arm near the singularity $|\theta_2 + \mu| = 90°$ and $\theta_4 = 0°$ with elbow pitch joint $\theta_3 = 45°$ using special solution 4.

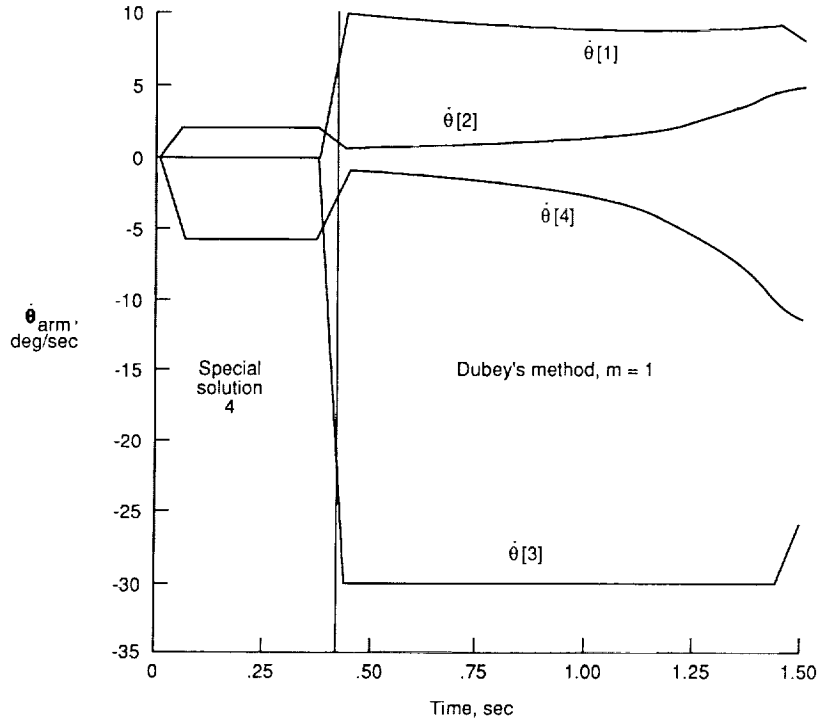

(c) Arm joint angle rates.

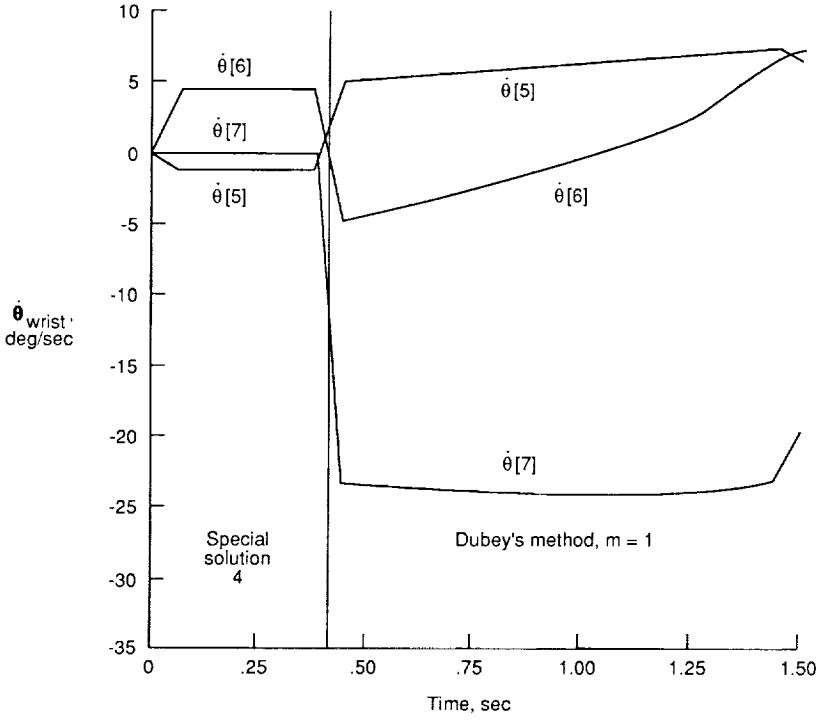

(d) Wrist joint angle rates.

Figure 19. Continued.

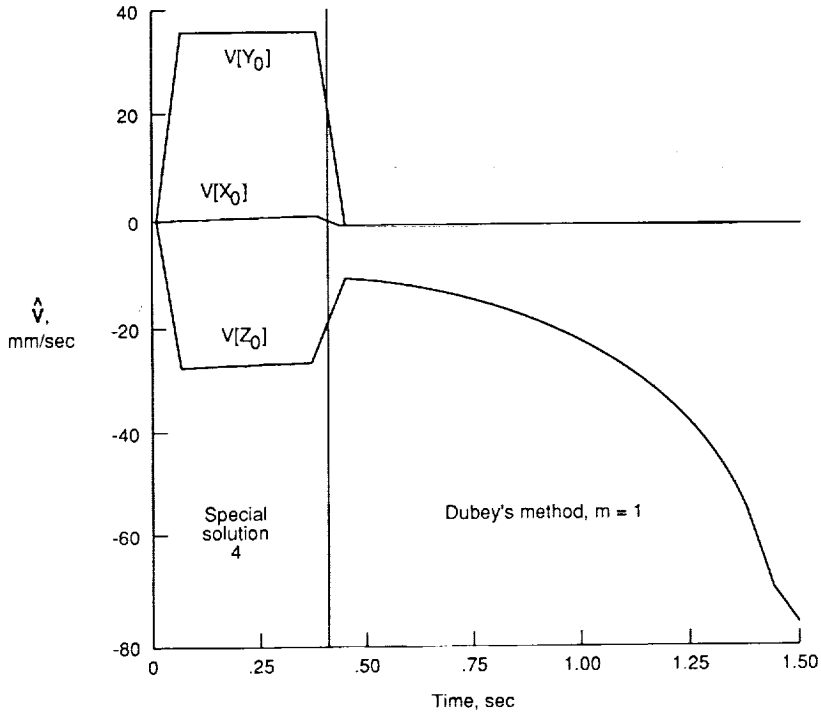

(e) Actual velocity of hand (in base coordinates).

Figure 19. Concluded.

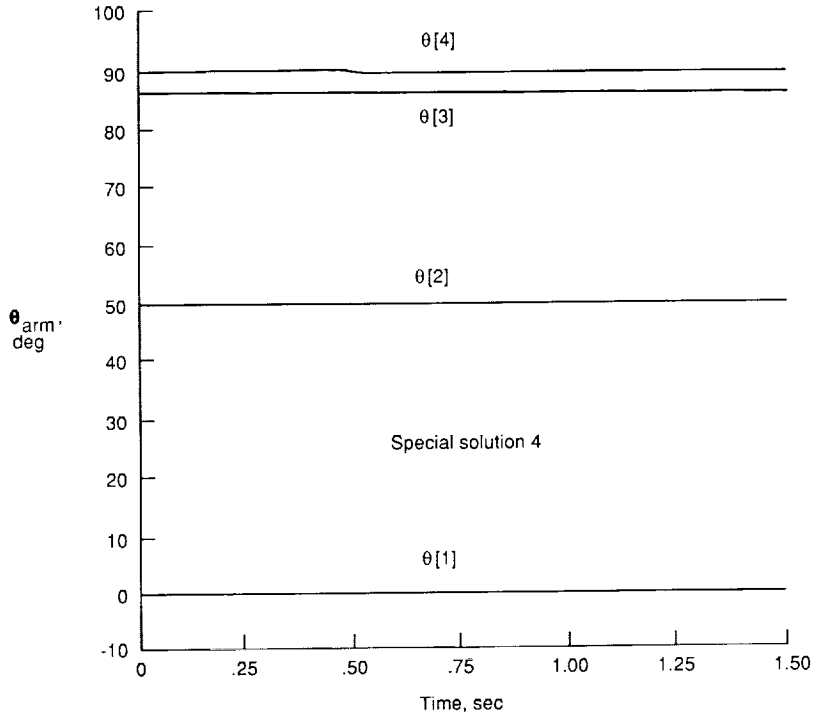

(a) Arm joint angles.

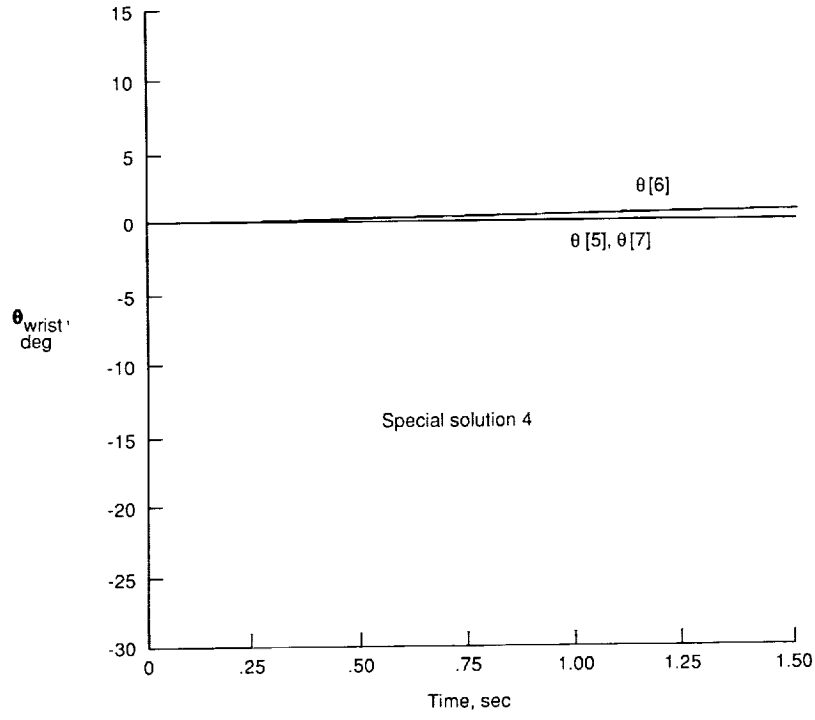

(b) Wrist joint angles.

Figure 20. Motion of arm near the singularity $|\theta_2 + \mu| = 90°$ and $\theta_4 = 0°$ with elbow pitch joint $\theta_3 = 85°$ using special solution 4.

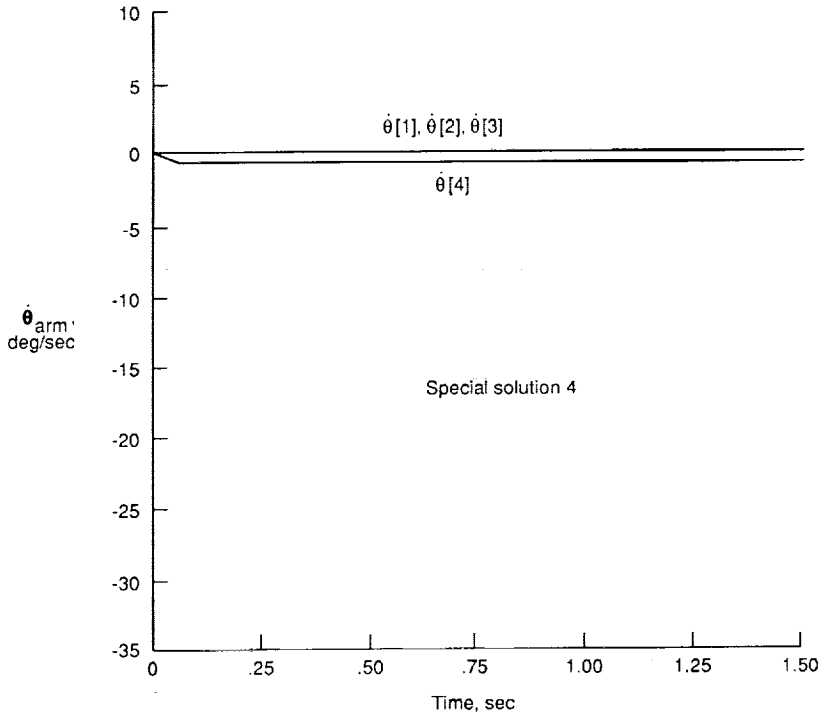

(c) Arm joint angle rates.

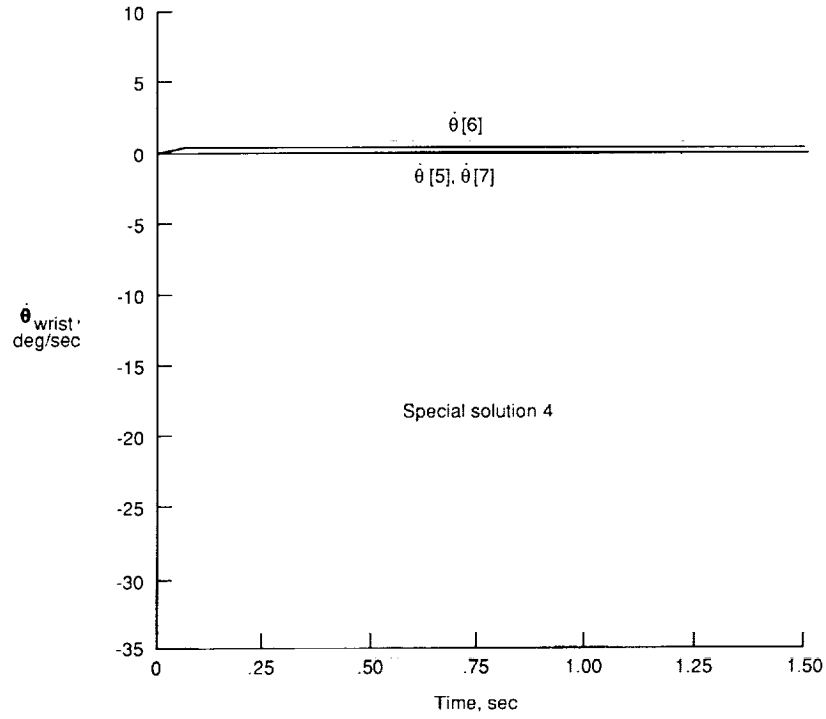

(d) Wrist joint angle rates.

Figure 20. Continued.

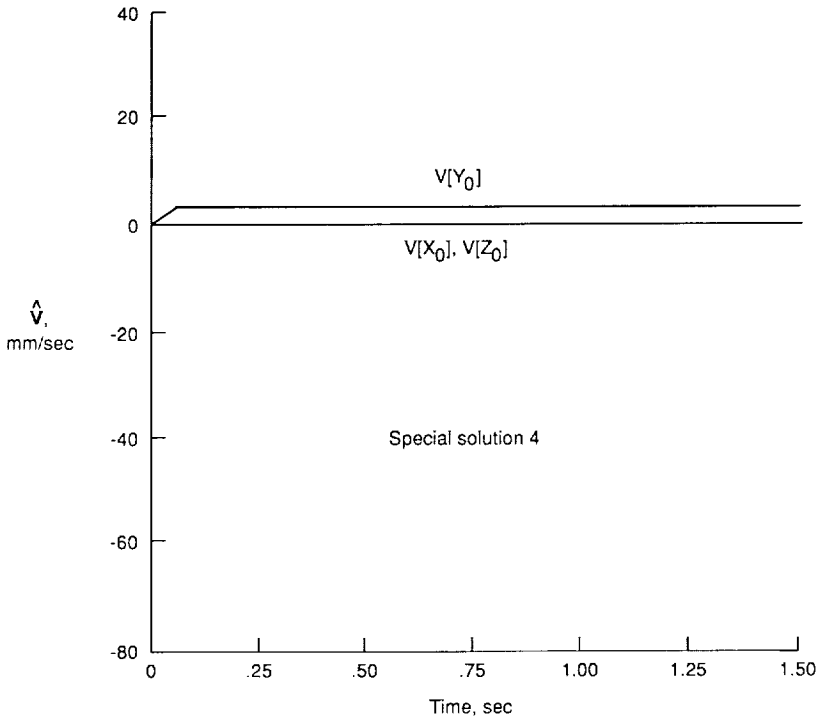

(e) Actual velocity of hand (in base coordinates).

Figure 20. Concluded.

NASA
National Aeronautics and Space Administration

Report Documentation Page

1. Report No.	2. Government Accession No.	3. Recipient's Catalog No.
NASA TP-2938		

4. Title and Subtitle	5. Report Date
Optimized Resolved Rate Control of Seven-Degree-of-Freedom Laboratory Telerobotic Manipulator (LTM) With Application to Three-Dimensional Graphics Simulation	October 1989
	6. Performing Organization Code
7. Author(s)	8. Performing Organization Report No.
L. Keith Barker and William S. McKinney, Jr.	L-16562
9. Performing Organization Name and Address	10. Work Unit No.
NASA Langley Research Center Hampton, VA 23665-5225	549-02-41-01
	11. Contract or Grant No.
12. Sponsoring Agency Name and Address	13. Type of Report and Period Covered
National Aeronautics and Space Administration Washington, DC 20546-0001	Technical Paper
	14. Sponsoring Agency Code

15. Supplementary Notes

16. Abstract

The Laboratory Telerobotic Manipulator (LTM) is a seven-degree-of-freedom robot arm built by the Oak Ridge National Laboratory for NASA. Two of the arms have been delivered to Langley Research Center for ground-based research to assess the use of redundant degree-of-freedom robot arms in space operations. Resolved rate control equations for the LTM are derived in this paper. The equations are based on a scheme developed at the Oak Ridge National Laboratory for computing optimized joint angle rates in real time. The optimized joint angle rates actually represent a trade-off, as the hand moves, between small rates (least-squares solution) and those rates which work toward satisfying a specified performance criterion of joint angles. In singularities where the optimization scheme cannot be applied, alternate control equations are devised. The equations developed in this paper were evaluated with a real-time computer simulation to control a three-dimensional graphics model of the LTM.

17. Key Words (Suggested by Authors(s))
Redundant
Real-time control
Singularities
Optimization

18. Distribution Statement
Unclassified—Unlimited

Subject Category 63

19. Security Classif. (of this report)	20. Security Classif. (of this page)	21. No. of Pages	22. Price
Unclassified	Unclassified	78	A05